ENGINEERING RESEARCH INSTITUTE
UNIVERSITY OF MICHIGAN
ANN ARBOR

TECHNICAL REPORT NO. 1

THE INFRARED ABSORPTION SPECTRA OF DIAMOND, SILICON, AND GERMANIUM

By

WILLIAM G. SIMERAL

Project M957

SIGNAL CORPS, DEPARTMENT OF THE ARMY
CONTRACT DA 36-039 sc-5581, SC PROJECT 152B-0, DA PROJECT 3-99-15-022
SQUIER SIGNAL LABORATORY, FORT MONMOUTH, N. J.

June 1, 1953

PREFACE

The following text has been approved as a dissertation for the doctorate at the University of Michigan. Since the author has derived support from a Signal Corps Contract both in stipend (Summers of 1951 and 1952) as well as in funds for equipment, the full account of the work is being submitted as a report to the Signal Corps.

The principal financial aid, however, was received from a University of Michigan Fellowship (1951-1952) and a National Science Foundation Fellowship (1952-1953).

The author is pleased to acknowledge the assistance which he has received from the staff of the Physics Department and from his fellow members of the "Infrared Group". In particular, he is indebted to Professor G. B. B. M. Sutherland who suggested the problem and who has been generous with advice during the course of the work and in the preparation of this manuscript. In addition, grateful acknowledgment is made to the following:

Dr. D. L. Wood, who has given advice pertaining to the experimental portions of this work on many occasions, particularly with regard to infrared instrumentation.

Dr. S. Krimm and Dr. C. Liang, who have assisted materially in obtaining spectra in the far infrared.

Mr. W. Childs, who operated the cyclotron during bombardment experiments.

Dr. K. N. Tanner, who helped in the vacuum ultraviolet instrumentation.

Dr. G. A. Morton, of the RCA Laboratories, who supplied samples of germanium.

The following firms and individuals have generously lent diamonds for use in this work:

The Diamond Trading Company (Mr. Grodzinski)

The Lazare Kaplan Company

Triefus and Company

Professor C. B. Slawson

Dr. W. C. Parkinson

In construction of equipment P. Weyrich, H. Roemer, and G. Kessler have contributed their not inconsiderable talents. A. Dockrill has been of great assistance in the work on the concentrated arc source.

Finally, the author wishes to take this opportunity to acknowledge the many important contributions which his wife has made to the preparation of this manuscript.

ERRATA

Page		
iv	Page number opposite	(l.2 read 14 for 6) (l.3 read 23 for 14) (l.4 read 30 for 23)
38	Line 19, read numerical for numberical	
77	Addendum line 15.	The linear range equals the quotient of the range in mg/cm^2 and the density.
113	Line 24, read numerical for numberical	
127	Line 23, read (8, 0, 0) for (8, 8, 0)	
131	Line 26, read (d) for (b)	
144	Read "See Figures 32 and 33" for "See Figure 34"	
1	In Table 1, interchange 2250 and 3000	

TABLE OF CONTENTS

LIST OF TABLES

Table
Number

LIST OF ILLUSTRATIONS

Figure
Number

INTRODUCTION

Because of its remarkable physical properties, diamond has been the subject of many experimental and theoretical investigations. Perhaps the best known properties of diamond are its great hardness, high index of refraction, and low specific heat at room temperature. Until recently, it was assumed that all diamonds were essentially identical. However, in 1934, Robertson, Fox, and Martin[1] reported two types of diamond, based on careful investigations of infrared absorption, position of ultraviolet cutoff, photoconductivity, and birefringence. The essential properties of the two types are given in Table 1.

Table 1

Property	Type I	Type II
Infrared Absorption	Near 4μ and near 8μ	Near 4μ only
Ultraviolet Cutoff	2250 A. U.	3000 A. U.
Photoconductivity	Poor	Ten times better
Birefringence	Present	Absent

Somewhat later Raman and Rendall[2] detected variations between the Laue diffraction patterns of different diamonds.

They reported that diamonds of Type I had extra streaks near certain Laue spots while Type II diamonds showed no such extra streaks. Also, Lonsdale[3] found that, in general, Type I diamonds had less mosaic texture than Type II diamonds. All of these workers found that Type I diamonds were more common and more perfect externally than Type II diamonds.

Later work[4,5] showed that many diamonds could not be classified as either Type I or Type II since their properties were intermediate between the two types. This fact has led to some confusion in the literature. One worker may describe a diamond as Type I because its ultraviolet cutoff falls at 2900 A. U., while another worker may describe the same diamond as Type II because it shows very little absorption at 8μ. In order to avoid the difficulty in the notation introduced by Robertson, Fox, and Martin, we have modified the notation in the following manner: With regard to ultraviolet absorption, a diamond will be described as UV II if its cutoff occurs between 2250 A. U. and 2500 A. U. It will be described as a weak UV I diamond if the cutoff falls between 2500 A. U. and 2800 A. U.; medium UV I, between 2800 A. U. and 3000 A. U.; strong UV I, greater than 3000 A. U. With regard to X-ray diffraction, X II indicates a diamond showing no extra streaks in the Laue diffraction pattern. X I indicates a diamond showing extra streaks, while the adjectives weak, medium, and strong, indicate the intensity of the streaks. With regard to infrared absorption, IR II denotes a diamond which displays no absorption at wavelengths longer than 6μ. IR I denotes a diamond which dis-

plays absorption at wavelengths longer than 6μ, while the adjectives weak, medium, and strong indicate the intensity of absorption at 8μ relative to the intensity of absorption at 4μ.

Raman and his coworkers have studied the properties of diamond in great detail.[6] They have found that the Raman scattering spectrum is the same for all diamonds. Variations between diamonds occur in their fluorescence spectra and their visible absorption spectra. The workers in India have made many observations of these properties. On the basis of his own theory of lattice dynamics[7] and on the basis of his experimental results, Raman has formulated a theory[8] to explain the anomalous properties of diamonds. The theory is based on the assumption that the local electronic configuration in diamond has four possible forms. This theory, as well as Raman's theory of lattice dynamics, has received severe criticism[3, 9, 10] and is not accepted by most workers in the fields of study concerned.

Blackwell and Sutherland[11] have proposed a different theory to account for the anomalous properties of diamonds. Their theory is based, in large part, on the experimental data obtained by Blackwell.[10] He performed experiments on a collection of several hundred stones. He studied: (1) Spectroscopic properties in the infrared, visible, and ultraviolet (2) Raman scattering, (3) Color, (4) Crystal habit and external perfection, (5) Several other properties. This work was devoted to the correlation of the various properties in an attempt to find regularities in the variations between diamonds. The theory put forward by

Sutherland and Blackwell proposed that the variations between diamonds are due to structural imperfections or foreign atoms.

The only subsequent work which is of importance is that of Dr. Grenville-Wells. The work was devoted to a continuation of Lonsdale's study of the X-ray diffraction properties of diamond. The work was similar to that of Blackwell in that correlations were found between mosaic texture, extra streak intensity, ultraviolet cutoff, and other properties.

The present work began in 1950. Because many of the diamonds from Blackwell's collection were available, it has been possible to obtain new data for the same stones for which considerable information was already available. Initially, the object of the work was to devise two types of experiments: (1) Those which would improve and extend Blackwell's data, (2) Those which would afford a test of the impurity theory. Included in the first set of experiments were observations of the absorption spectra of diamonds in the far infrared, in the vacuum ultraviolet, and in the region of atmospheric absorption near 6μ. In the second set of experiments were variations of infrared and ultraviolet absorption in individual diamonds, the effects on infrared absorption caused by deuteron and neutron bombardment, and comparisons between the spectra of diamonds and those of silicon and germanium of various states of purity.

As the work progressed, it became evident that the main difficulty in the interpretation of observation lay in the fact that very little effort had been made to apply existing theory of crystal spectra to the case of diamond. On the other hand, many of the phenomena connected with the elec-

tronic structure can be interpreted, at least in a qualitative fashion, in terms of existing theory. The band structure of the electronic energy levels has received new theoretical treatment.[13] However, the extra streaks in the Laue diffraction pattern and the varying absorption at 8μ in diamond remain unexplained.

Consequently, the theoretical part of this work is mainly concerned with an explanation of the infrared absorption spectrum of diamond. Our approach has been through H. M. J. Smith's[14] calculation of the frequency distribution of diamond based on the Born[15] theory of lattice dynamics. Smith was mainly concerned with the explanation of the second order Raman spectrum of diamond. Our goal has been to establish what the absorption spectrum of an ideal diamond should be, and then to examine the theoretical justification of Raman's theory and of Blackwell's and Sutherland's theory in accounting for those features of the spectrum which are not associated with the ideal case. For the latter work we have used the theory developed by I. M. Lifshitz[16] to explain the anomalous variation of intensity of certain infrared bands. Finally, it was found that the theories developed for diamond apply equally well to silicon and germanium since these substances have crystal structures and associated physical properties similar to those of diamond.

Chapter 1

REVIEW OF PREVIOUS EXPERIMENTAL WORK

1.1 X-ray

In 1913, the Braggs[17] determined the structure of diamond. The Bragg structure consists of two interpenetrating face-centered cubic lattices displaced from one another one quarter of the way along the space diagonal. This structure is shown in Figure 1. Such a structure has a center of symmetry midway between each neighboring pair of carbon atoms. Each carbon atom has four symmetrically placed first neighbors located at the vertices of a tetrahedron. The most recent measurement of the unit cell dimension is by Straumanis[18] who finds the cube side to be 3.668 A. U. which gives a nearest neighbor distance of 1.544 A. U. In Figure 2 we show the structure of diamond in terms of the bonds between neighboring atoms.

The perfection of individual diamond crystals has been the subject of considerable study. Ehrenberg, Ewald, and Mark[19] measured the angular width of the Bragg reflections for certain diamonds. In the most favorable cases, the measured width approaches the theoretical width for an ideal crystal. Such narrow reflections imply regions of perfect crystal which are many thousands of layers in depth.

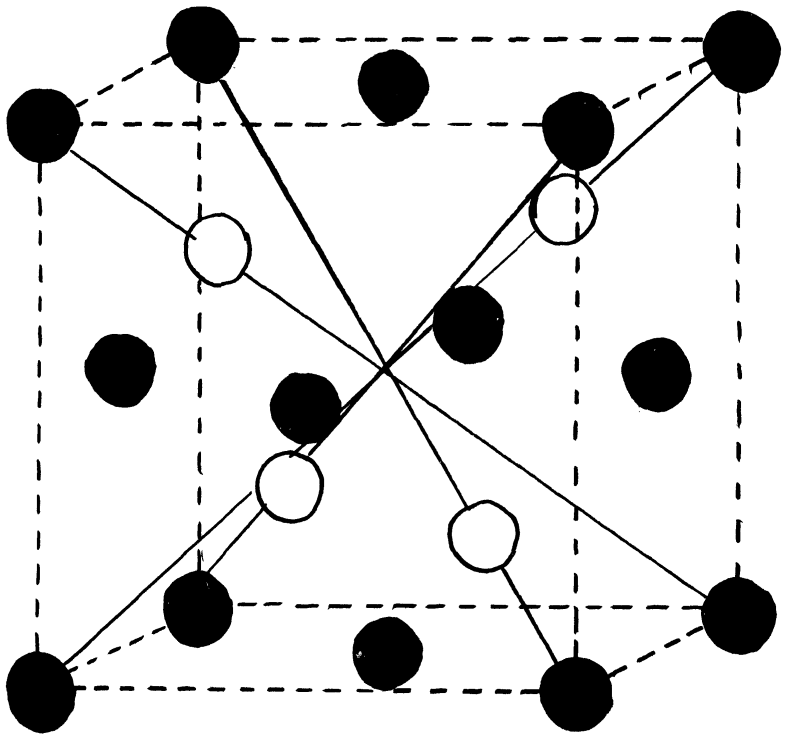

Fig. 1

THE BRAGG STRUCTURE FOR DIAMOND

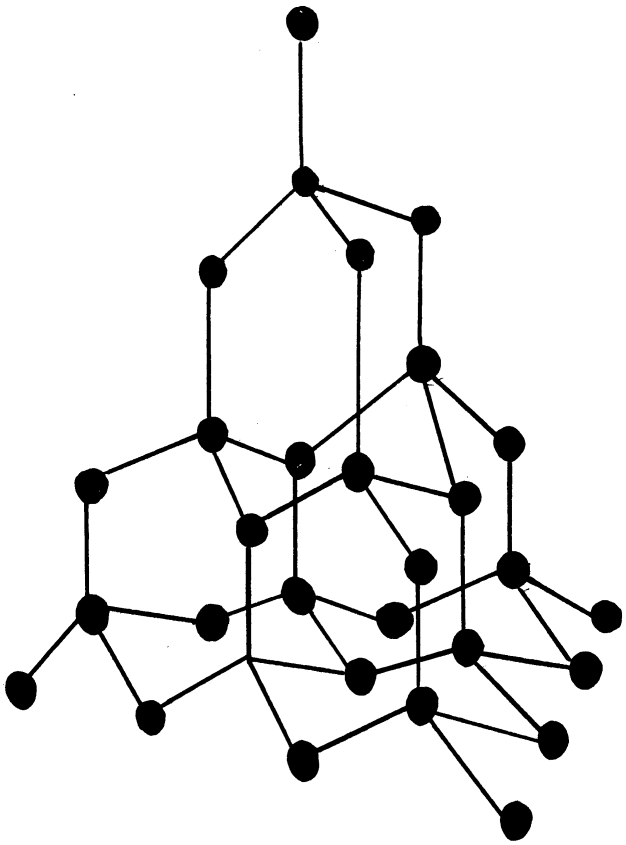

Fig. 2

COVALENT BONDS IN DIAMOND

In 1940, Raman and Nilakantan[2] found extra reflections on Laue photographs of diamond. They proposed a new theory for interpreting these reflections. Prior to 1940, the theory developed by Faxen[20] and Waller[21] based on Born's[15] lattice dynamics had proved adequate to explain diffuse spots associated with reflections. Diffuse spots are normally temperature sensitive and have a natural explanation in terms of thermally excited lattice vibrations. Raman and Nilakantan found that the extra streaks in diamond were relatively sharp and temperature insensitive. They were led to propose a completely new theory which was then applied to diamond and other substances. The arguments covering this new theory are in the literature.[9, 22] The majority of the workers in the field of X-ray diffraction are inclined to minimize the importance of Raman's theory, and, in fact, many consider it to be completely in error. In any event, Lonsdale[23] has shown that the extra streaks are separate and distinct from the thermal diffuse spots which are found in other crystals. She found that both thermal diffuse spots (primary extra reflections) and the extra streaks (secondary extra reflections) appear in the diffraction patterns of diamond. The diffuse spots occur in all diamond patterns, and they are temperature sensitive. The sharper extra streaks vary in intensity from diamond to diamond and are insensitive to temperature. In some diamonds no secondary extra reflections are detected.

Grenville-Wells[12] studied the occurrence of the extra streaks in a large collection of stones. The extra streaks

always appear at the same positions with roughly constant relative intensities. Hoerni and Wooster[24] have verified the work concerning the position of the streaks and have made a study of the intensity distribution within the streaks as well as the relative intensity of streaks. Their results are summarized in Table II. For those streaks studied (111, 220, 311, and 331) it is found that the extra streaks have an intensity distributed according to the relation $D \sim |F_{hkl}|^2 R^{-n}$ where D is the scattering density along the spike in reciprocal space corresponding to the extra streak, R is the distance from the corresponding reciprocal lattice point from which the spike extends, F_{hkl} is the structure amplitude of the reciprocal lattice point as determined by Brill[25] and $n = 2.2 \pm 0.1$ for the measured points. From the relative intensities it can be determined that when "h" has a given value, independent of the value of k and l, the quantity $D/|F_{hkl}|^2$ for a spike parallel to (100) always has the same value. Similar statements hold for "k" and "l" spikes parallel to (010) and (001) respectively. The results for the spikes extending from 111 are the only discrepancy in this overall picture. Hoerni and Wooster indicate that the F_{111} value obtained by Brill may be too high. According to Hoerni and Wooster, the relations between the indices h, k, l, and the intensity of the spikes determine certain features of a stratification parallel to the cube faces, and the inverse square law ($n \sim 2$) is to be expected if the stratification is subject to random variations.

Table 2

THE OCCURRENCE OF EXTRA STREAKS IN THE X-RAY DIFFRACTION PATTERN OF DIAMOND

Indices of Reciprocal Lattice Point	Zone Indices of Spike		
	(100)	(010)	(001)
111	87	87	87
220	76	76	absent
113	100	100	absent
222	75	75	75
004	5	5	30
331	7	7	104
224	72	72	30
115	present	present	absent
333	absent	absent	absent

Numbers indicate relative intensity.

[J. Hoerni and W. A. Wooster, Experientia 8, 297 (1952).]

Lonsdale[3] and Grenville-Wells[12, 26] have used the method of divergent beam X-ray photography to study the mosaic texture of diamonds. Before giving their results, we wish to make the following point. The term mosaic texture is employed throughout X-ray literature. While the term arises from the concept of perfect crystalline blocks which form a mosaic to make up a real crystal, the use of this picture of a real crystal is only a mathematical idealization. Structural defects will have definite effects on the X-ray pattern. For a theoretical treatment one is forced to approximate these defects by a mosaic of small perfect blocks. When the blocks are very large, the crystal may appear to be nearly perfect, i.e. exhibit narrow Bragg reflections, high extinction, and poor divergent beam photographs. When the blocks decrease in size the result is broadened Bragg reflections, decreased extinction, and improved divergent beam patterns. Finally, James[27] has pointed out that the width of Bragg reflections is not always correlated to the amount of extinction, "...there is no strict correlation between the breadth of the reflection curves and the amount of small scale irregularities. Some crystals with comparatively narrow reflection curves show quite small extinction." Consequently, in the following, it should be realized that the relative perfection of crystal as measured by X-ray techniques depends upon the technique used.

In the work on mosaic texture by Lonsdale and Grenville-Wells an attempt has been made to correlate the intensity of extra streaks with the extent of the mosaic texture. Their

results are not clean cut. While it is generally true that strong extra reflections occur in stones which are the least mosaic, the correlation is by no means universal. Grenville-Wells has found some rare diamonds which are not mosaic nor do they show extra streaks. Such diamonds are ideal from the X-ray standpoint. On the other hand, Grenville-Wells has increased the amount of mosaic structure by heat treatment and by bombardment without altering the intensity of the extra reflections. One must conclude that the occurrence of the extra streaks cannot be associated with lack of mosaic structure, in general, but that the specific anomalies of structure which cause the extra reflections usually do not occur in naturally mosaic diamonds. In addition, the structure defect responsible for the extra reflections is not seen as mosaic structure in the divergent beam technique.

The remaining experimental X-ray work has concerned the 222 reflection. This reflection is forbidden if the scattering at each lattice site is spherically symmetric. The 222 reflection occurs for all diamonds. However, the intensity of this reflection varies, and Grenville-Wells[12] finds that it occurs with greatest intensity in diamonds showing strong extra streaks. The occurrence of the 222 reflection is usually attributed to the tetrahedral distribution of the outer electrons in the valency bonds. Heidenreich[28] objects to this interpretation since the contribution of the valence electrons to scattering is rather small. However, Moffett and Coulson[29] have shown that the X-ray diffraction pattern is consistent with

localized electronic charge extending along the bond directions. The fact that the 222 reflection varies in intensity can be explained by alteration in the electronic distribution to increase the asphericity of scattering at lattice sites. It is clear that almost any distortion of the structure will produce such an effect at sites near the distortion.

Beyond qualitative statements, no interpretation of the secondary extra reflections is in existence. Born[30] wishes to ascribe the streaks to strain in the lattice, perhaps associated with displaced atoms. Lonsdale[23] is reticent to accept any such theory because of the small amount of mosaic structure present in many diamonds showing extra streaks.

We summarize the current status of X-ray data as follows: (1) Certain diamonds exhibit secondary extra reflections which indicate that the usual Bragg model is incomplete in some respect since no other crystal exhibits similar reflections. (2) There is some evidence that the extra streaks may be connected with stratification parallel to the cube faces occurring in a random manner. (3) The extra streaks most frequently occur in diamonds having no mosaic structure, but cases occur where mosaic diamonds show extra streaks and vice versa. (4) The 222 reflection is found to be stronger in diamonds showing extra streaks.

1.2 Ultraviolet and Visible

In the present problem we are concerned with the absorption and fluorescence spectra of diamonds in the range from

2000 A. U. to 6000 A. U. The spectrum of each diamond is essentially unique in that the absorption coefficients and emission intensities vary from diamond to diamond. We shall consider the following: (1) The ultraviolet transmission limit or cutoff, (2) Ultraviolet and visible absorption bands, (3) Fluorescence bands.

1.2.1 Ultraviolet Cutoff

Robertson, Fox, and Martin[1] showed that while some diamonds transmit to wavelengths as short as 2250 A. U. with total absorption at shorter wavelengths, many diamonds will transmit no wavelengths shorter than 3100 A. U. Ramanthan[4] discovered that diamonds are not divided into two definite classes by the positions of their ultraviolet cutoffs. He found that the position of cutoff may fall at any point between the limits of 2250 A. U. and 3100 A. U, (see Figure 3 and Figure 4). Blackwell[11] measured the position of cutoff for over one hundred stones. He was able to correlate the position of cutoff with infrared band intensities. We shall discuss these correlations in the infrared section.

At the time Raman and Nilakantan[2] published their first observation of the secondary extra X-ray spots, they also noted that those diamonds which transmit to 2250 A. U. show no extra spots. More recently, Grenville-Wells[12] has made a correlation between the occurrence of the secondary extra spots and the position of the ultraviolet cutoff. The correlation is necessarily qualitative since the extra spot intensities were judged on a qualitative basis. Nevertheless, the

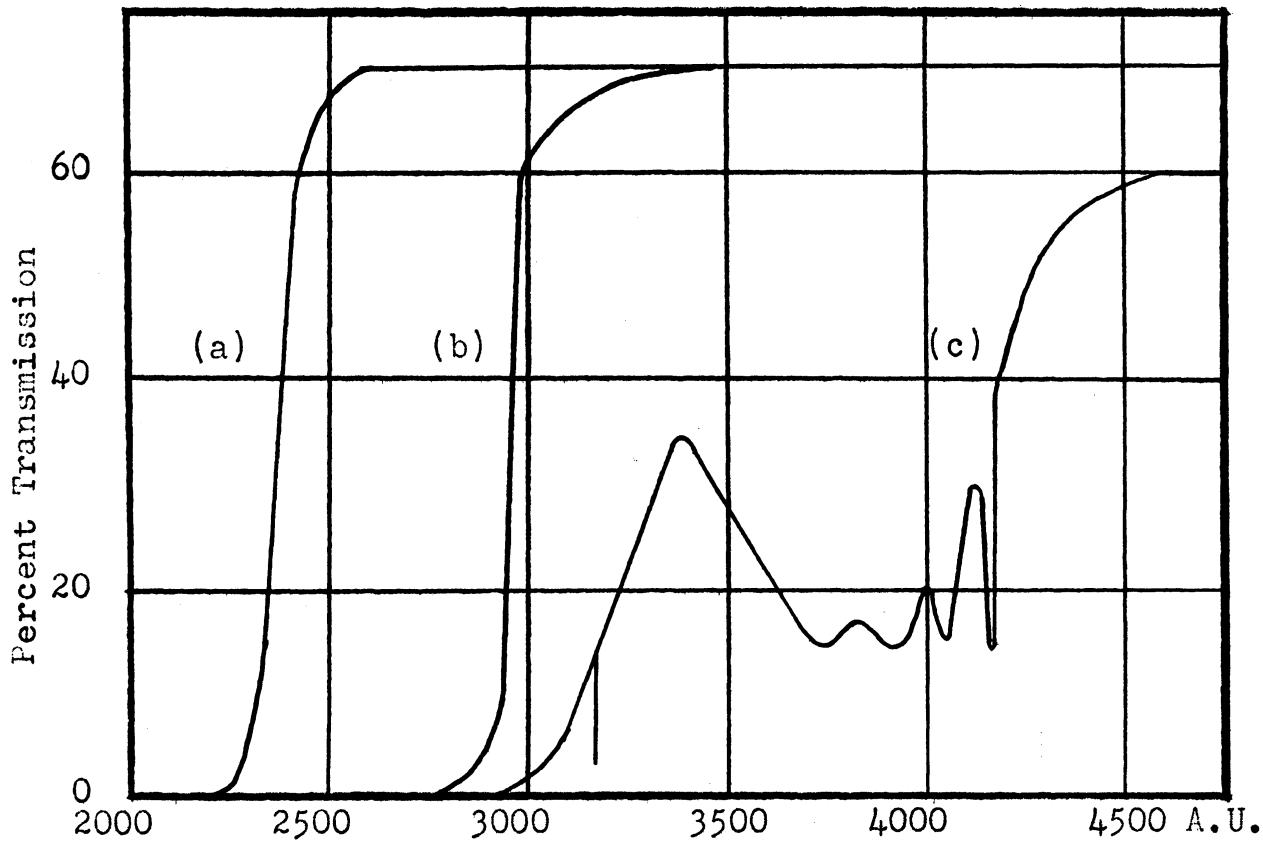

(a) BP-2 (UV II) ; (b) M-4 (Weak UV I); (c) SLF 127 (Medium UV I)

Fig. 3

ULTRAVIOLET AND VISIBLE ABSORPTION SPECTRA OF DIAMONDS

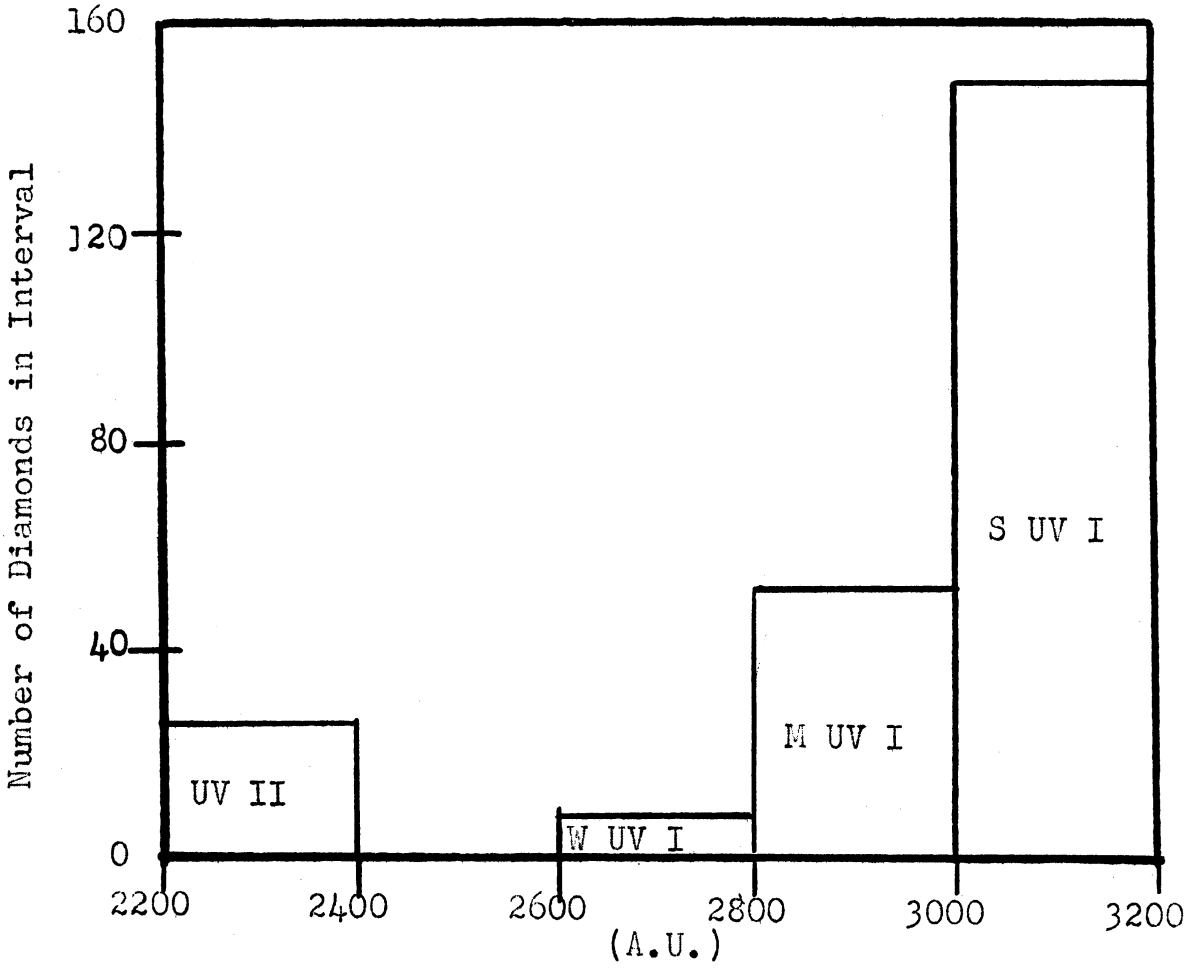

Fig. 4

THE FREQUENCY OF OCCURRENCE OF UV CUTOFF

IN VARIOUS WAVELENGTH INTERVALS

results generally confirm the original statement by Raman and Nilakantan. However, there are some exceptions to the correlation of ultraviolet transmission and absence of extra spots. In particular, extra spots have been found in some UV II stones, whereas some medium UV I stones have no detectable extra spots.

Various experiments[10, 3] have shown that many diamonds are not uniform in their ultraviolet transmission properties. Certain regions of a given diamond may be transparent to the 2537 A. U. mercury line while other areas may be opaque to this wavelength. With this fact established, it becomes possible to explain cases in which ultraviolet absorption above 2250 A. U. is measured in stones which show no extra spots. X-ray techniques utilize a relatively small volume of crystal, while standard ultraviolet absorption measurements utilize a larger volume. Consequently, transparent regions with no extra spots may be "seen" by X-rays, but masked by surrounding regions in ultraviolet absorption measurements. On the other hand, the occurrence of extra spots for ultraviolet transparent diamonds would appear to be a real exception to the usual correlation.

An interesting result of the discovery that large diamonds are often non-uniform is that a large collection of small, perfect octahedra assembled by Grenville-Wells[26] contains a larger proportion of ultraviolet transparent diamonds than any similar collection hitherto reported. Grenville-Wells explains this result as a direct consequence of the fact that small crystals are less likely than are

large crystals to contain regions of varying properties. The existence of such a collection also tends to disprove the statement, often made,[1, 10] that UV II and IR II diamonds are externally imperfect, although the statement is surely true for large diamonds.

1.2.2 Ultraviolet and Visible Absorption Bands

Table 3 lists all of the known lines and bands commonly found in diamonds in the absorption spectrum from 2250 A. U. to 6000 A. U.[10] We are not concerned with all of these lines but list them for completeness. The lines between 2300 A. U. and 3208 A. U. are, of course, only observed in diamonds whose cutoffs occur at some shorter wavelength than that of the line involved. The lines between 3034 and 3208 A. U. appear with constant relative intensities. However, their absorption coefficients vary from diamond to diamond. The strongest line in this group is at 3157 A. U. In a large collection of diamonds ranging from UV II to strong UV I, Blackwell found that the intensity of the 3157 A. U. line could be correlated with the position of cutoff. As the cutoff moves towards short wavelengths, the intensity of the 3157 A. U. line (and the intensity of each line associated with it) decreases.

The 4155 A. U. line has several diffuse maxima at shorter wavelengths associated with it. The group is shown in Figure 5a as a plot of cm^{-1} displacement from the 4155 A. U. line. The diffuse maxima follow the 4155 A. U. line in intensity. Blackwell has measured the intensity of the 4155 A. U. line in many diamonds. He finds there is no correlation

Table 3

PRINCIPAL LINES AND BANDS OBSERVED IN THE ULTRAVIOLET AND VISIBLE SPECTRUM OF DIAMOND

Wavelength in Angstroms	Intensity	Wavelength in Angstroms	Intensity
2359	VS	4041	
2364	VS	3951	Maxima of Diffuse Region of Medium Intensity
2399	S	3847	
Weak lines sometimes occur between 2400 and 3000		3766	
		4155	S
3034	W	4200	VW
3068	W	4400	W
3157	S	4530	W
3181	W	4647	W
3208	W	4770	S

Blackwell's Data

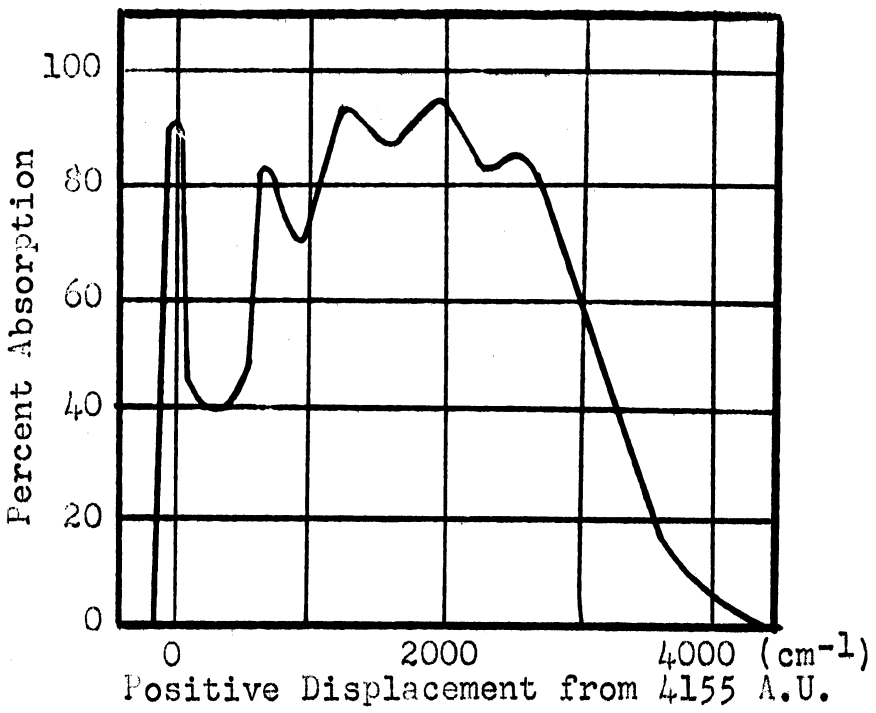

(a)

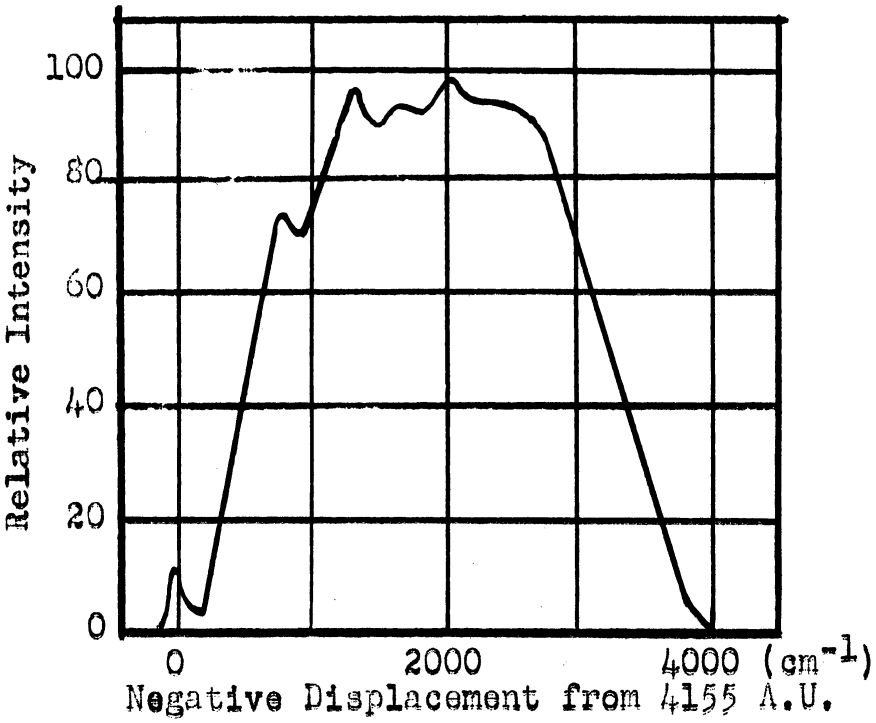

(b)

Fig. 5

(a) ABSORPTION NEAR 4155 A.U. IN DIAMOND

(b) FLUORESCENCE NEAR 4155 A.U. IN DIAMOND

between the absorption coefficients of the lines at 4155 A. U. and 3157 A. U. Because of the correlation between the position of UV cutoff and the intensity of the 3157 A. U. line, it follows that there is no correlation between the position of cutoff and the intensity of the 4155 A. U. line. By "no correlation" we mean that while the 4155 A. U. line does not occur in UV II diamonds, it may appear with variable intensity in UV I diamonds having the same cutoff.

1.2.3 Fluorescence Bands

There are several colors of fluorescence which occur in diamonds.[10] We are concerned with the most commonly observed fluorescence, which is blue. When diamonds are irradiated with radiation of wavelength shorter than 4155 A. U., while many are non-fluorescent, many others fluoresce blue with varying intensities. The spectrum of the blue fluorescence consists of a sharp line at 4155 A. U. together with a group of diffuse maxima at longer wavelengths. This spectrum is shown in Figure 5b as displacement in cm^{-1} from the line at 4155 A. U. When this spectrum is compared to the similar blue absorption bands, Figure 5a, it is found that, although the maxima are displaced in opposite directions from 4155 A. U., the structure of the diffuse bands is similar for absorption and emission.

Blackwell has visually estimated the intensity of the blue fluorescence for many diamonds. He has also measured the intensity of the 4155 A. U. fluorescence line in some of these stones. He finds that (1) the relative intensity of the 4155 A. U. line and the diffuse bands is not constant

from diamond to diamond. The 4155 A. U. line may be absent or very strong for a given intensity of the diffuse group. (2) The intensity of the fluorescence line at 4155 A. U. does not follow the intensity of the absorption line at 4155 A. U. The only established correlation between the blue emission and absorption is that blue fluorescence never occurs in stones which show no blue absorption. The converse statement does not hold. (3) Blue fluorescent stones tend to cutoff at wavelengths below 3100 A. U. whereas most non-fluorescent UV I diamonds cutoff near 3200 A. U.

Mani[32] has shown that blue fluorescence increases in intensity at low temperatures. It is found that all of the spectrum near 4155 A. U. becomes sharper and more intense at liquid air temperatures.

1.3 Infrared Absorption

Robertson, Fox, and Martin[1] were the first to show that diamonds are not all alike in the intensity of absorption at 8μ. They classified diamonds as either absorbers or non-absorbers in the 8μ region of the spectrum. Four typical infrared spectra found in diamonds are shown in Figure 6. The spectrum is seen to consist of a group of bands near 5μ, which appears in all diamonds, plus a group of bands near 8μ which can either appear or be absent. Sutherland and Willis[5] showed that the absorption coefficients of all the bands at wavelengths shorter than 6μ are constant for all diamonds while the absorption coefficients of the bands at

wavelengths longer than 6μ vary from zero to values larger than the coefficients for the short wavelength bands. In addition, they showed that the relative intensities of the long wavelength bands, when they occur, vary significantly.

Blackwell[10] has made an important contribution to the infrared absorption data. All of his measurements on ultraviolet and visible absorption, fluorescence, and other properties have been related to the corresponding infrared effects. Blackwell's results on properties other than infrared absorption have been discussed. In the infrared, Blackwell found several general spectral features and a group of anomalous bands. In most cases, the anomalous bands appear in diamonds of unusual color or crystal habit. We shall omit reference to these bands since they are deemed extraneous. In Table 4 are listed all of the principal infrared bands as located by Blackwell. The bands at wavelengths longer than 6μ have been divided into Group A (Blackwell's Group I) (7.8, 8.3, 9.2, 12.8μ) and Group B (Blackwell's Group II) (7.0, 7.3, 7.5, 8.5, 10.0) for the following reason: It was found that the bands in Group A follow one another in intensity and the bands in Group B follow one another in intensity. That is, Group A band intensities correlate and Group B band intensities correlate. However, there is, in general, no correlation of intensities between bands of Group A and Group B. Group B is also unique in that the 7.0, 7.3, and 7.5 bands are quite narrow while all other bands in both groups are quite broad (see Figure 6). Although the intensities of the Groups are not correlated,

Table 4

MAXIMA OF INFRARED ABSORPTION BANDS IN THE SPECTRA OF DIAMONDS

Wave-length (Microns)	Frequency (Wave-numbers)	Inten-sity	Wave-length (Microns)	Frequency (Wave-numbers)	Inten-sity
2.8	3570	W	7.51 (B)	1332	VW
3.2	3125	W	7.80 (A)	1282	S
4.03	2480	M	8.31 (A)	1203	S
4.59	2180	S	8.54 (B)	1171	W
4.98	2008	S	9.15 (A)	1093	M
7.01 (B)	1426	VW	9.97 (B)	1003	W
7.29 (B)	1372	W	12.8 (?)	784	VW

Blackwell's Data

pend on the integrated intensity of the emitted light. Consequently, the effects are determined principally by the diffuse bands near 4155 A. U. rather than the intensity of the 4155 A. U. line itself. Therefore, although it is found that the intensity of the line at 4155 A. U. cannot be correlated with any of the other spectral features, correlations with overall "blue fluorescence" are not precluded. Blackwell finds that blue fluorescence never occurs in the absence of blue absorption. This implies that Group B infrared absorption also occurs in blue fluorescent diamonds. This point is verified experimentally. In addition, it is found that, relative to bands in non-fluorescent diamonds which have Group B absorption, blue fluorescent diamonds have strong Group B absorption and weak Group A absorption. Finally, Blackwell finds that, while, in general, there is no correlation between Group A and Group B band intensities, the "blue fluorescent" diamonds form a special class for which the intensities of the two groups are correlated in the sense that their absorption coefficients follow one another in magnitude.

The final correlation of importance is between infrared absorption and X-ray extra spots. Unfortunately, very few data are available on this point. Original work by Raman and Nilakantan[2] and a small amount of work by Blackwell[10] confirm the fact that extra spots occur in diamonds having absorption at 8μ. This fact can be inferred from the previously mentioned qualitative correlation between extra spot intensity and position of ultraviolet cutoff. However, the

work is not sufficiently quantitative to determine the correlation between extra spot intensity and a particular group of bands in the infrared.

When diamonds are heated to 400° C, the only detectable change in the infrared spectrum is a decrease in the intensity of the 7.29μ (Group B) band by a factor of 2/3,[10] This band also shifts to longer wavelengths as the temperature increases by a factor of 1 cm^{-1} /50° C. Heating to 1700° C did not introduce any change in the room temperature infrared spectrum in specimens examined by Blackwell.

1.4 Other Properties

Several other physical properties of diamond are known which exhibit anomalies similar in some ways to those already described. These will now be briefly discussed together with some important properties which show no anomalies. The latter are the Raman scattering spectrum and the density. We shall deal with them first.

1.4.1 Raman Effect

All diamonds show a strong, narrow, weakly polarized Raman line at 1332 cm^{-1}.[10, 33] After many studies, it is well-established that there is no effective change in this line from diamond to diamond. The line moves to lower frequencies as the temperature increases. Its displacement with temperature is approximately the same as noted for the 7.29μ band in absorption.[34]

For certain large, ultraviolet transparent diamonds, Krishman[35] has succeeded in recording a weak set of Raman

bands extending to an upper frequency limit of 2665 cm^{-1}. Figure 26 shows this group of bands. The 2537 A. U. line of mercury is the only exciting line which is sufficiently intense to scatter this set of bands with enough energy to record. Consequently, no UV I diamonds have been studied. It is generally assumed that the second order Raman scattering is the same for all diamonds.

1.4.2 Density

The most accurate measurements of density have been made by Tu[36] and by Bearden.[37] Their average results are 3.5142 and 3.51536 ± .00004 g/cc at 23.5° C respectively. No such accurate methods have been employed in attempts to find density variations between diamonds.[1, 10] No significant density variations have been found.

1.4.3 Color, Crystal Habit, and External Crystal Perfection

The three properties listed are variable between diamonds. Blackwell[10] has studied the variation of these properties and has attempted to correlate them with spectroscopic properties. There appears to be no new information to gain from introducing the highly involved relationships found in this phase of Blackwell's work. We have already mentioned that Grenville-Wells[12] assembled a collection of externally perfect, colorless octahedra. The full range of X-ray and spectroscopic anomalies is shown by her collection. Consequently, the variables of color, crystal habit, and perfection appear to be extraneous to our work.

However, since some color changes have occurred in experiments performed in the present study, it is pertinent

to mention that Blackwell found that blue diamonds are invariably IR II, brown are either IR II or weak IR I, and green diamonds are strong IR I.

1.4.4 Birefringence

From its cubic symmetry, the diamond lattice is expected to be isotropic. However, many diamonds exhibit patterns of birefringence when viewed between crossed polarizers.[1] The birefringence may be due either to strain introduced through external distortion or to lattice imperfections. Since both factors may be in operation, and since only strain due to imperfections is of interest, the results are difficult to interpret.[38] In favorable cases, Raman and Jayaraman have shown that sometimes there is similarity between patterns of birefringence and patterns of fluoresence. One deduces that both effects arise from a common lattice imperfection. In general, the results from the study of birefringence cannot be interpreted in such a way as to give concrete information as to the origin of anomalies in diamond properties.

The Indian school[39] has placed considerable stress on the laminae seen in certain birefringence patterns. The laminae occur parallel to octahedral and dodecahedral planes. According to Raman's theory for diamond,[8] which we will discuss in a later section, the laminae occur at the boundaries between regions of differing local electronic configuration.

1.4.5 Photoconductivity

Diamonds, which are normally good insulators, sometimes become conductive when exposed to ultraviolet light.[1] It is

found that the photoconductivity of UV II diamonds is as much as ten times the photoconductivity of UV I diamonds.

1.4.6 Impurities

All diamonds contain detectable amounts of chemical impurities. Chesley[40] made qualitative spectrographic analyses of thirty-three diamonds, listing their ultraviolet absorption properties as well. He found no correlation between the type of impurity and the position of the ultraviolet transmission limit. Table 5 lists the common impurities.

Straumanis[18] lists the impurities found in two diamonds used for X-ray work. The impurities are shown in Table 5. From his X-ray results and the density measurements of Tu[36] and Bearden,[37] Straumanis concludes that his diamonds are essentially perfect with respect to spacing, vacant sites, and interstitial atoms. However, his measure of perfection depends upon atomic weight and density data which is necessarily less accurate than spectroscopic or X-ray data.

1.5 Summary

From our review of previous experimental results we can draw certain conclusions about the correlations between anomalous properties. We assume that the exceptions to correlations which sometimes occur can be neglected. On this basis, we can state that whenever a diamond differs from ideal UV II, X II, IR II the following phenomena will occur, the occurrence of one inferring the occurrence of the others:

Table 5

IMPURITIES FOUND IN DIAMOND

Impurity (a)	Diamond 1	Diamond 2	Impurity (b)	Occurrence
Al	3	3	Al	A
B	1	-	Ba	S
Ca	1	4	Ca	A
Co	2	-	Cr	S
Hf	-	1	Cu	S
Fe	?	1	Fe	S
Pb	?	?	Pb	S
Mg	4	2	Mg	S
Mn	-	-	Na	S
Pt	-	1	-	-
Si	4	2	Si	A
Ag	-	2	Ag	S
Sn	-	-	Sr	S
Ti	2	3	Ti	S
Zn	2	-	-	-

(a) M. E. Straumanis and E. Z. Aka, J.A.C.S., 73, 5643 (1951).

(b) F. G. Chesley, Amer. Min., 27, 20 (1942).

4 Major contaminant

1 Faint trace

A: Occurs in all diamonds tested

S: Occurs only in some diamonds

Class I: (1) X-ray streaks

(2) Ultraviolet cutoff at wavelengths greater than 2500 A U.

(3) Group A absorption in the infrared

(4) Absorption at 3157 A. U.

These Class I properties are correlated in the sense that the magnitudes of the effects are proportional, i. e. as the intensities of effects (1), (3), and (4) increase, the ultraviolet cutoff moves towards longer wavelengths.

In some of the diamonds displaying Class I properties, another group of phenomena occurs:

Class II: (1) Absorption at and near 4155 A. U.

(2) Group B absorption in the infrared

These Class II properties are correlated in the sense that the absorption coefficient at 4155 A. U. is proportional to the Group B absorption coefficients.

Finally, in some diamonds displaying both Class I and Class II properties, a third group of phenomena occurs:

Class III: (1) Diffuse fluorescence near 4155 A. U.

(2) Group A absorption coefficients proportional to Group B absorption coefficients

(3) Group B stronger with respect to Group A than in non-class III diamonds.

In this class, the correlations are not so clean-cut. The listing of properties is meant to convey that the presence of strong blue fluoresence seems to introduce a regularity between the effects of Class I and Class II, i. e. the normally independent intensities of Group A and Group B are now correlated.

Chapter 2

PRESENT EXPERIMENTAL WORK

2.1 Apparatus

(2.1.1 Near Infrared)
(2.1.2 Far Infrared)
(2.1.3 Vacuum Ultraviolet)
(2.1.4 Ultraviolet Transmission)

2.1.1 Near Infrared

SPECTROMETERS: Commercial spectrometers were used to obtain spectra in the range from 2 to 33μ. These spectrometers are made by the Perkin-Elmer Corporation of Norwalk, Connecticut. Because the Perkin-Elmer spectrometers have been fully described elsewhere, we shall mention only the general features of the instruments.

The Model 21[41] is a double-beam recording spectrometer equipped with a sodium chloride prism. This instrument records percent transmission versus wavelength from one to fifteen microns. In regular use, a sample 10 by 25 mm is required to cover the area of the energy beam. An adapter makes it possible to use samples as small as 2 by 15 mm. Smaller samples cover only part of the entrance slit and consequently reduce the energy at the thermocouple.

The Model 12C[42] is a single-beam recording spectrometer in which give different prisms (LiF, CaF_2, NaCl, CsBr, KRS-5) may be used. With these prisms the wavelength interval from one to 35 microns can be covered with resolution of the order of two wavenumbers. Sample size requirements for the 12C are the same as those for the 21.

The Model 112[43] is a single-beam recording spectrometer which is a modified version of the 12C. The modification consists of the introduction of the Walsh[44] optical system. This system causes the radiation to be sent through the prism four times instead of twice (Littrow system monochromator). The effect of the alteration is to increase the resolving power of the spectrometer. In addition, since the radiation is chopped after it has been dispersed the effect of scattered radiation is greatly reduced. Scattered radiation beyond 25μ makes the 12C spectrometer very unreliable. For example, at 25μ, 25 percent of the energy detected by the thermocouple is due to scattered radiation. In the 112 instrument less than 2 percent of the energy at 25μ is due to scattered radiation.

REFLECTING MICROSCOPE: It has been noted that the spectrometers used in this work require samples at least 2 x 15 mm for optimum performance. A sample smaller than this will cover only part of the length of entrance slit. With such a sample, only part of the beam enters the spectrometer. In order to bring the amount of energy at the thermocouple up to the minimum (determined by the sensitivity of the thermocouple and the gain of the amplifier) which is

needed for recording spectra it is necessary to increase the slit width. The spectra obtained under such conditions will show less resolution. The sample size which can be used is determined, therefore, by the resolution required. Since many of the diamonds used in this work will cover only a small fraction of the slit length, and also because there is interest in the spectra of individual portions of diamonds, a reflecting microscope has been used.

The microscope used is one constructed by D. L. Wood.[45] In Figure 7 is shown a schematic drawing of the microscope and its relation to the monochromator. In all of the present work the monochromator and auxiliary equipment have been those of the 12C spectrometer.

The microscope design is based on the theory of Schwartzchild[46] as applied by Burch.[47] Its advantage over a refracting microscope is the fact that its properties are achromatic. Because of the obstruction of the beam by the small convex mirror and the hole in the large convex mirror, approximately 45% of the numberical aperture is lost when both the large concave and the small convex mirrors are spherical. Wood[48] ground his large spheres sufficiently aspherical to reduce the obstruction to 14% of the numerical aperture. The effective focal length of the system is 0.30 cm. The numerical aperture, not corrected for obstruction, is 0.75. Since the numerical aperture of the Model 12C monochromator is 0.12, the magnification for optimum operation is 0.75/0.12 or about 6. Wood's system is not limited to this magnification, since for a range of magnification

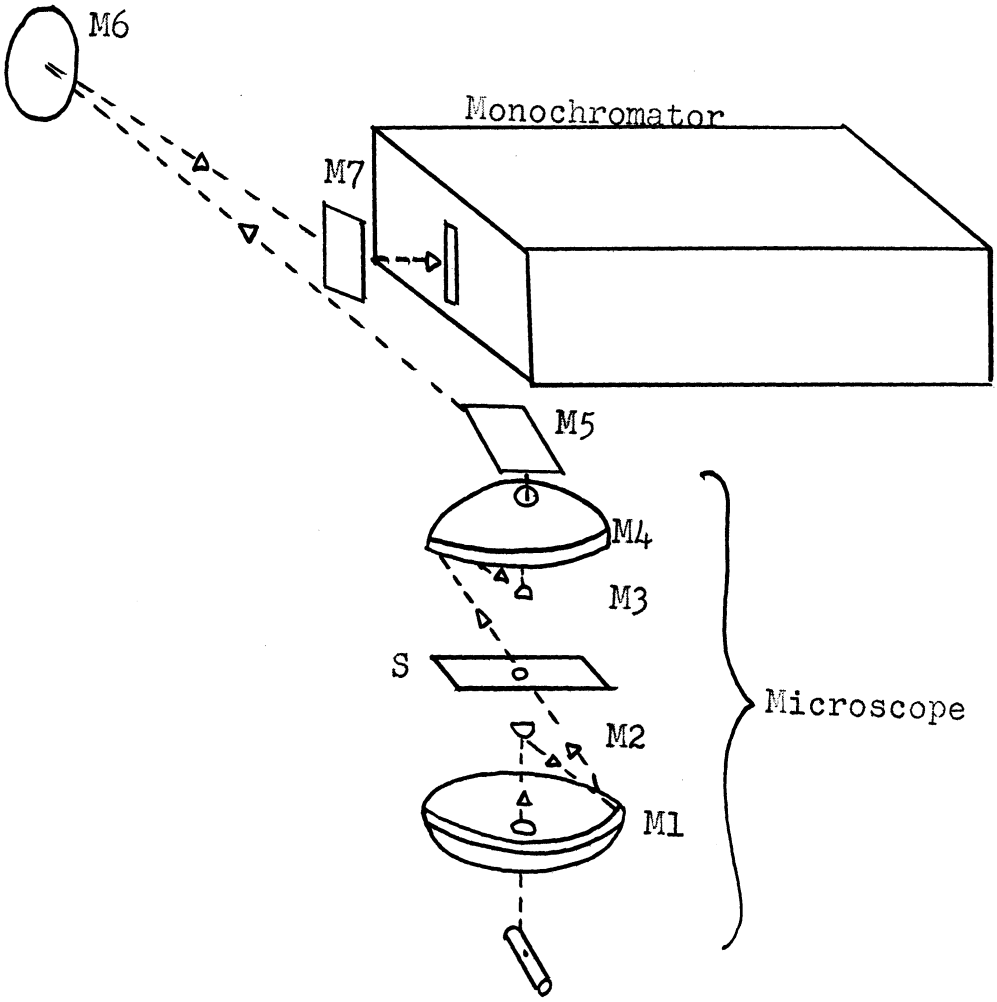

Fig. 7

REFLECTING MICROSCOPE

mirror M_6 can be adjusted so that the collimator of the spectrometer is filled. In practice, with a field as small as 100 by 300μ, the microscope makes it possible to record spectra using slit widths about twice the widths used in "macro" operation.

The limitations of the reflecting microscope are (1) Resolution is reduced by a factor of two from "macro" operation. (2) Opening the slit of the monochromator beyond the width of the image of the source on the slit (0.6 mm) will produce no gain in energy. At long wavelengths (beyond 15μ) where "macro" slit widths are greater than 0.3 mm, the microscope cannot be used.

2.1.2 Far Infrared

To measure spectral absorption from 30 to 100μ (330 to 100 cm^{-1}) a vacuum grating instrument has been used. This instrument was constructed by Randall and coworkers and has been described elsewhere.[49] The basic elements of the spectrometer are (1) an incandescent chromel metal strip which supplies the energy, (2) an off-axis parabola, (3) a plane grating, (4) a reststrahlen plate, (5) a thermocouple detector, (6) a galvanometer amplifier, (7) a tuned electronic amplifier (13 seconds / cycle), and (8) a recording potentiometer. The reststrahlen plate and the grating are changed from one wavelength interval to the next. In obtaining spectra from 30 to 100μ one is required to alter the grating-reststrahlen combination at least four times,

i. e. four separate runs are necessary for each sample. One is seriously limited by the small amount of energy available. For satisfactory results a sample must cover most of the exit slit. The minimum sample dimensions are about 30 x 5 mm.

2.1.3 Vacuum Ultraviolet

In the current work some measurements have been made of spectral absorption in the region from 1200 to 2000 A. U. The instrument used is a Cario-Schmidt-Ott vacuum fluorite spectrograph, which has been described elsewhere.[50] A schematic diagram is shown in Figure 8. The instrument's characteristics are below the Figure. The recorded spectrum, (Hilger Q1 Special plates were used), extends from about 1200 A. U to the red of the visible with dispersion decreasing rapidly at wavelengths longer than 2000 A. U. Atmospheric absorption below 2000 A. U. can be effectively eliminated by pumping continuously with a Welsh Duoseal vacuum pump.

A hydrogen discharge lamp served as a source of continuous radiation. A drawing of the lamp with its accompanying apparatus is shown in Figure 9. In operation, the discharge tube and the lower halves of the tubes enclosing the aluminum electrodes are immersed in a tank of water. Hydrogen gas, from a cylinder, brought to atmospheric pressure by a mercury bubbler, is pulled through a capillary tube into the discharge tube. The pumping rate and the dimensions of the capillary regulated the rate of gas flow into the discharge tube and hence the pressure within the discharge

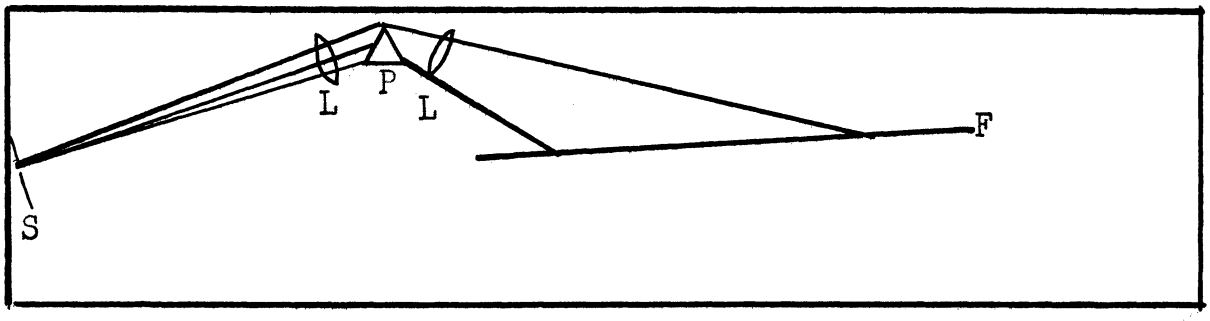

S : Entrance Slit ; L : Fluorite Lenses

P : Fluorite Prism; F : Plate Holder

Scale: $\frac{1}{2}$ size ; Focal Length: 10 cm ; Speed: f/12

Plate Factor: 6 A.U. at 1250 A.U.

Fig. 8

CARIO-SCHMIDT-OTT SPECTROGRAPH

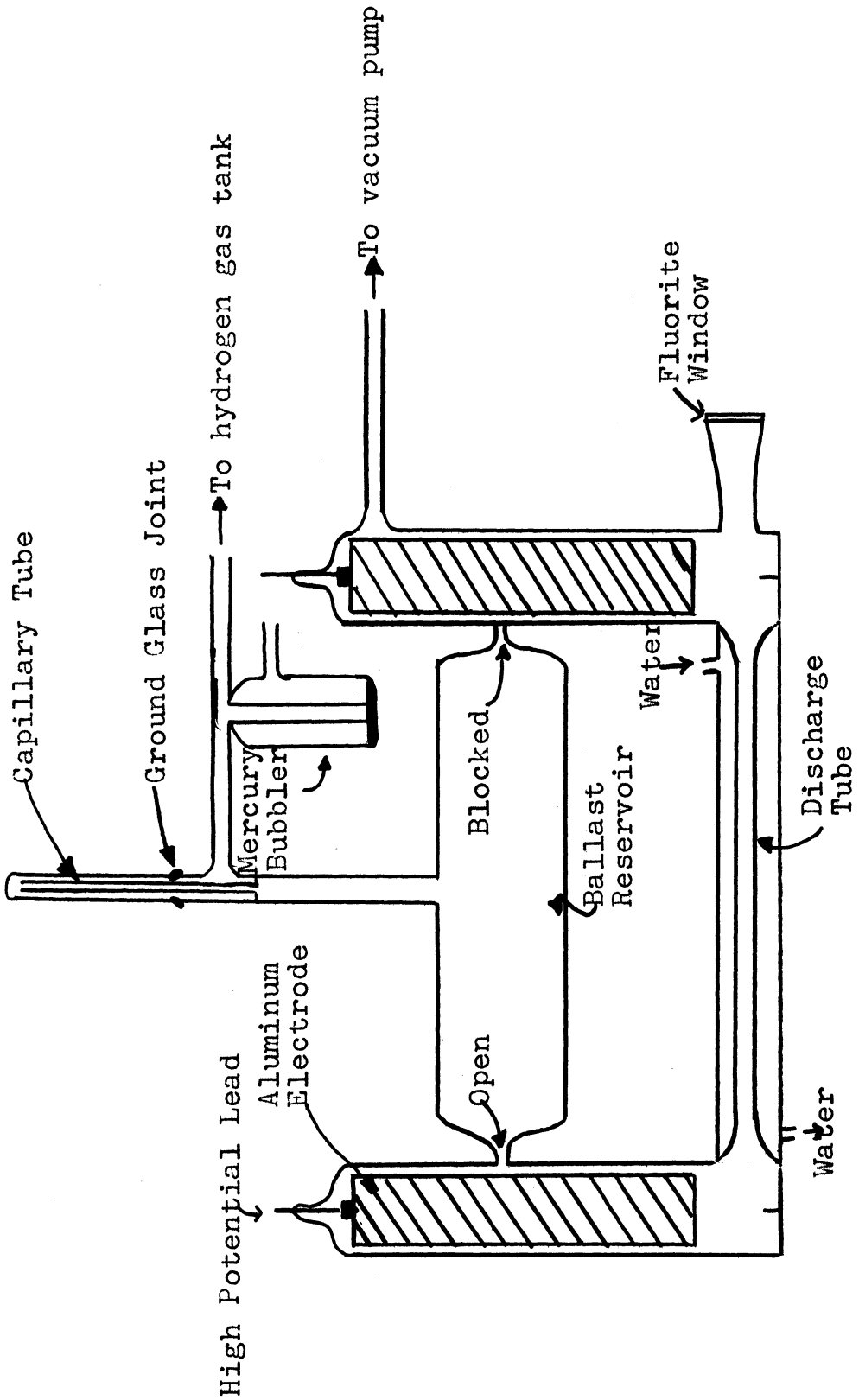

Fig. 9

HYDROGEN DISCHARGE LAMP

tube. The glass tube covering the capillary is seated on a ground glass joint and can be removed to adjust the length of the capillary by breaking off small sections. By proper regulation, a discharge of any desired character can be produced. The lamp has been operated at approximately 200 volt amperes, the hydrogen continuum can be recorded in a few seconds.

For the present work no accurate calibration has been necessary. Lines in the hydrogen spectrum, the Schumann Runge bands of oxygen, and mercury vapor lines provided reference points for estimating wavelengths. Scattered light is serious at short wavelengths and accounts for roughly 10% of the observed intensity at 1500 A. U.[51]

2.1.4 Ultraviolet Transmission

A technique has been developed for examining the variation in the transmission of ultraviolet light in a diamond. The apparatus is shown in Figure 10. The grating monochromator is a standard commercial instrument made by Bauch and Lomb. With a mercury vapor lamp as a source, monochromatic light is available at the exit slit. This light is reflected through a diamond mounted in a holder. An enlarged image of the diamond produced by a quartz lens, is formed at the focal plane of a camera. This image can be recorded photographically or observed visually by means of a plate covered with anthracene crystals which fluoresce in ultraviolet light. Aberrations in the system and scattering of the light make it necessary to use diamonds

which have flat sides. For less uniform stones, a contact print of the transmission pattern can be obtained by placing the sample directly on the photographic plate. Incident monochromatic light then produces an unmagnified pattern which can be enlarged photographically.

2.2 Account of Experimental Work Performed

(2.2.1 The Near Infrared Spectrum of Diamond)
(2.2.2 The Far Infrared Spectrum of Diamond)
(2.2.3 Infrared Spectra of Powdered Solids)
(2.2.4 The Infrared Spectrum of Germanium)
(2.2.5 The Ultraviolet Absorption of Adamantane)
(2.2.6 The Absorption of Diamond in the Vacuum Ultraviolet)
(2.2.7 Bombardment Experiments

2.2.1 The Near Infrared Spectrum of Diamond

6.5 BAND: Twenty diamonds in the present collection were large enough to permit use of the double-beam spectrometer to record absorption spectra from one to 15μ. These diamonds included 1 IR II, 3 W IR I, 2 M IR I, and 17 S IR I. Fourteen of the diamonds (1 M, 13 S IR I) showed a weak band near 6.5μ. This band has not been reported by other investigators. The reason for its detection in the present work lies in the fact that the double-beam instrument automatically compensates for the intense water vapor absorption between 6 and 7μ. In previous work, single-beam spectrometers were used, and observations between 6 and 7μ were difficult, especially for the detection of weak bands. When the 6.5μ band is strong enough for accurate observation, it appears as a doublet with maxima at 6.48μ (1540 cm^{-1}) and 6.57μ (1520 cm^{-1}). In Figure 11 the spectra of two strong IR I diamonds are shown

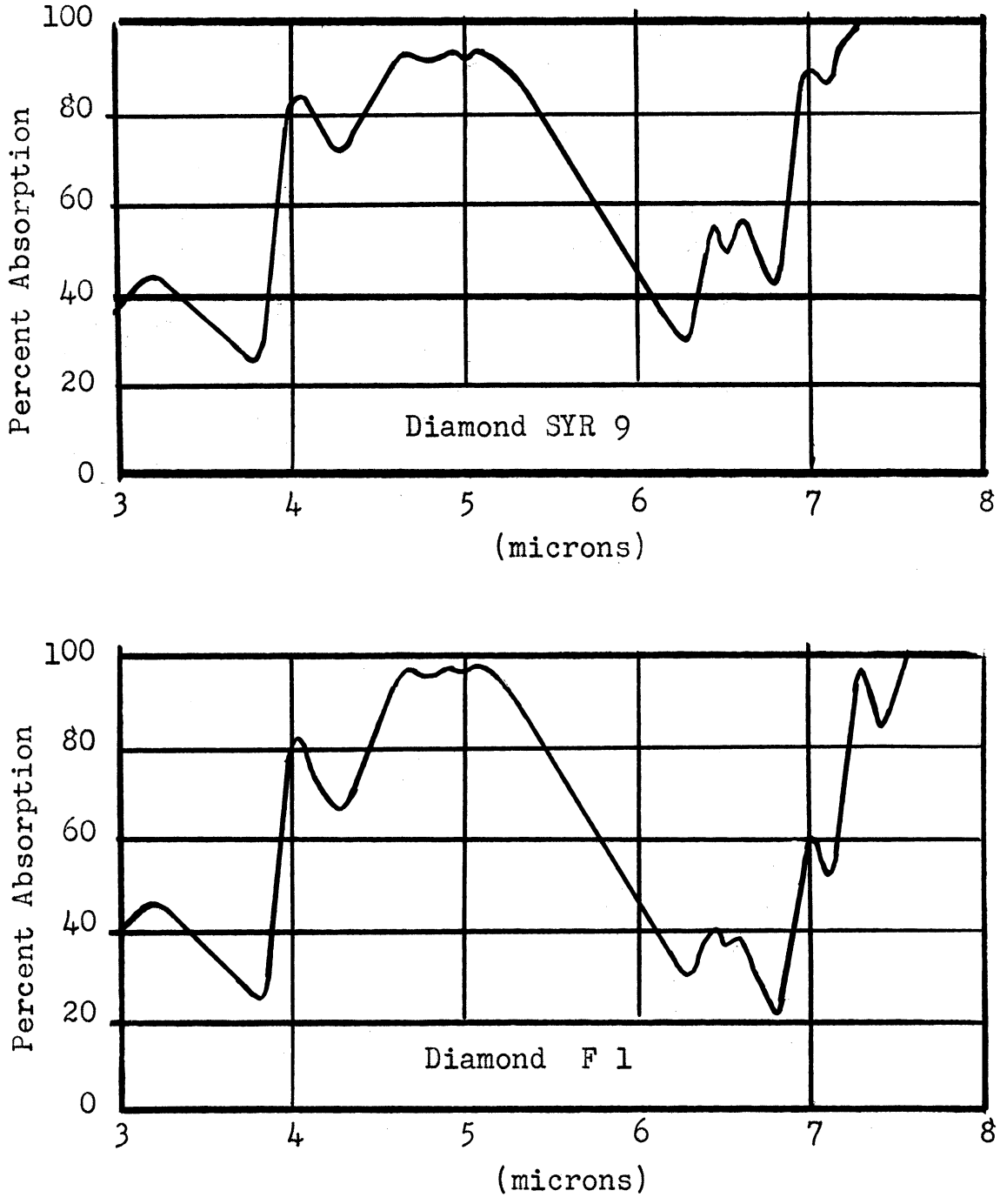

Fig. 11

TWO SPECTRA SHOWING THE 6.5 MICRON BAND

in which the 6.5μ band is relatively strong. This band does not appear in the IR II diamond or the weak IR I diamonds. Its intensity in IR I diamonds does not appear to be correlated with either Blackwell's Group A or Group B. In Table 6 the absorption coefficient for the 6.5μ band is given for the diamonds examined. We define the absorption coefficient (here, and in the following section) as k in the expression $I/I_o = 10^{-kt}$, where $I/I_o \cdot 100$ is the measured percent transmission, and t is the sample thickness in centimeters. We attribute the lack of correlation between 6.5μ and other IR I bands to two sources: (1) The band is weak and difficult to observe with accuracy. (2) The absorption at 6.5μ due to the long wavelength portion of the 5μ band and the short wavelength side of Group B bands. These contributions to the absorption at 6.5μ introduce errors in intensity of absorption assigned to the band.

BAND INTENSITY MEASUREMENTS: Unless scattering of the light occurs, due to imperfect surfaces, the percentage of incident light transmitted by all diamonds is constant from 1 to 2.5μ. The loss of energy in this wavelength interval is due to reflection. In addition, as Blackwell[10] has shown, the intensity of absorption in the near infrared spectra of diamonds is never sufficient to alter the reflection coefficient at absorption bands by a significant amount. Since one can adjust the percent transmission scale of the double-beam instrument so that the recorded transmission between 1 and 2.5μ is 100%, all of the recorded

Table 6

THE ABSORPTION COEFFICIENT OF THE 6.5μ BAND

Diamond	Type	t(mm)	K (6.5μ)-(cm^{-1})
B2	SI	1.32	0
BP2	II	1.89	0
F1	SI	3.84	0.12
F2	SI	3.96	0
F3	SI	3.56	0.10
I7	MI	3.0	0.41
I20	WI	4.0	0
M4	WI	0.79	0
S1	SI	4.67	0.34
S2	SI	4.19	0.25
S3	SI	5.36	0.57
SLF127	SI	2.55	0
SL09	SI	3.10	0.42
SL015	SI	0.54	0.33
SL025	SI	0.53	0.20
SL042	SI	3.75	0.10
SL044P2	SI	0.69	0.80
SYR1	SI	3.45	0.38
SYR8	SI	0.30	0.30
SYR9	SI	0.51	0.51

spectra can be automatically compensated for loss by reflection. The absorption coefficient at any wavelength can then be determined from the recorded spectrum without assumptions as to the position of the base line.

In order to test the validity of previous experiments which showed that the absorption coefficients of the bands from 2.8 to 6.0μ are constant, we have adopted the following method. Spectra are adjusted to compensate for loss by reflection as already described. The resulting spectra are plotted as log log I_o/I vs wavelength, where I/I_o is the measured fractional transmission. Such plots are independent of sample thickness except for a vertical displacement along the log log scale. This is shown as follows:

(1) $I/I_o = 10^{-kt}$

(2) $\log_{10} I_o/I = kt$; $\log_{10} \log_{10} I_o/I = \log k + \log t$

Besides their independence of thickness, these log log plots have the virtue that wide variations of the absorption coefficient are represented on a logarithmic scale where they are more obvious than on a linear scale where variations in k are overexaggerated. However, regions in which k is zero or nearly zero cannot be represented on log log plots. When the double-beam spectra are plotted in this manner, it is found that a linear shift along the log log scale will superimpose (within experimental error) the bands between 2.5 and 6.0μ in 17 of the 20 diamonds examined with the double-beam spectrometer. Three of the diamonds (F2, I20, T38) were too rough to give acceptable spectra

in the short wavelength region. The resulting contour is shown in Figure 12. These results verify the previous observations by Sutherland and Willis[5] and by Blackwell[10] that the absorption coefficients for bands from 2.5 to 6.0μ are the same for all diamonds.

The log log I_o/I presentation is also useful to show the variable absorption at wavelengths greater than 6.0μ. Plots for T15 (W IR I) and SYR8 (S IR I) are shown in Figure 12. The short wavelength portions are superimposed so that the differences at long wavelength are independent of thickness.

CORRELATION OF INFRARED AND ULTRAVIOLET ABSORPTION: The reflecting microscope has been used to detect variations in the spectrum between different parts of individual diamonds. Only one clear example of absorption variation within a single diamond was found. The ultraviolet transmission patterns of all suitable diamonds (i. e. flat sides) were examined using the apparatus described on page 44 . The 2537 A. U. line of mercury was used for illumination. This wavelength lies in a region where UV I diamonds are opaque but UV II diamonds transmit. Patches of transmitted 2537 A. U. light indicate the presence of UV II regions. The pattern is viewed through the use of the anthracene coated plate. In 50 diamonds (listed in appendix) only two stones showed variations in transmission at 2537 A. U. One of these stones (K2) was too rough to separate the effect of scattering from the variation in absorption. When K2

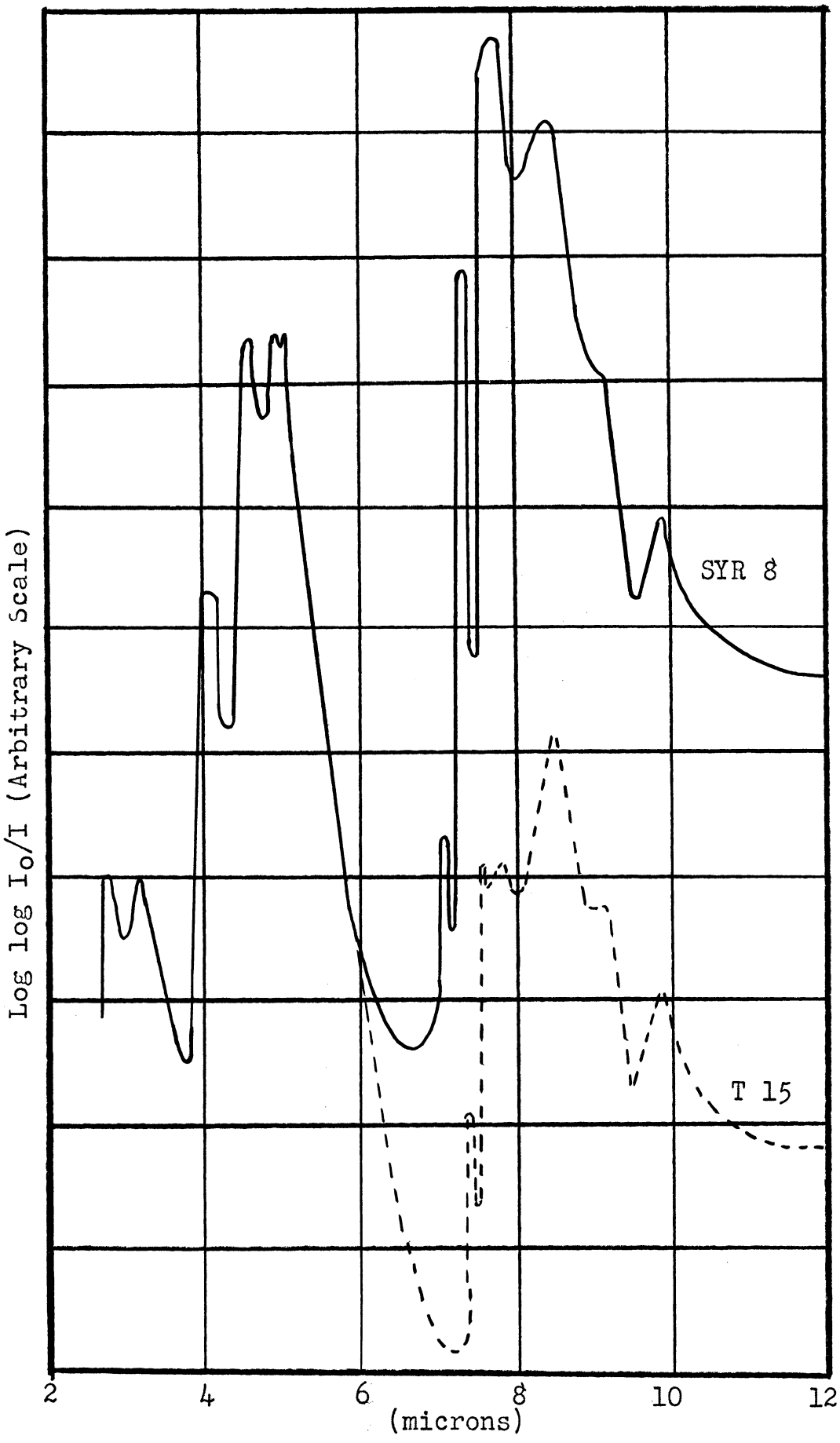

Fig. 12

LOG LOG I_o/I VS WAVELENGTH FOR DIAMOND

was examined with the reflecting microscope, the rough surfaces caused too much refraction of the beam to permit reliable estimates of the change in absorption coefficient between different points in the stone. Diamond M4 (W IR I) showed a clear transmission pattern which is sketched in Figure 13. Using the reflecting microscope, spectra were recorded for several points in the diamond. Using log log I_o/I plots the variations in the 8μ regions were apparent. In Table 7 below Figure 13 these variations are listed in terms of the absorption coefficient at 7.8μ. The correlation with the transmission pattern is obvious. This result confirms Blackwell's results obtained for the variations between different stones, i. e. the intensity of absorption at 7.8μ increases as the position of the ultraviolet cutoff moves to longer wavelengths.

ABSORPTION OF POLARIZED LIGHT: Because many diamonds display birefringence patterns, we have looked for dichroism in the infrared which might accompany the birefringence. On a "macro" scale, the spectrum of SLF127 (S IR I) was recorded using the double-beam instrument equipped with reflection polarizers. No effects were observed. Since the birefringence is localized, a better experiment was the recording of spectra using the reflecting microscope with a polarizer. In this case, individual regions in SLF127 and T37 (IR II) which displayed birefringence were tested for dichroism. Again, no effects were observed.

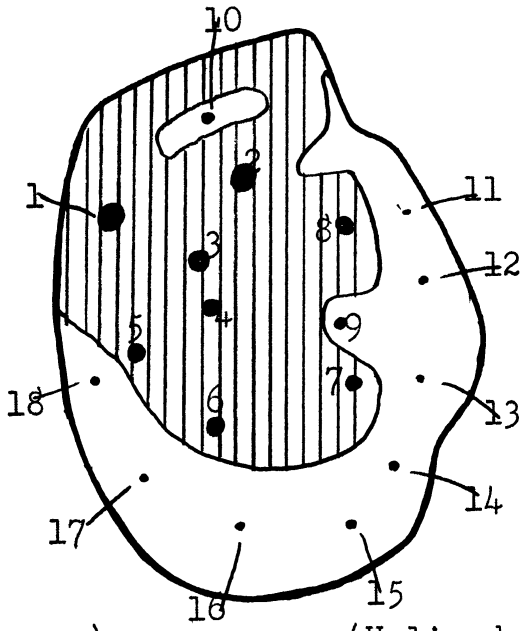

(Lined region-opaque) (Unlined region-transparent)

Fig. 13

TRANSMISSION PATTERN OF DIAMOND M4 FOR 2537 A.U. LIGHT

Table 7

The Absorption Coefficient at 7.8 Microns for Points in Diamond M4

Point	K(cm^{-1})	Point	K(cm^{-1})	Point	K(cm^{-1})
1	4.8	7	1.2	13	0.3
2	4.0	8	2.0	14	0.4
3	2.8	9	0.5	15	0.5
4	1.6	10	0.6	16	0.3
5	1.4	11	0.2	17	0.3
6	1.2	12	0.3	18	0.3

2.2.2 Far Infrared Spectra of Diamonds

300 TO 900 cm^{-1}: In this region, the CsBr prism was used, mounted in the Model 112 spectrometer. The reflecting microscope cannot be used at these wavelengths for reasons already discussed. Because the energy from the "blackbody" source drops off rapidly with wavelength, samples must cover a larger portion of the slit height than in the experiments from 1 to 15μ. (See page 37). Consequently, spectra from 300 to 600 cm^{-1} have been obtained only for the large flat diamonds in our collection. The diamonds examined include one IR II (BP2), one weak IR I (M4) and six strong IR I (F1, S1, S2, S3, SLF127, SL025). The spectra of F1, S2, and SLF127 from 300 to 1400 cm^{-1} are shown in Figure 14.

In the long wavelength region we have found no absorption in the IR II diamond. However, two bands occur in all IR I diamonds. These bands are located at 20.8μ (480 cm^{-1}) and at 30.5μ (328 cm^{-1}). The 21μ band was first reported by Danielson[31] in 1951. The 30μ band has not been reported previously.

In Table 8 we list the absorption coefficients for the 21 and 30μ bands together with other IR I bands. The bands at 21 and 30μ are typical IR I bands in that their absorption coefficients vary from diamond to diamond. In order to investigate any connection between the two long wavelength bands and other IR I bands we have prepared the charts shown in Figure 15 in which are plotted the absorption coefficients of bands which may be related. Chart (a) demonstrates that

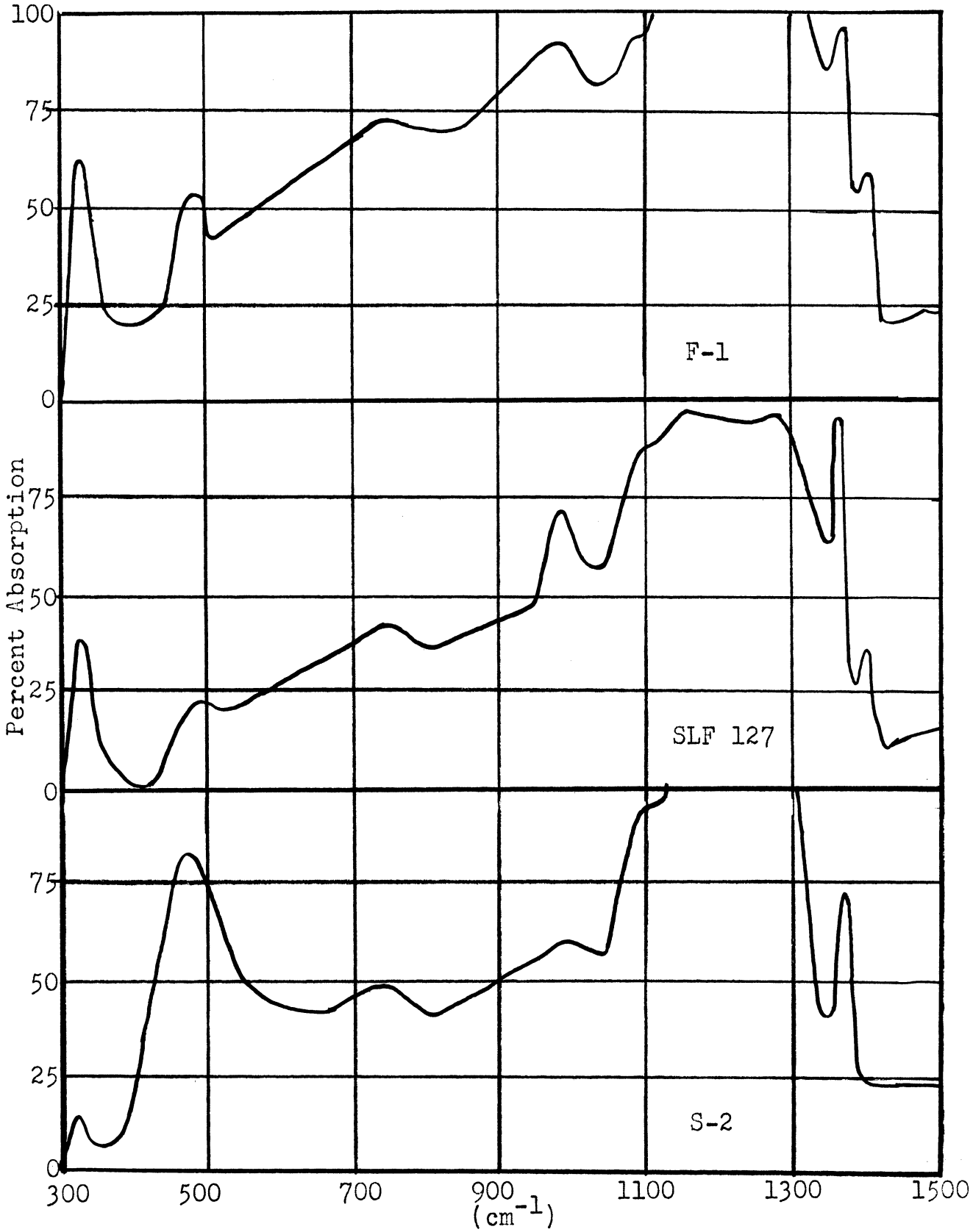

FIG. 14

SPECTRA OF 3 DIAMONDS FROM 300 TO 1500 CM^{-1}

Table 8

THE ABSORPTION COEFFICIENTS FOR THE LONG WAVELENGTH BANDS IN DIAMOND

Diamond	t(mm)	Undetermined Group			Group B			Group A
		21μ	30μ	13μ	7.0μ	7.3μ	10μ	7.8μ
F1	3.84	0.86	1.1	1.4	1.0	H	2.9	H
N4	0.79	0.5	0.3	0	0	0	0	3.1
S1	4.67	1.0	1.25	1.5	1.05	H	3.2	H
S2	4.19	1.8	0.17	0.72	.10	0.57	0.95	H
S3	5.36	0.93	2.4	2.0	1.75	H	5.3	H
SLF127	2.55	0.46	0.87	0.97	0.81	3.2	2.2	4.9
S1025	0.53	3.7	1.0	2.5	1.0	5.2	3.2	19.6

Note: H indicates a band too intense to measure.

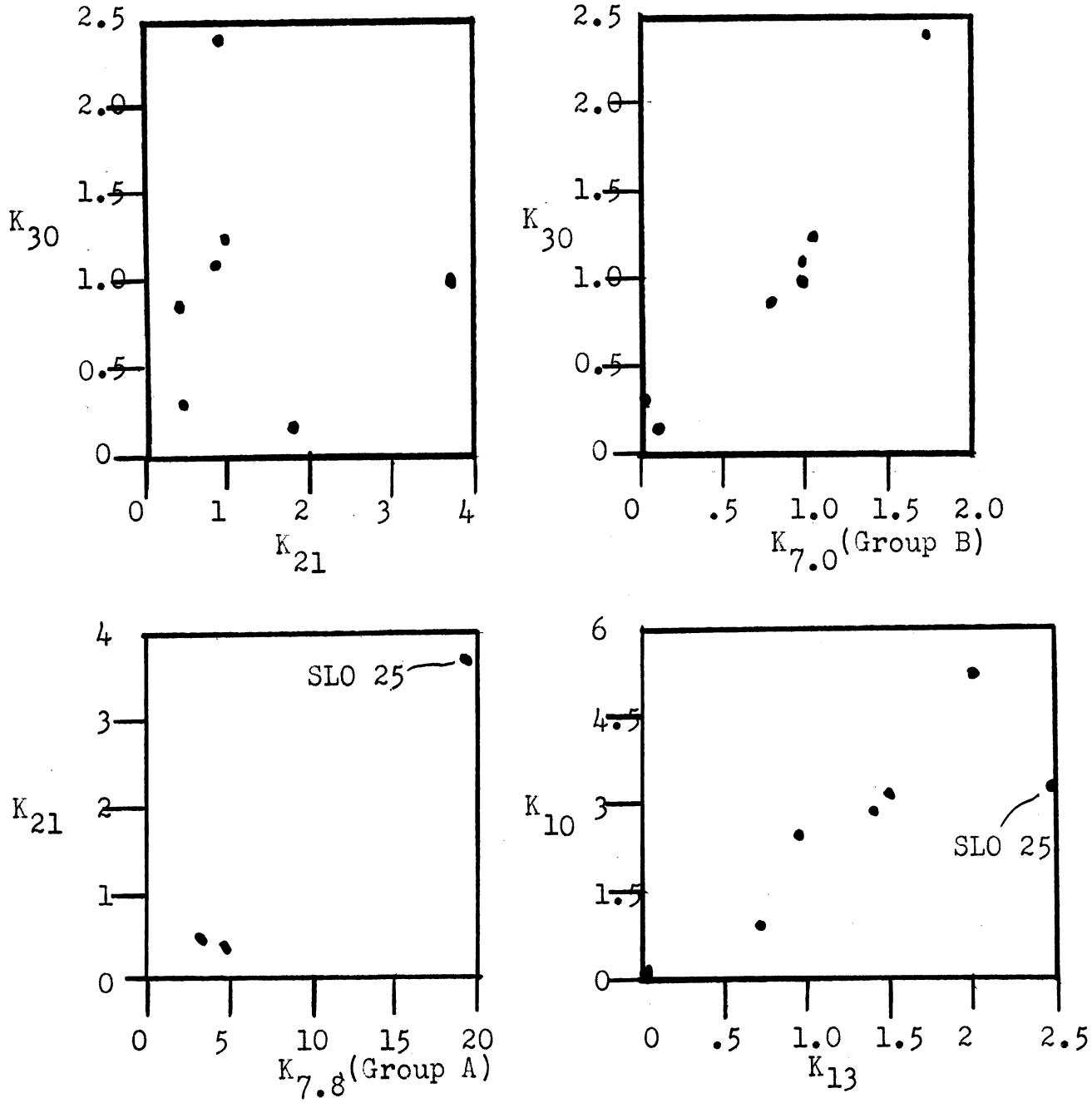

Fig. 15

RELATIONS BETWEEN ABSORPTION COEFFICIENTS OF IR I BANDS

the absorption coefficient of the 30μ band varies independently of the absorption coefficient of 21μ band. Chart (b) demonstrates that the 30μ band is a Group B band in that its absorption coefficient is essentially proportional to the absorption coefficient of the 7.0μ band (see page 26). Chart (c) demonstrates that the 21μ band is probably a Group A band. There are only three cases in which the 7.8μ band is weak enough (in intensity) to measure accurately, but the wide range of K_{21} and $K_{7.8}$ covered, gives good support to our statement.

The 13μ band (Blackwell's 12.75μ band) has not been correlated with a particular group in the past. Blackwell made a few measurements of the band and assumed that it was a Group A band. In Chart (d), Figure 15, the correlation is shown between 10μ (a Group B band) and 13μ. Except for SL025, the relationship appears to be quite good. We explain the deviation of SL025, by pointing to the fact the K_{21} is very high in SL025. The remaining Group A bands associated with 21μ will also be strong and will tend to upset correlations between Group B bands lying in the wavelength interval where both Group A and Group B absorption occur, i. e. between 7.8 and 30μ. We have intentionally chosen 10μ rather than 7μ as the representative Group B band because it lies closer to 13μ than the other Group B bands and should be affected by Group A absorption in a manner similar to 13μ. In fact, the position of the point for SL025 gives a good indication that the absorption band at 21μ has a tail extending to at least 13μ and that Group A

absorption at 10μ is less than Group A absorption at 13μ. If this conjecture about SL025 is accepted, our measurements can be interpreted to mean that the 13μ band is a Group B band.

30 TO 100μ: Two samples large enough to use in the vacuum grating instrument (page 40) were made from (1) Four strong IR I diamonds of average thickness 0.63 mm. This sample is designated as SLO. Stones SL015, 25, 44(a) and 44(b) were used. (2) Three strong IR I diamonds of average thickness 3.74 mm. This sample is designated F since F1, 2, and 3 were used. Neither sample shows absorption bands at wavelengths longer than 30μ. By comparing transmission in the overlapping regions between the records obtained in the near infrared, the CsBr region, and the far infrared it was established that the transmission measured at 35μ and beyond was equal to the transmission measured between 1 and 2.5μ. That is, the only losses at long wavelengths are due to reflection. The reason that one cannot rely on the absolute value of the transmission measured at long wavelengths is that the stones used are not flat or uniform in thickness. The radiation is often completely blocked by certain rough portions of the diamonds. The results are incorporated in Figure 16 in which the infrared spectrum of F1 is shown from 100 to 3800 cm^{-1}.

2.2.3 The Infrared Spectra of Powdered Solids

In the course of our work in the far infrared, the possibility of using diamond dust for a sample was considered.

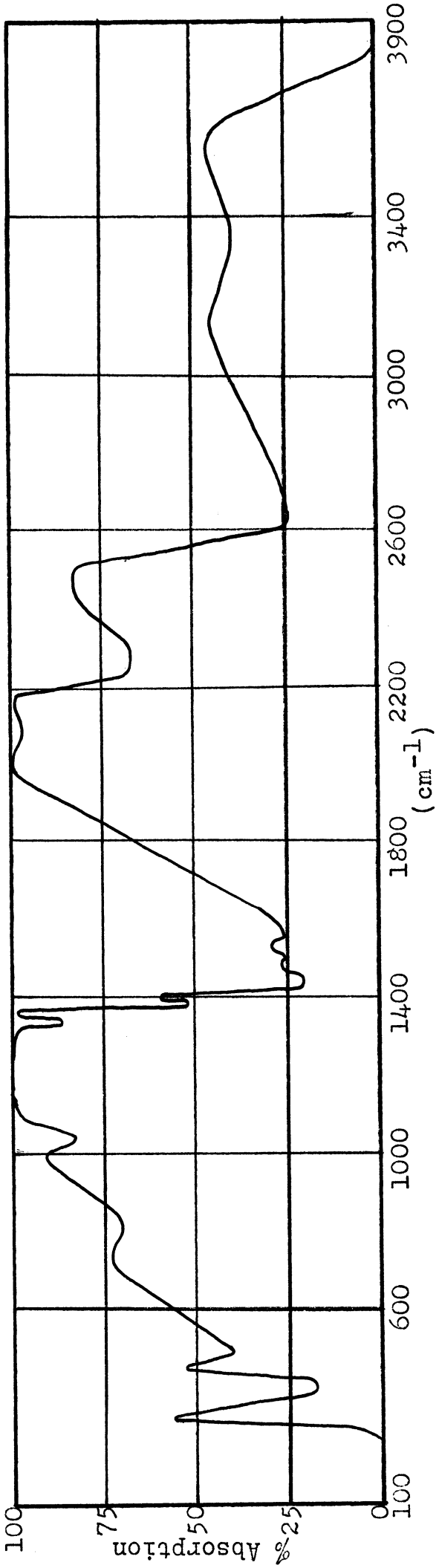

Fig. 16

THE INFRARED ABSORPTION SPECTRUM OF DIAMOND F-1

Such a sample would be useful in that it could be made as large in area as necessary to cover the whole length of the exit slit of the spectrometer. Diamond dust obtained commercially proved to be contaminated with SiC and/or SiO_2. This was established by recording spectra of powdered samples of these materials (see Figure 17). Methods of purification proved unsatisfactory. Consequently, it was not possible to use diamond dust in the experimental work in the far infrared.

The spectrum of silicon powder was also recorded. (See Figure 17). It will be noted that a strong band occurs at 9μ. A similar band occurs in all the other powder spectra. A similar band also occurs in the spectrum of crystalline silicon.[52] However, it seems probable that this band is due to SiO_2.[53] The similarity of the powder spectra points to this fact. A further discussion of this point is given on page 157.

2.2.4 The Infrared Spectrum of Germanium

Lord[54] and Briggs[55] have published absorption spectra for crystals of germanium for the region from one to 35μ. However, it was desirable to obtain additional spectra in this region for use in our calculations. In addition, the germanium absorption spectrum beyond 35μ is of interest and has not been published. We have received samples of germanium crystals from Dr. G. A. Morton of the R. C. A. Laboratories, and we are indebted to Dr. Morton for supplying these samples.

The samples were of varying thickness and purity. Samples A_1 (8.90 mm), A_2 (2.54 mm), and A_3 (0.99 mm) were relatively pure (impurity concentration 10^{13} atoms/cc) according to their electrical properties (resistivity between 30 and 38 ohm cm). Pure germanium would have a resistivity of approximately 47 ohm cm.[56] Samples B_1 (8.80 mm) and B_2 (2.44 mm) had arsenic added to a concentration of about 10^{16} atoms/cc (resistivity between 0.4 and 0.6 ohm cm).[56] Arsenic is known to act as an electron donor in germanium.[57] The positive arsenic ion is located at a lattice site where it is tetrahedrally bound to neighboring atoms. The extra electron is essentially free to add to the number of carriers. Consequently, germanium with arsenic impurities is "n" type since the conduction takes place through the movement of electrons (as opposed to conducting by holes). While this section was in preparation, a communication by Collins[58] has appeared in which it is stated the "n" type germanium displays absorption at long wavelengths which increases with λ^2. This absorption is independent of lattice absorption and is characteristic of absorption by free carriers.

Absorption spectra for our samples were obtained from 1 to 100μ. The spectra are shown in Figures 18, 19, and 20. In Table 9 the observed maxima are given together with the absorption coefficients at these maxima. In Figure 18 the absolute transmission from 1 to 15μ is given. Beyond the sharp cutoff at 1.75μ, each sample increases in transmission to a maximum of about 40%. The surfaces of the

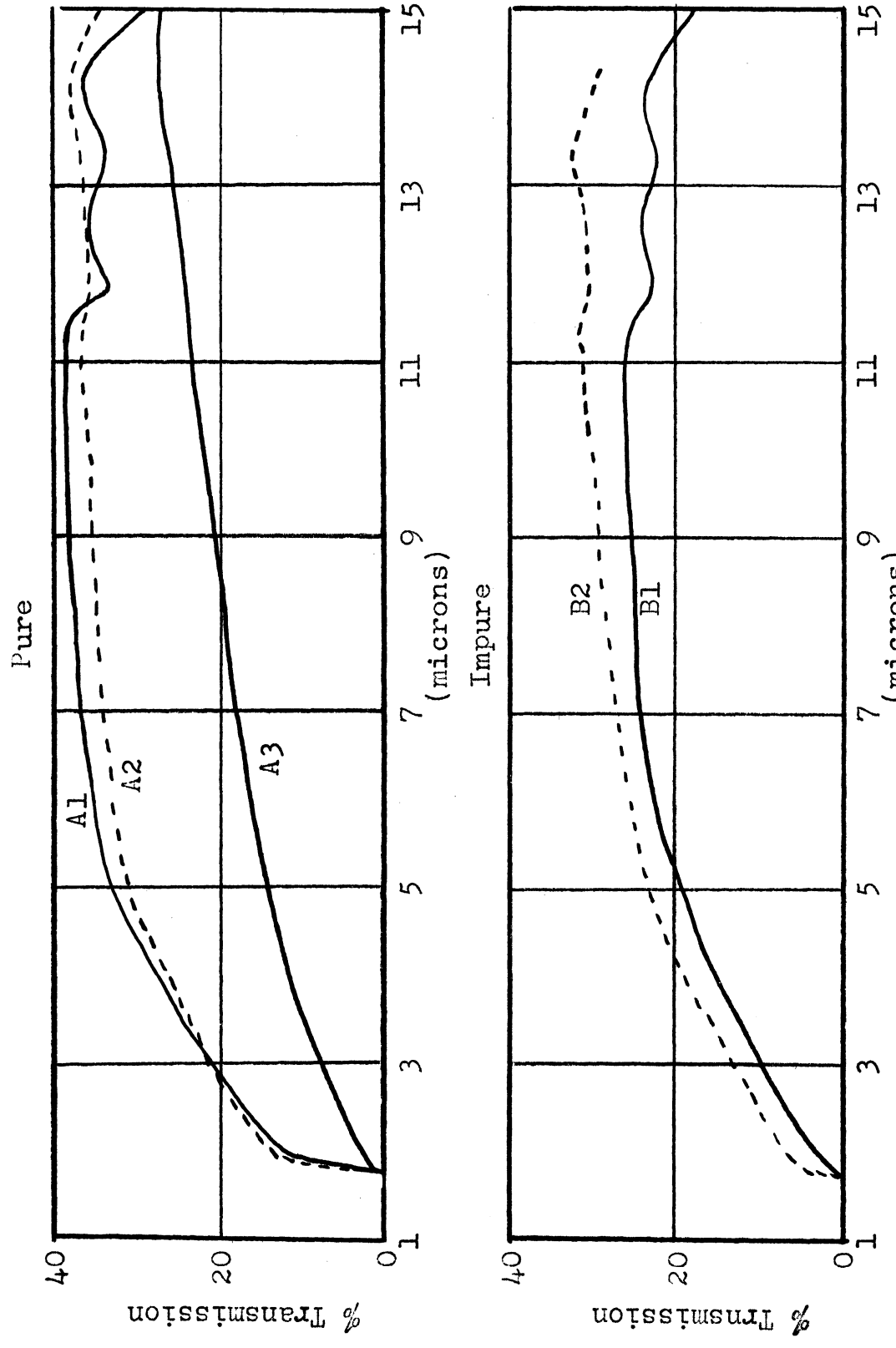

Fig. 18

TRANSMISSION OF GERMANIUM FROM 1 TO 15 MICRONS

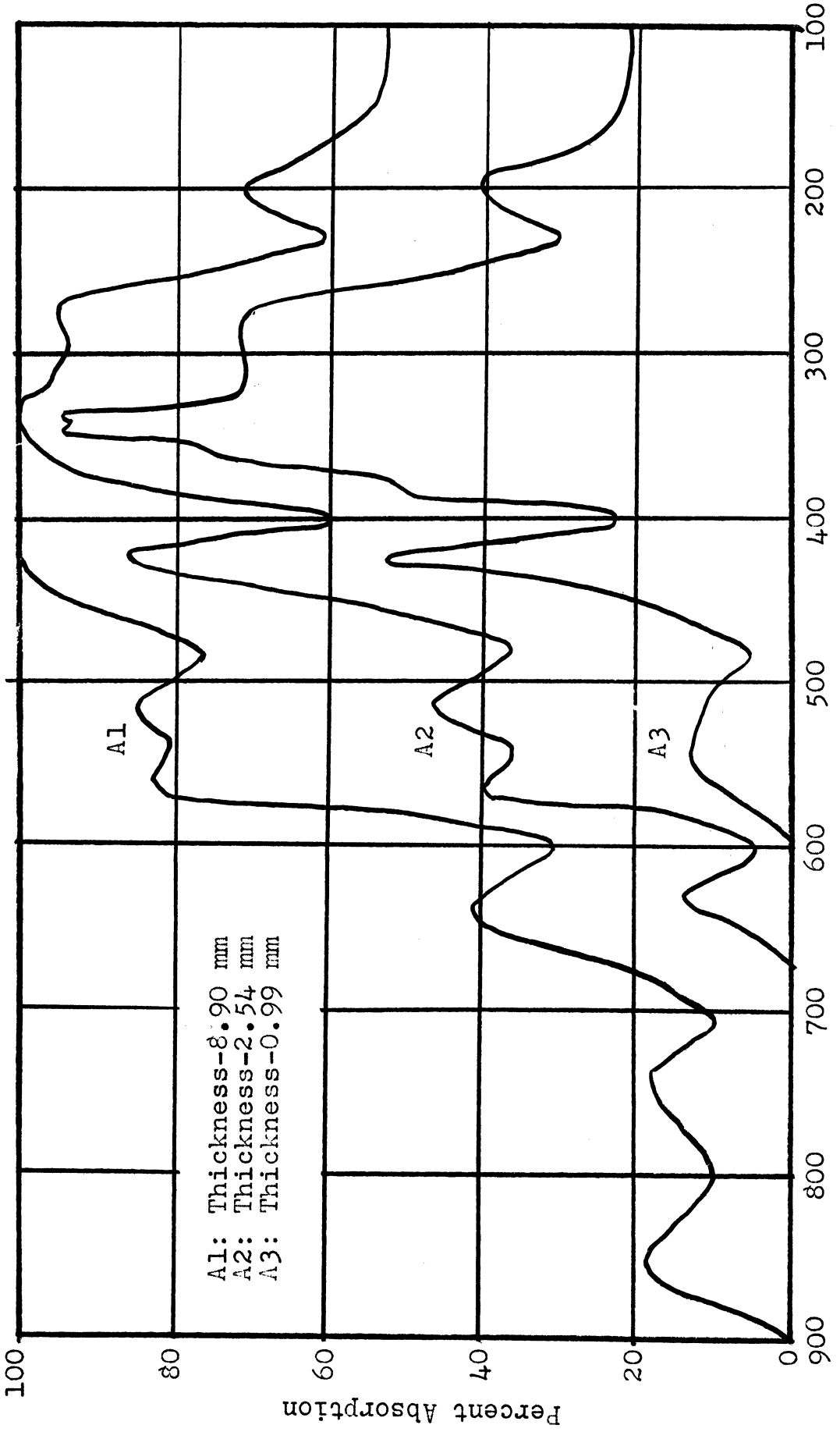

Fig. 19

ABSORPTION SPECTRA OF 3 PURE GERMANIUM CRYSTALS

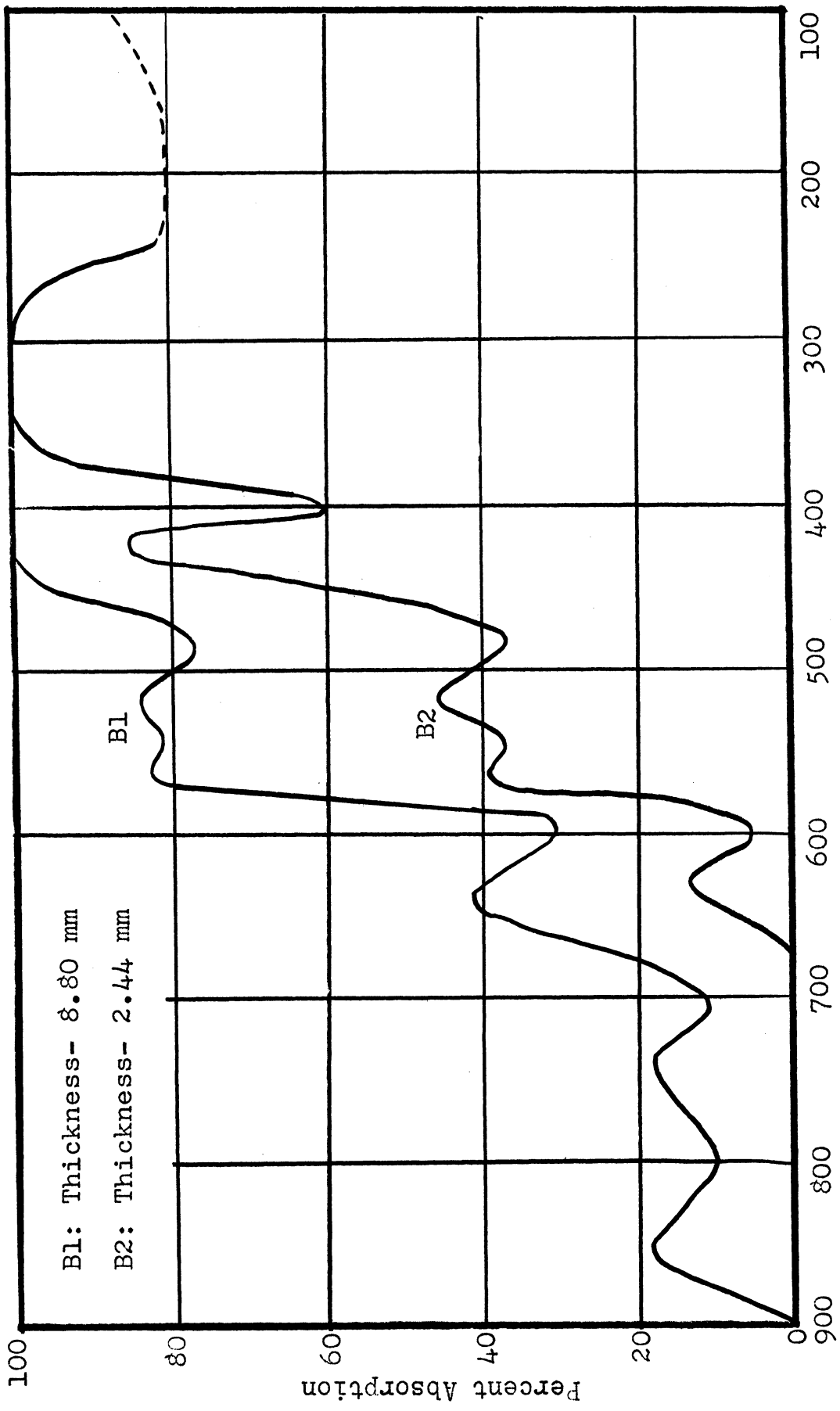

Fig. 20

ABSORPTION SPECTRA OF 2 IMPURE GERMANIUM CRYSTALS

Table 9

ABSORPTION MAXIMA IN THE GERMANIUM SPECTRUM

Position		Absorption Coefficient (cm^{-1})	Position		Absorption Coefficient (cm^{-1})*
μ	cm^{-1}		μ	cm^{-1}	
11.87	845	0.10	23.8	420	3.3
13.35	750	0.10	29.0	345	25
15.6	640	0.30	36.3	275	5.3
17.9	560	0.85	50.0	200	2.2
19.2	520	1.00			

* To the base 10

samples were only rough ground, so that the departure from constant transmission between 3 and 10μ (observed by Briggs[52] and others) may be attributed to scattering. In addition, the absolute transmission at wavelength where scattering is not important (near 10μ) varies from sample to sample, and the loss is greater than that due to normal reflection as measured by Briggs ($\sim$ 50%). The excess loss is attributed to diffuse reflection by rough portions of the surface and is not due to absorption. A comparable situation occurs with diamonds which have been sawn but not polished. For all samples except A_3, the transmission between 6 and 10μ is essentially constant. For the spectra between 100 and 1000 cm^{-1} (Figures 19 and 20) we have assumed that the loss

due to all types of reflection is the same as that measured between 1000 and 1600 cm^{-1} (10 to 6μ). Since in sample A_3, the transmission increases continuously from 6 to 14μ, we assume that the reflection loss from 100 to 700 cm^{-1} is the same as that at 700 cm^{-1} (14μ).

In the spectra between 300 and 900 cm^{-1} (Figures 19 and 20) the absorption coefficients for all of the bands appear to be the same in all five samples regardless of purity. Beyond 300 cm^{-1}, the impure samples (B_1 and B_2, Figure 20) absorb too strongly to make accurate measurements of the absorption coefficients, but there is no question that they absorb more strongly than the pure samples. On this point, we agree with Collins.[58] Concerning the magnitude of the increase of absorption between pure and impure samples, Collins states that this absorption is due to free carriers and that it increases as λ^2. On the other hand he finds that the amount of the observed "free carrier" absorption is several orders of magnitude greater than that predicted by theory. In the absence of published data (Collins' work appears as an abstract), it is not possible to examine these conclusions in detail. However, in all cases, Collins assumes that the absorption due to lattice vibrations is the same in all samples. It seems a remarkable coincidence that the increased absorption in impure samples sets in at precisely the place where fundamental lattice absorption occurs (Collins and Fan[59] have already proposed that the 345 cm^{-1} band in germanium is a fundamental lattice absorption). In diamond, where no

free carrier absorption is expected, absorption in the fundamental region also changes from sample to sample. Since our pure germanium samples show absorption at the longest wavelengths, i. e. fundamental bands occur in the region from 100 to 300 cm^{-1}, it is difficult to exclude the possibility that at least part of increased absorption in impure samples is due to a change in the absorption coefficients of the fundamental bands.

2.2.5 The Ultraviolet Absorption of Adamantane

Adamantane is a hydrocarbon, $C_{10}H_{16}$, having the structure shown in Figure 21. If the hydrogens are omitted, the structure of adamantane is similar to the local structure of diamond (Figure 2). Since the position of the ultraviolet cutoff is determined by the electronic configuration, it is reasonable to expect that the cutoff for adamantane should be close to the cutoff of the similar structure, diamond.

Platt[60] has shown that the position of the cutoff of aliphatic compounds moves to longer wavelengths as the branching around the C-C bond increases (see Table 10). The highest branched structure is diamond in which each C-C bond is surrounded by 6 branches. From Platt's data, one expects such a substance to cutoff near 1800 A. U. However, the cutoff is not sharp in all substances and can be expected to move to longer wavelengths as the concentration increases. Similarly, one expects adamantane to cut off at some wavelength longer than 1800 A. U.

The cutoff of adamantane was determined by making transmission measurements on a solution of the substance in either

Table 10

VARIATION OF ULTRAVIOLET CUTOFF WITH BRANCHING

Number of Branches Around C-C Bond	Type	Example	Transmission Limit (A. U.)
0	-C-C	Ethane	1550-1560
1	-C-C-C-	Propane	Not Measured
2	-C-C-C-C-	n-pentane	1700-1730
3	C 1 -C-C-C-C-	3-Methylhexane	1730-1740
4	C C 1 1 -C-C-C-C-	2,3-dimethylhexane	1770
5	C C 1 1 -C-C-C-C- 1 C	2,2,3-trimethylpentane	1785
6	C C 1 1 -C-C-C-C- 1 1 C C	2,2,3,3-tetramethylpentane	1795

Platt's [60] Data

cyclohexane or n-hexane. The cells used were either 1cm in thickness made of fused quartz or 0.1 mm in thickness made by using a lead shim between two fluorite windows. All transmission measurements were made with a Beckmann Model DU spectrophotometer.

In agreement with Potts[61] we found that the purest solvents available from commercial suppliers transmitted feebly from 2500 to 2000 A. U. By shaking the solvents with sulfuric acid, the contaminants could be reduced so that transmission measurements could be made to 2000 A. U.

The transmission of adamantane is shown in Figure 22. The concentration was measured for only one case, where it was found to be about 0.5 mg/cc. The cell thickness of 1 cm with such a concentration of adamantane is equivalent to about 10^{-4} cm of diamond. Since the measured concentration of 0.5 mg/cc in a one cm path produces a long gradual absorption which transmits only 10% at 2300 A. U., one is led to the conclusion that either the sample of adamantane was contaminated or the absorption of adamantane is different from that of diamond which has a sharp cutoff (see Figure 3). Attempts to purify the solutions of adamantane did not alter the absorption.

Another characteristic of the absorption spectrum of adamantane is the shoulder near 2250 A. U. In higher concentration, the shoulder could represent the beginning of total absorption. Since the shoulder lies close to the cutoff of UV II diamonds, it may be characteristic of the similar electronic configurations in adamantane and diamond.

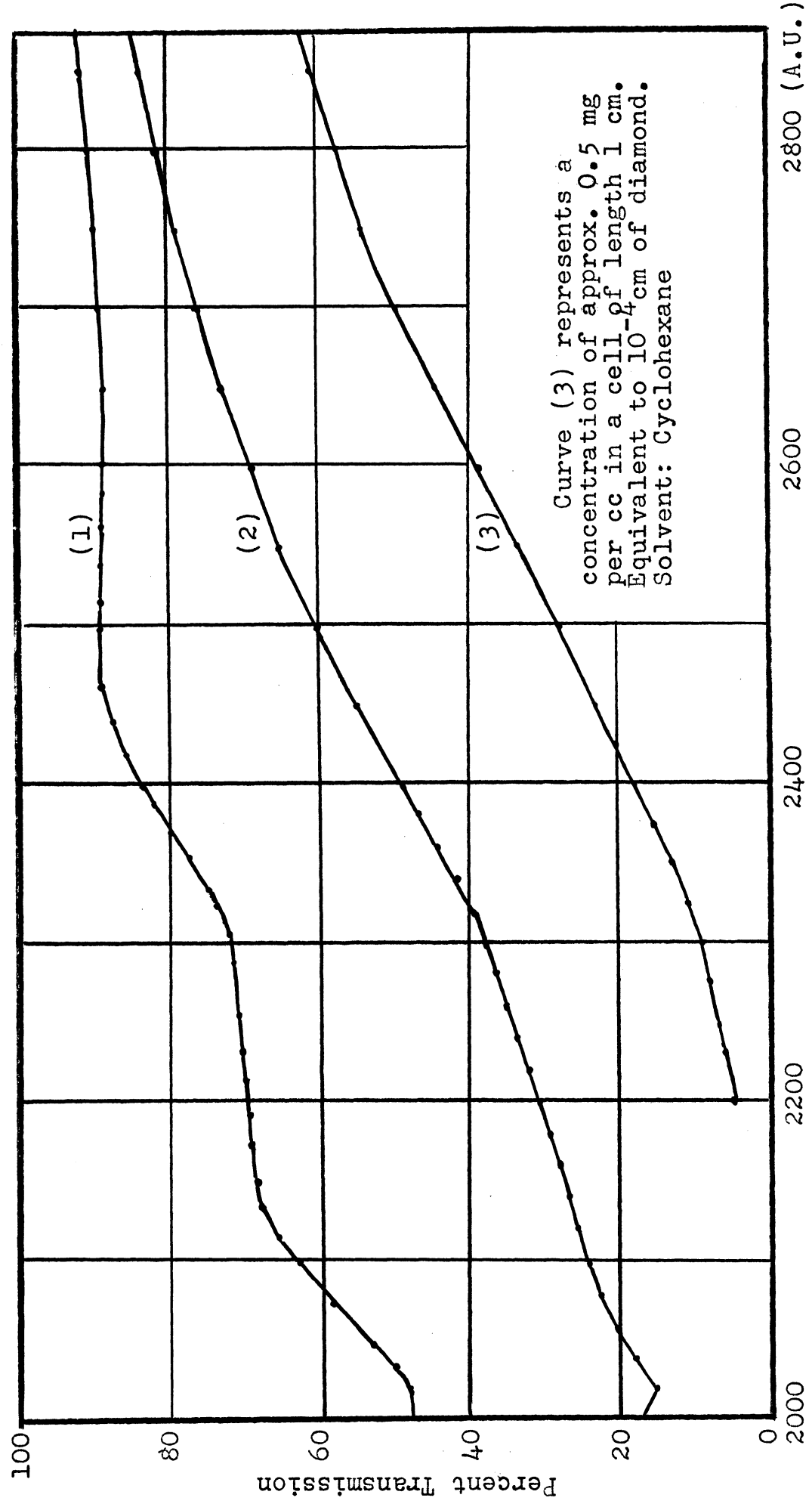

Fig. 22

THE ULTRAVIOLET ABSORPTION SPECTRUM OF ADAMANTANE

2.2.6 The Absorption of Diamond in the Vacuum Ultraviolet

The position of the ultraviolet cutoff is generally assumed to be the long wavelength edge of a broad continuum extending into the X-ray region. However, until recently, calculations of the electronic structure predicted a cutoff nearer 1500 A. U. In order to determine whether or not any region of transmission exists between 1200 A. U. and the cutoff of diamonds, we used the fluorite spectrograph described on page 41 . The diamonds which were examined included 5 S IR I, 1 W IR I, and 2 IR II. The diamonds are listed in Appendix B together with their IR and UV characteristics. None of these diamonds showed measurable transmission at wavelengths shorter than the position of its cutoff (between 2250 and 3200 A. U., depending on the sample). We conclude that the position of the ultraviolet cutoff is a true absorption band. We discuss the recent theoretical work concerning this point in section 3.2.

2.2.7 Bombardment Experiments

In 1905, Crookes[62] reported that the color of diamonds could be altered. A diamond exposed to cathode rays, in vacuum, for one year turned black on its surface. Heating to 600° C restored the original color. Exposing a diamond to radium radiations for one year turned it blue. This color could not be removed. In 1942, Cork[63] reported that bombardment of diamonds by 10 Mev deutrons turned their surfaces green. This color could be removed by heating. Later, Blackwell and Sutherland,[64] in an attempt to test their impurity theory by introducing defects in diamonds, placed

diamonds in the Harwell pile. Several weeks of exposure to the pile radiations (principally fast neutrons) caused the diamonds to turn black (presumably a volume effect). No infrared energy was transmitted by the bombarded diamonds, so that the effect of bombardment on 8μ absorption could not be determined. Grenville-Wells[65] performed similar experiments in which the diamonds were bombarded for as much as a month. In this case, the diamonds turned black, but it was still possible to observe the X-ray diffraction pattern. No effect was found on the intensity of the extra streaks. She found similar effects in color change on heating diamonds in vacuum.[66] In this case, the formation of graphite can be detected by X-ray. The similar effects in experiments on bombardment and heat treatment lead to the conclusion that the diamonds are changed to graphite locally.

Since, in the previous experiments, pile irradiations had been carried on for several weeks before observation of the effects was made, it was considered worthwhile to examine the effects in the infrared before the diamond is rendered opaque to infrared radiation. Four diamonds, GM39 (S IR I), GM40 (S IR I), GM74 (IR II), and GM75 (W IR I), were sent to Oak Ridge for insertion in the pile. After six hours in the pile, all four diamonds showed a slight blackening, but they were still transparent in the visible and showed no changes in their infrared spectra. Additional bombardment for 24 hours rendered all four diamonds nearly opaque in the visible (a faint amount of red light was transmitted). By

reflected light the diamonds appeared black. In the infrared, no changes in the spectrum could be detected.

We also placed two diamonds in the University of Michigan cyclotron where they were bombarded with 10 Mev deuterons. T37 (IR II) was bombarded for a total of 100 microampere minutes. It turned pale green on its surface, but no change occurred in its infrared absorption spectrum. K3 (IR I) was bombarded for a total of 250 microampere minutes. It turned pale brown on its surface, and again no change occurred in its infrared spectrum. By examining the edge of T37 under a microscope, the depth of penetration of the color change was measured to be approximately 0.2 mm. This corresponds to the range of 10 Mev deuteron in diamond as calculated from curves given by Cork.[67] For carbon, his curves indicate a range of approximately 90 mg/cm^2. The density of diamond is 3.51 g/cc. Consequently, the calculated range is 0.25 mm. Since the penetrating power of fast neutrons is higher than that of deuteron, and since the flux density in the pile is higher than that in the cyclotron, it is not likely that enough defects could be introduced by bombardment with deuterons to produce changes in the infrared spectrum which were not produced by neutron bombardment.

Although we have made no measurements of the ultraviolet absorption spectrum of the bombarded diamonds, the visible absorption is sufficient evidence that the electronic structure has been altered on a large scale by neutron bombardment. Since no comparable effect in the infrared spectrum is pro-

duced by short periods of neutron bombardment, while long periods of neutrom bombardment evidently materially change the character of the local structure by turning it to graphite, we conclude that neutron bombardment of diamonds introduces defects different from those causing infrared absorption at 8μ. Since vacant sites are the most probable defects introduced by bombardment, we deduce that a random distribution of vacant sites is not responsible for the anomalous absorption at 8μ.

2.3 Summary

In our experimental work on diamonds we found an absorption band at 6.5μ and another at 30μ, neither of which has been reported previously. While the 6.5μ band appeared only in IR I diamonds, it was not associated uniquely with other IR I bands. The 13μ and 30μ were shown to be Group B bands, and the 21μ band to be a Group A band. We verified the fact that the bands between 2.5 and 6.0μ occur with the same absorption coefficients in all diamonds. The variation in ultraviolet absorption (.2537 A. U.) in diamond M4 correlated with the variation in the absorption coefficient of the 7.8μ band. We found no dichroism in the infrared at those points which show birefringence in the visible. Between 33 and 100μ there was no absorption, and the reflection loss proved to be essentially equal to that between 1 and 2.5μ. Bombardment by neutrons and deuterons did not alter the infrared spectra of diamonds, although marked changes occurred in the visible spectrum. From these experiments, we concluded that vacant

sites are not the defects causing anomalous absorption in the infrared.

A comparison of the spectra of powdered SiO_2 and powdered Si indicated that the 9μ band in silicon may be due to SiO_2. A comparison of the spectra of 3 pure Ge samples and 2 impure Ge samples showed that the absorption coefficients were the same for all samples at wavelengths shorter than 30μ, but that the impure samples absorb more strongly at wavelengths larger than 30μ.

We found that adamantane absorbs strongly near the position of the ultraviolet cutoff of UV II diamonds (2250 A. U.). No diamond tested showed transmission between 1200 A. U. and the position of the ultraviolet cutoff, proving that the cutoff is the long wavelength edge of a continuum.

Chapter 3

REVIEW OF PREVIOUS THEORETICAL WORK

Although a rigorous theoretical treatment of the physical phenomena which display anomalies in diamond has not been made, these are in existence well developed theories which have been successful in explaining similar phenomena in other substances. In addition, when it is said that some properties of diamonds display anomalies, it is implied that a normal behavior can be predicted. Finally, there are two theories, that proposed by Raman,[8] and that proposed by Blackwell and Sutherland,[11] which try to account for the observed anomalies.

In this section, we will present portions of the general theory which has been developed for several of the physical phenomena in which we are interested. From this theory, the normal behavior for an ideal diamond will be inferred, whenever possible. In those cases, where anomalous properties in other substances parallel the anomalous properties of diamond, the pertinent facts will be discussed. Finally, with this background of accepted theory, the proposed theories of Raman and of Sutherland and Blackwell will be discussed.

3.1 Infrared Absorption

To explain the infrared absorption spectrum of diamonds there are two questions which must be answered. (1) What

is the absorption spectrum of an ideal diamond having the Bragg structure? (2) What causes the variation in the observed spectrum?

The absorption spectrum in the infrared must arise from transitions to vibrational levels. Consequently, we must investigate the vibrational spectrum of the ideal diamond lattice. We will digress slightly to review the development of the theory of the vibrational spectrum of the crystalline lattice.

As is well-known, the temperature variation of the specific heat of crystalline solids is a function of the frequency distribution of the normal vibrations of the solid. Historically, it was because some substances, (principally diamond), displayed a molar specific heat considerably lower than the classical Dulong and Petit value of 6 calories / mole° K that the problem of the temperature coefficient of the specific heat received attention. Originally, Einstein[68] applied the concept of the Planck quantized harmonic oscillator by assuming that, to first approximation, the atoms of a monatomic crystal do not interact and that they all vibrate with the single frequency, ν_E, characteristic of the vibration about their equilibrium position. This approximation accounted for many of the observed features of the variation of specific heat with temperature. The total energy of the crystal is now represented as the thermal average of 3N oscillators of frequency ν_E. Since the average energy of a Planck oscillator at temperature T is $E = \frac{h\nu_E}{e^{h\nu_E/kT}-1}$ the total energy of the crystal is $E = 3RT \frac{\theta_{E/T}}{e^{\theta_{E/T}}-1}$ where

$\theta_E = h\nu_{E/k}$ and has the dimensions of temperature. The corresponding specific heat varies as $C_v = 3R\ (\theta_{E/T})^2\ e^{-\theta_{E/T}}$ at temperature low with respect to θ_E. Experimentally the specific heat at low temperatures does not approach zero exponentially, but varies more slowly with T. Consequently, while the Einstein approximation fits high temperature specific heat data, it fails at low temperatures.

Nernst and Lindemann[69] made a modification of the Einstein equation. They obtained considerably better agreement with experiment by introducing a second term, $\theta/2$, i. e. $E = 3RT\ .1/2\ \frac{\theta/T}{e^{\theta/T} - 1} + \frac{\theta/2T}{e^{\theta/2T} - 1}$. However, at low temperatures the predicted specific heat varies exponentially with temperature.

The next major step in calculating the frequency distribution was performed by Debye.[70] The Debye theory treats the crystalline solid as an elastic continuum with the provision that elastic waves shorter in wavelength than the atomic spacing are not supported by the lattice. Consequently, the Debye spectrum is characteristic of a continuum except that there is a high frequency limit. It is further assumed that the crystal is isotropic and that there is no dispersion of the elastic waves. The Debye spectrum is composed of modes whose density increases as the square of the frequency, reaching a maximum at the high frequency limit. The position of the limit is established so that there be only 3N modes. For the energy of the crystal Debye obtained

$$E = 9RT\ (T/\theta_D)^3 \int_0^{\theta_{D/T}} \frac{x^3 dx}{e^x - 1} \quad \text{where} \quad \theta_D = \frac{h\nu_D}{k}\ ,\ x = h\nu/kT$$

ν_D is the upper frequency limit and θ_D is called the Debye temperature. At low temperatures $C_v \approx 464 \ (T/\theta_D)^3$ cal/mol° K. The Debye results fit experimental data over a wide range of temperatures. In particular the low temperature values of specific heat fit the T^3 variation more closly than the exponential variation. Because the Debye function for specific heat can be tabulated as molar C_v vs θ_D/T, it is a simple matter to calculate the effective θ_D for any substance at a given temperature when the specific heat at that temperature is known. Consequently, specific heat data are frequently represented as a plot of effective θ_D vs T. Deviations from constant θ_D represent deviations of the solid from the ideal Debye solid.

It is important to recognize that even the very successful Debye theory is only an approximation to the true frequency spectrum of crystalline solids. Through the work of Born and von-Karman[71] a rigorous treatment of the calculation of the frequency spectrum is possible, at least in principle. Born pointed out that the problem involved is essentially a classical problem of normal vibrations. If one assumes a potential for the forces binding the atoms together, then the equations of motion and the eigenfrequencies for small vibrations can be calculated. We shall present the detail of this theory in a later section. Born calculated the frequency distribution for simple linear lattices. From his calculations, it was apparent that the principal errors in the Debye approximation are (1) the assumption that there is no dispersion of the elastic waves, (2) the neglect of the effects due to having

more than one atom per unit cell. Nevertheless, the Born theory predicted the same temperature variation of specific heat at very low temperatures as the Debye theory. Consequently, very little interest was displayed in making the laborous computations for the Born method until significant variations from the Debye approximation were found experimentally.[72]

In a series of papers, Blackman[73] applied the Born theory to several simple lattices, in particular, the simple cubic lattice. While it was necessary to make assumptions concerning the forces between atoms, he found that certain general features of the frequency distribution were present regardless of the nature of the assumed forces. In particular, while there is a strong maximum near the upper frequency limit of the distribution, there is also a weaker secondary maximum at some lower frequency. In Figure 23 we show the relation between Blackman's results and those of the Debye theory. Blackman showed that the effect of the secondary maximum is to cause a minimum in the θ_D vs T curve. Following Blackman, Fine[74] calculated the frequency distribution of the normal modes of a face centered cubic lattice and Leighton[75] calculated the distribution for a body-centered cubic lattice. In each calculation, special assumptions must be made concerning the nature of the forces between atoms.

For real crystals three calculations have appeared in the literature: (1) NaCl by Kellerman,[76] (2) Diamond by H. M. J. Smith,[14] (3) Germanium by Hsieh.[77] We will discuss these calculations in a later section. In the calculations for

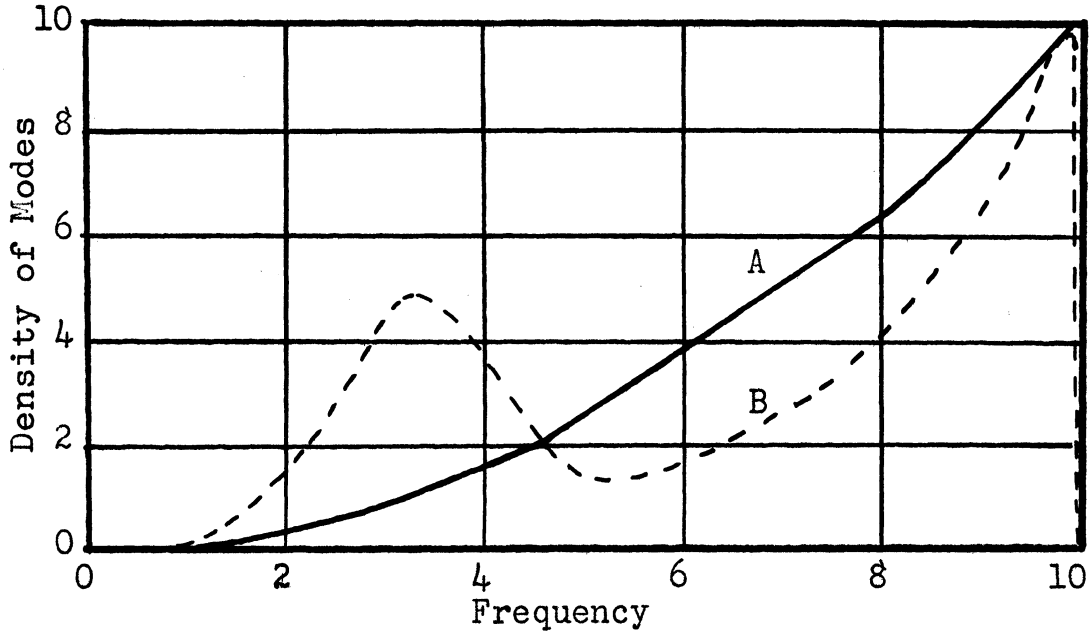

A. After Debye B. After Blackman

Fig. 23

COMPARISON OF DEBYE AND BLACKMAN FREQUENCY DISTRIBUTIONS

real crystals, only the elastic constants must be known in order to calculate the frequency distribution, if the assumed force field does not contain more constants than there are elastic constants. Consequently, when one uses the Born theory, one calculates the frequency spectrum, the specific heat, and related phenomena such as spectral absorption without recourse to experimental data other than the elastic constants. For a cubic crystal three parameters, which can be directly measured, determine the calculations.

When reviewing the status of the Born theory, which is based on firm classical theory and which Born[9] has shown fits the requirements of quantum theory also, it appears that the problem of the frequency spectrum of the crystalline solid has received a satisfactory solution. However, Raman[7] has not agreed with the Born theory and has chosen to formulate a new treatment of the frequency spectrum. Raman's theory is not supported by basic reasoning, but it is based on Raman's interpretation of the observations he has made experimentally. Before describing Raman's theory of lattice dynamics, we must point out that the Raman theory of the anomalies in the properties of diamond is a separate theory which stands apart from the theory under discussion. Raman arbitrarily divides crystal vibrations into two classes: (1) Those which are on "...a large scale and may be described without any reference to the fine structure of the solid. These are the elastic vibrations...". (2) Those which are "essentially dependent on the fine structure of the solid." According to Raman,

the first class is a continuous distribution of frequencies while the second class is made of "discrete and enumerable monochromatic frequencies in the infrared region of the spectrum." No proof of the preceding statements exists. In addition, Raman originally discarded the contribution of the first class to the specific heat. Here he made an error which could be shown experimentally. Since the second class can give only a sum of Einstein contributions to the specific heat, the low temperature specific heat must go to zero exponentially according to the Raman theory. Recently, however, in order to explain the specific heat of diamond, a coworker of Raman[78] has used 3 Debye functions and 9 Einstein functions. With 12 adjustable parameters, it is not surprising that the specific heat curve can be matched. Blackman[79] has compared predictions by Raman with those according to the Born theory for the specific heats of crystalline solids and shows that the Born results, which require no adjustable parameters, are superior to Raman's results. MacDonald[80] reviewed the Raman theory and concluded that the Raman theory is no more than an extension of the Nernst-Lindemann theory which achieves success through the introduction of many adjustable parameters.

Let us now consider the absorption spectrum of a crystalline solid. Using Born's dynamics one predicts that the only active frequencies are those corresponding to modes which are represented by elastic waves whose wavelength is comparable to the wavelength of light.[81] In terms of atomic dimensions, the wavelengths of such elastic waves are essentially infinite.

Consequently, one finds that the absorption spectrum should consist of a few sharp lines whose corresponding modes involve the vibrations of atoms in the unit cell against one another. Corresponding atoms in all unit cells vibrate in phase. For all other wavelengths, the dipole moment change will cancel to zero and no absorption occurs. Similar statements hold for Raman scattering. Raman[82] has not recognized that the Born distribution has only a few allowed frequencies in absorption as well as in Raman scattering, and claims that his theory of lattice dynamics is born out by the fact that the first order Raman scattering spectra of many crystals are composed of discrete lines. On the other hand, when the overtone and combination spectra of crystals are considered Raman has difficulty in explaining the occurrence of broad bands. Since the Born spectrum is expected to have broad overtone and combination bands, a final blow is dealt Raman's theory of lattice dynamics. We shall discuss the selection rules in greater detail in a later section. However, it is now clear that we need only consider the Born theory of lattice dynamics.

We can now answer the first question: "What is the absorption spectrum of an ideal diamond?" It must consist of no more than discrete lines in the fundamental portion of the spectrum and should consist of some broad combination bands. We will show later that no discrete lines are allowed in the fundamental region due to symmetry selection rules. In any case, it is clear that the appearance of the broad IR I bands at wavelengths longer that 7μ is in violation of the general

selection rules for any crystalline solid. Therefore, we can conclude that IR II diamonds display the absorption spectrum of an ideal diamond. IR I diamonds must depart, in some manner, from the Bragg structure.

It is in connection with the variation of the IR I diamonds from ideal behavior that the theories of Raman and of Sutherland and Blackwell have been proposed. Raman[8] claims, without analytical support, that there are four possible configurations for the electronic structure around individual carbon atoms. His diagrams for these configurations are shown in Figure 24. It can be seen from the figure that the structures differ from one another only in the directions indicated by the arrows lying along the tetrahedral bonds. What the nature of the forces may be that support the atoms in the Td I, Td II, and OH II structures has never been explained. In addition, the electronic density derived from X-ray measurements is consistent only with OH I, i. e. the Bragg structure as represented in Figure 1. As with his lattice dynamics, the basic tenets of the Raman theory for diamond are not well-founded in theory but are only qualitative ideas.

Since, in Raman's theory, there are four possible electronic configurations, varying mixtures of the four configurations are supposed to produce the observed variations in properties. In the infrared, the structures with no center of symmetry (Td) account for IR I bands while the structures with center of symmetry (Oh) account for the absence of these bands in IR II diamonds. It is assumed that all vibrations in the Oh structure are automatically centrosymmetric and those

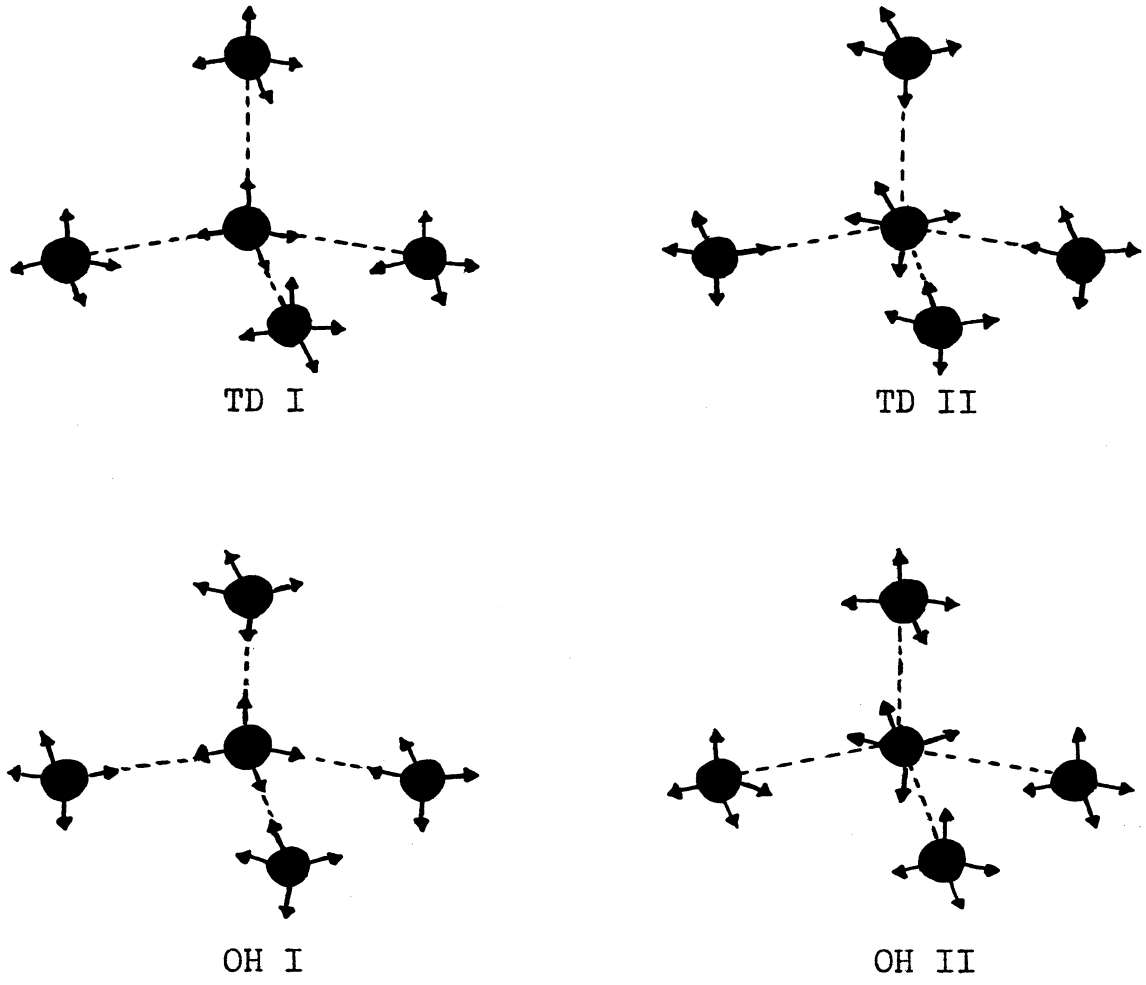

Fig. 24

THE FOUR POSSIBLE ELECTRONIC STRUCTURES OF DIAMOND

(AFTER RAMAN)

in the Td structure are non-centrosymmetric. This theory is extended by the addition of Raman's lattice dynamics. The combination of his two theories leads Raman to the conclusion that the broad absorption from 7 to 12μ is due to the "resonance interaction" of nine discrete frequencies.[83] The band at 7.8μ is supposed to have the same origin as the band at 7.51μ (1332 cm^{-1}) in the Raman spectrum. As Sutherland[84] has pointed out, it is not explained how the interaction can affect the energy levels involved when observing the bands in absorption while it does not affect them when observing the band in scattering. Without further ado, we state that there is no support on any theoretical grounds for the Raman theory for diamond.

Another theory for the anomalies in the properties of diamonds is that proposed by Sutherland and Blackwell.[11] They proposed that defects in the lattice structure cause the anomlies. This theory did not receive any theoretical justification when it was proposed. It was simply stated that the presence of impurities or structural defects could cause a breakdown in the local symmetry of the structure and hence break down selection rules which forbid the fundamentals. Blackwell[10] pointed out that the Born vibrational spectrum of diamond, as calculated by Smith,[14] was very similar to the observed absorption spectra of IR I diamonds. Since these bands do not appear in IR II diamonds, they must be normally forbidden. Hence some structural anomaly must occur in IR I diamonds which breaks down the selection rules. In a later section, we will amplify this theory and attempt to give it theoretical justification.

3.2 Ultraviolet Cutoff

Clearly, the onset of absorption whether at 3200 A. U. or 2250 A. U. is associated with electronic transitions. Since diamond is an insulator we may expect that the electronic zone structure can be represented in the band approximation as a filled band separated by a relatively wide gap from an empty conduction band. In this respect, it differs from silicon and germanium only in the width of the gap separating the filled and conduction bands. These qualitative statements are supported by several calculations of the electronic structure of diamond. The first such calculation was made by Kimball.[85] He found that the eight electrons per unit cell just fill the lower zone system which exists at the observed interatomic distance. He calculated the gap between the filled and unfilled bands to be 7ev (1700 A. U.). Pauling[86] and Slater[87] discussed the form of the Heitler - London function appropriate to valence crystals such as diamond. Pauling showed that the particular linear combination of one s function and 3p functions which are orthogonal and which has maximum directional localization have maximum electron density along the tetrahedral direction, i. e. along the directions connecting nearest neighbors in the Bragg structure. The calculations of electron density by Coulson[29] from X-ray data confirm the Pauling and Slater view. In 1951, Hall[88] made a calculation of the electronic structure of diamond based on this valency description of the crystal. He obtained substantially the same energy levels as those calculated by

Kimball. In 1952, Herman[12] made a new calculation of the electronic structure of diamond using more refined methods. He found a separation of the filled and unfilled levels equal to approximately 6ev which corresponds to a wavelength of about 2050 A. U. This value is close to the observed cutoff of UV II diamonds at 2250 A. U. There can be little doubt that the ultraviolet cutoff in UV II diamonds corresponds to transitions from the filled valency bands to the unfilled conduction bands.

Now we must consider the fact that many diamonds do not transmit to as short wavelengths as 2250 A. U. Some alteration in the electronic structure must occur in UV I diamonds. In the zone structure, the longer wavelength absorption implies the existence of levels lying in the forbidden region between the filled and unfilled bands. The role of such intermediate levels in determining the electric properties of silicon and germanium is well-known in the theory of semiconductors.[89] In general, these levels are introduced by the presence of impurities, vacant sites, or structural imperfection. We can be confident that the explanation for the ultraviolet absorption in UV I diamonds lies in this same field. The theory of Blackwell and Sutherland is entirely consistent with the viewpoint that structural anomalies alter the electronic structure in UV II diamonds. The connection between the infrared and ultraviolet absorption lies in the fact that both phenomena depend on the periodicity of the lattice. In the collective electron[90] treatment each electron is described by a wave function extending throughout the lattice, and it is the

periodic field of the lattice which leads to a separation of the permissible states into zones. Deviations from the ideal periodic structure alter the field of the lattice and hence alter the zone structure. Similarly, in Born's lattice dynamics the elastic waves which represent the normal modes of the lattice are plane waves only so long as the lattice has its ideal periodicity. Deviations from the periodicity alter the forms of the normal modes and hence alter the phase relationships between unit cells.

3.3 X-ray

In the review of experimental work we have pointed out that there is no explanation for the occurrence of secondary extra spots in X I diamonds. Therefore, we shall not attempt to review the various existing theories involved in the associated X-ray phenomena. It is certain, however, that current theories of X-ray diffraction do not predict the extra spots in any crystalline material regardless of its symmetry. Consequently, it is safe to assume that X I diamonds depart from the ideal Bragg structure in some manner. However, since the principal features of the diffraction pattern of X I diamonds do fit the Bragg structure, and since there is a marked regularity in the position of the extra spots, any departure from the ideal Bragg structure must not change the gross structure over wide regions of the crystal, and it must have some definite orientation with respect to the axes of the crystal.

3.4 Blue Fluorescence and Absorption

The electronic transitions associated with absorption and fluorescence near 4155 A. U. in diamond are similar to those observed in ionic crystals where the transitions are associated with energy levels introduced by imperfections such as vacant sites or impurity atoms. However, it is not certain what the origin of the levels in diamond may be. Raman[37] argues that the fluorescence is fundamental to the lattice while Bishui[91] and others argue that the fluorescence is dependent upon structural imperfections. We shall not attempt to present the arguments in detail. However, since blue fluoresence and absorption occur with variable intensity and are sometimes absent, it is certain that if the levels involved in the transitions are fundamental to the lattice, the transitions must be normally forbidden, and they occur when some modification of the structure occurs which breaks down the selection rules. Consequently, it is surely valid to assume that blue fluorescence and absorption are characteristic of a lattice imperfection.

3.5 Other Properties

(3.5.1 Conductivity)
(3.5.2 Particle Counting)
(3.5.3 Thermal Conductivity)

3.5.1 Photoconductivity

The property of photoconductivity is intimately related to the electronic structure. It is known[1] that while UV II diamonds normally conduct electricity when exposed to ultra-

violet light, UV I diamonds exhibit much lower conductivity under similar conditions. This means that in UV II diamonds, absorption of light quanta can raise electrons to the conduction band, and while some of these electrons are trapped or scattered, many migrate to the anode. The problem is reduced to considering (1) from which levels are the electrons initially excited by the light quanta, (2) the nature of the electron traps. In our discussion of the ultraviolet cutoff, we have established that UV II diamonds are essentially ideal in their electronic structure. This implies that the photoconduction electrons in UV II diamonds are excited from the tail of the fundamental absorption band, i. e. the edge of the filled band, to the conduction band. If the structure is ideal, only lattice scattering of the electrons deters their movement through the solid. However, the absorption lines between 2250 A. U. and 2500 A. U. in many UV II diamonds indicate that there are energy levels in the forbidden zone near the conduction band. These levels may be associated with electron traps. However, the density of these levels in UV II diamonds must be low compared to UV I diamonds. In UV I diamonds there are many levels (4155 A. U. to 2250 A. U.) in the forbidden zone. These levels are associated with imperfections some of which may serve as electron traps. Consequently, the photoconductivity of UV I is very small. As Seitz[90] points out, excitations from wavelengths well within the absorption band cannot be expected since the reflectivity will be high and few quanta will penetrate into the body of the solid. Similarly, in UV I diamonds, few quanta of sufficient energy to raise electrons

from the edge of the filled band to the conduction band will penetrate the solid, since the absorption coefficient (and hence the reflectivity) is large in this wavelength region.

3.5.2 Particle Counting

The variation of the ability of diamonds to act as particle counters has recently received new qualitative theoretical consideration.[92] Ahearn has pointed out that the counting properties of the diamonds can be related to the type and configuration of the imperfections. He proposes that the imperfections may occur in clusters so that a diamond may be composed of conductive channels next to insulating regions. We shall not present further details of this proposal, but while Ahearn's proposal is not rigorously proved, it shows that the variations in counting properties are consistent with a model of clusters of imperfections, the precise arrangement of which will influence the counting properties. His proposal is especially important in view of the variation of counting properties within a given diamond.[93] The fact that there appears to be no unique correlation between particle counting ability[30] and the UV and IR properties is probably related to the fact that in particle counting, the existence of many electron traps will deter the counting ability. For example, fluorescent diamonds are usually poor counters.[94] One infers that the levels associated with fluorescence at 4155 A. U. are connected with imperfections which act as electron traps. On the other hand, UV II diamonds are presumably ideal in struc-

ture and hence contain few of Ahearn's clusters of imperfections. Consequently, a good particle counter can be expected to have UV and IR properties intermediate between our II and strong I.

3.5.3 Thermal Conductivity

The experimental values for the thermal conductivity of diamond at low temperatures has been said to be consistent with Ahearn's proposal of clusters of imperfections.[95, 96] Klevens has applied his theory of the effect of particle size on thermal conductivity to show that the experimental values for diamond can be explained in terms of imperfections of the order of 20 to 60 interatomic distances. "Either the imperfections form linear arrays of length large and diameter small compared with these wavelengths or they form clusters whose diameters are of the same order as the size of the wavelengths." Since the thermal resistance depends upon both scattering by the lattice and scattering by imperfections, there is clearly a relationship between this deduction by Klevens and other properties which we have discussed, all of which depend upon lattice periodicity and departures from ideal periodicity. Unfortunately, no data are available on the variation of thermal conductivity between diamonds or its correlation to other physical properties.

3.6 Summary

We have seen that all of the important anomalies in the structure sensitive properties of diamond are consistent with

the existence of imperfections in the structures of UV I, IR I, and X I diamonds. In each case, the discussion has been qualitative in the sense that no specific imperfection has been proposed, and no quantitative calculations have been made. In addition, while each of the electronic phenomena such as ultraviolet cutoff, fluorescence and absorption in the visible, etc. has some counterpart in the observed phenomena in other crystals, i. e. the introduction of energy levels in the forbidden zone, the infrared absorption spectrum and the X-ray diffraction pattern have no such counterpart since only diamond shows the observed anomalies. In fact, since this work has started it has been shown that absorption bands occur in the spectra of silicon and germanium which are comparable to 8μ bands in diamond in position, although their intensities appear to be constant. We shall discuss this later. But these two points remain unique, (1) Variation in intensity of absorption near 8μ and (2) Occurrence of extra streaks in the X-ray pattern. No other substance is known to show these properties. In the following sections we will attempt to show how far current theory can go in explaining the positions of the bands in the infrared spectrum of diamond, and we will also show that the same theory applies to the spectra of silicon and germanium. Finally, we shall attempt to account for the anomalous variation in intensity of the 8μ bands in diamond.

Chapter 4

PRESENT THEORETICAL WORK

4.1 The Frequency Distribution of Lattice Vibrational Modes

(4.1.1 Diamond)
(4.1.2 Germanium)
(4.1.3 Silicon)
(4.1.4 Analyses of the Fundamental Branches)

4.1.1 Diamond

The broad absorption bands observed in the infrared spectrum of the diamond crystal must have their origin in the vibrational modes associated with the diamond lattice. The theory of the crystalline lattice as developed by Born[15] states that the frequency distribution of the normal modes will be characterized by 3p analytically distinct functions (normally called "branches"), where p is the number of atoms per unit cell in the crystal. Diamond is made up of two interpenetrating face-centered lattices, displaced one quarter of the way along the space diagonal. Such a lattice can be generated from a unit cell containing two atoms, one belonging to each of the face-centered lattices. Consequently, for diamond, $p = 2$, and the frequency distribution will be made up of 6 branches.

In order to calculate the form of the distribution of modes in a given branch, one must set up the so-called

"Dynamical Matrix".[97] This matrix is formed in the following manner: (1) Assumptions are made as to the form of the forces between atoms. (2) The three equations of motion for each atom are calculated on the basis of classical mechanics. (3) Solutions in the form of triply periodic functions are substituted in the equations of motion. The periodicity is expressed through three phases, φ_i. The φ space is equivalent to the well-known reciprocal lattice. (4) After substitution, one has 3p equations in the 3p amplitudes of the assumed solutions. One now demands that these 3p equations be satisfied simultaneously. A matrix of the coefficients of the amplitudes is formed. This is the dynamical matrix $D(\varphi_i)$ with added terms on the diagonal, i. e. $(D(\varphi_i) - \omega^2 I)$ where $\omega = 2\pi\nu$, ν = the frequency of the periodic solution. The condition that all 3p equations have a non-trivial solution requires that the determinant $|D(\varphi_i) - \omega^2 I|$ vanish. This determinant is 3p square. Consequently, for each point in φ space $(\varphi_1, \varphi_2, \varphi_3)$ there are 3p corresponding values of ν. These 3p solutions are the values of the frequency for the 3p branches at that point in φ space.

The number of modes having frequencies between ν and $\nu + d\nu$ is the distribution function $N(\nu)$. Each branch can be formed separately in the following manner. (1) A number of uniformly spaced points in φ space are chosen. (2) The value of ν for the branch at each point is calculated using the dynamical matrix. (3) A small interval of frequency, $\Delta\nu$, is chosen. (4) The number of calculated ν's falling in each interval is plotted vs the average frequency of the interval. (5) n such counts are made, shifting the boundaries of each

interval by $\Delta\nu/n$ each time. (6) $N_i(\nu)$ for the i^{th} branch is a curve through the plotted points. Clearly, the accuracy of such a calculation is increased by increasing the number of points used in ϕ space.

We have, so far, neglected the calculation of the force constants entering into the dynamical matrix. In general, it is found that force constants corresponding to the assumed force field can be expressed in terms of elastic constants, C_{ij}. In the case where a solid has n independent elastic constants, n independent force constants can be determined by the elastic constants.

In the particular case of diamond, H. M. J. Smith[14] performed a calculation following the method outlined above. For diamond there are three independent elastic constants, C_{11}, C_{12}, C_{44}, which have been determined experimentally.[98] Consequently, 3 independent force constants can be determined. Smith chose a force field which involved a completely general first neighbor interaction, demanding only that the corresponding potential be expandable in a Taylor series in the displacements. Only terms corresponding to small displacements from equilibrium are retained. Because of the symmetry of the lattice, such a field requires only two constants for specification (Smith's α and β). Since there are three elastic constants, the field is overspecified and one identity results between the C_{ij}. In addition, the general theory predicts that the upper limiting frequency of the total distribution $N(\nu)$ will be Raman active. This frequency, ν_R, is observed. ν_R can be expressed in terms of α and hence in terms of the C_{ij}.

Consequently, a second identity is obtained: a = unit cell side; m = mass of carbon atom.

Identity 1: $\frac{4\,C_{11}\,(C_{11} - C_{44})}{(C_{11} + C_{12})^2} = 1$; Identity 2: $\frac{4\pi^2\,C^2\,\frac{m}{2a}\,\nu_R^2}{8\,C_{11}} = 1$

The measured values are:

$C_{11} = 9.5 \times 10^{12}$ dynes/cm

$C_{12} = 3.9 \times 10^{12}$

$C_{44} = 4.3 \times 10^{12}$

$\nu_R = 1332\ cm^{-1}$

$2a = 3.56 \times 10^{-8}$ cm

$m = 1.995 \times 10^{-23}$ g

Using these values, identity 1 gives the result 1.11 vs 1; identity 2 gives the result 0.46 vs 1.

Since the second identity is so poorly satisfied, Smith added an additional force field in the calculation. This field is central between second neighbors and characterized by a single force constant "μ". Using ν_R, one identity can be established between the C_{ij}.

Identity 3: $\frac{8A\,(A + 8C_{11} - 16C_{44})}{(3A - 8C_{11} + 16C_{12})^2} = 1$; $A = 4\,\pi^2\,C^2\,\frac{m}{2a}\,\nu_R^2$

Using the listed values of the constants, identity 3 gives 1.4 vs. 1. On the basis of these results Born[99] has pointed out that there are three possibilities: (1) The elastic constants are in error, (2) The second neighbor forces are not central, (3) More distant neighbors interact. If either of the latter two possibilities is true, Smith's formulation is inadequate. Since no better solution was available, Smith

chose to examine the elastic constants.

There is one experimental check of C_{11} and C_{12} in the value of the bulk modulus, 1/K: $1/K = 1/3(C_{11} + 2\,C_{12})$. The observed values of $K^{100,\ 101}$ are 0.16 and 0.18 x 10^{-16} /megabar. The average, 0.17 x 10^{-6} /megabar, gives $1/K = 5.9 \times 10^{12}$ dynes/cm^2. The observed values of C_{11} and C_{12} give $1/K = 5.77 \times 10^{12}$ dynes/cm^2. The discrepancy is 2% whereas the deviation of the observed bulk modulus is 6%, so that C_{11} and C_{12} must be essentially correct. On this basis, Smith calculated as follows:

$$\nu_R = \frac{1}{2\pi C}\sqrt{\frac{8\alpha}{m}} = 1332\ \text{cm}^{-1}: \quad \alpha = 0.157 \times 10^6\ \text{dynes/cm}$$

$$\alpha + 8\mu = 2aC_{11} \qquad : \quad \mu = 0.0226 \times 10^6$$

$$\beta = 1/4\,[2a\,(C_{11} + 2\,C_{12}) + \alpha - 16\mu]: \quad \beta = 0.104 \times 10^6$$

$$C_{44} = \frac{1}{2a}[\alpha - \beta^2/\alpha + 4\mu]: \quad C_{44} = 5.0 \times 10^{12}$$

The observed value of C_{44} is 4.3 x 10^{12}. The alteration by Smith is 14%.

With the revised value of C_{44}, identity 3 now gives the result 1.04 vs 1. This represents improved agreement over the previous result of 1.4 vs 1.

In order to clarify the concepts involved in these calculations, it is worthwhile to consider the physical interpretation of the three force constants α, β, and μ. The expression for the highest frequency of the lattice, ν_R, is $\nu_R = \frac{1}{2\pi C}\sqrt{\frac{8\alpha}{m}}$. The corresponding mode is the vibration of one face-centered lattice against the other along the bond direction. Since a simple diatomic C-C stretching mode would give $\nu = \frac{1}{2\pi C}\sqrt{\frac{2K}{m}}$, it is clear that α can be interpre-

as a bond stretching force constant. The constant β does not, by itself, determine a mode, but it is analogous to the coefficients of the cross terms in the potential function of a polyatomic molecule. The constant "μ" can be interpreted as a constant between second neighbors comparable to the force constants used in the central force field approximation for polyatomic molecules[102] since the corresponding potential is central.

To this point, the only justification for altering the measured value of C_{44} is that the identities which follow from Smith's force field are not satisfied by the unaltered C_{44}. Predictions based on the altered C_{44} can be used to test its validity. One such prediction is the variation of specific heat with temperature. This variation is determined by $N(\nu)d\nu$. Smith used her calculated $N(\nu)$ to determine C_v vs T and obtained excellent agreement with experiment. Smith also calculated a different $N(\nu)$ using the α and β given on page 101, but setting $\mu = o$. This calculation does not correspond to the true case for diamond since the values of α and β used were originally calculated on the assumption that $\mu \neq o$. However, we shall make use of both calculations in later sections. In order to avoid confusion in nomenclature we will name the calculations as follows:

Calculation A: $\alpha = 0.157 \times 10^6$, $\beta = 0.104 \times 10^6$, $\mu = 0.0226 \times 10^6$

Calculation B: $\alpha = 0.157 \times 10^6$, $\beta = 0.104 \times 10^6$, $\mu = 0$

Calculation A is based on a force field which includes both

first and second neighbor interaction and is valid for diamond if the alteration of C_{44} is accepted. Calculation B is based on a force field which includes only first neighbor interaction but is not valid for diamond for the reason given above. The plots of N (ν) vs ν obtained by Smith for the two calculations are shown in Figure 25 (A, B). Her data are given in Table 11 (A, B).

Another check of the altered value of C_{44} is offered by Smith's analysis of the observed second order Raman effect. Rather than assuming that the potential includes anharmonic terms, Smith assumed that there is "electrical anharmonicity."[102] Because of this anharmonicity certain overtones and combinations are allowed. Without considering the theory in detail, it is sufficient to state that she determined that the following bands are allowed in second order Raman scattering: (1) The first overtones of all branches, (2) The sum and difference bands involving branches 1 and 2, 1 and 3, 2 and 3, 4 and 5, 4 and 6, 5 and 6. In calculations A, used here, branches 1 and 2 are degenerate. The contours of the combination and overtone distributions were obtained by numerical integration in the manner described for $N_i(\nu)$. In this case, one combines the two frequencies of the branches involved at each point in ϕ space and then obtains the distribution of the combined values of ν. Smith's results are shown in Figure 26. She found that the observed spectrum could be matched if the relative intensities of the allowed branches was I(33): I(44): I(11): I(13) = 40:12:1:1;

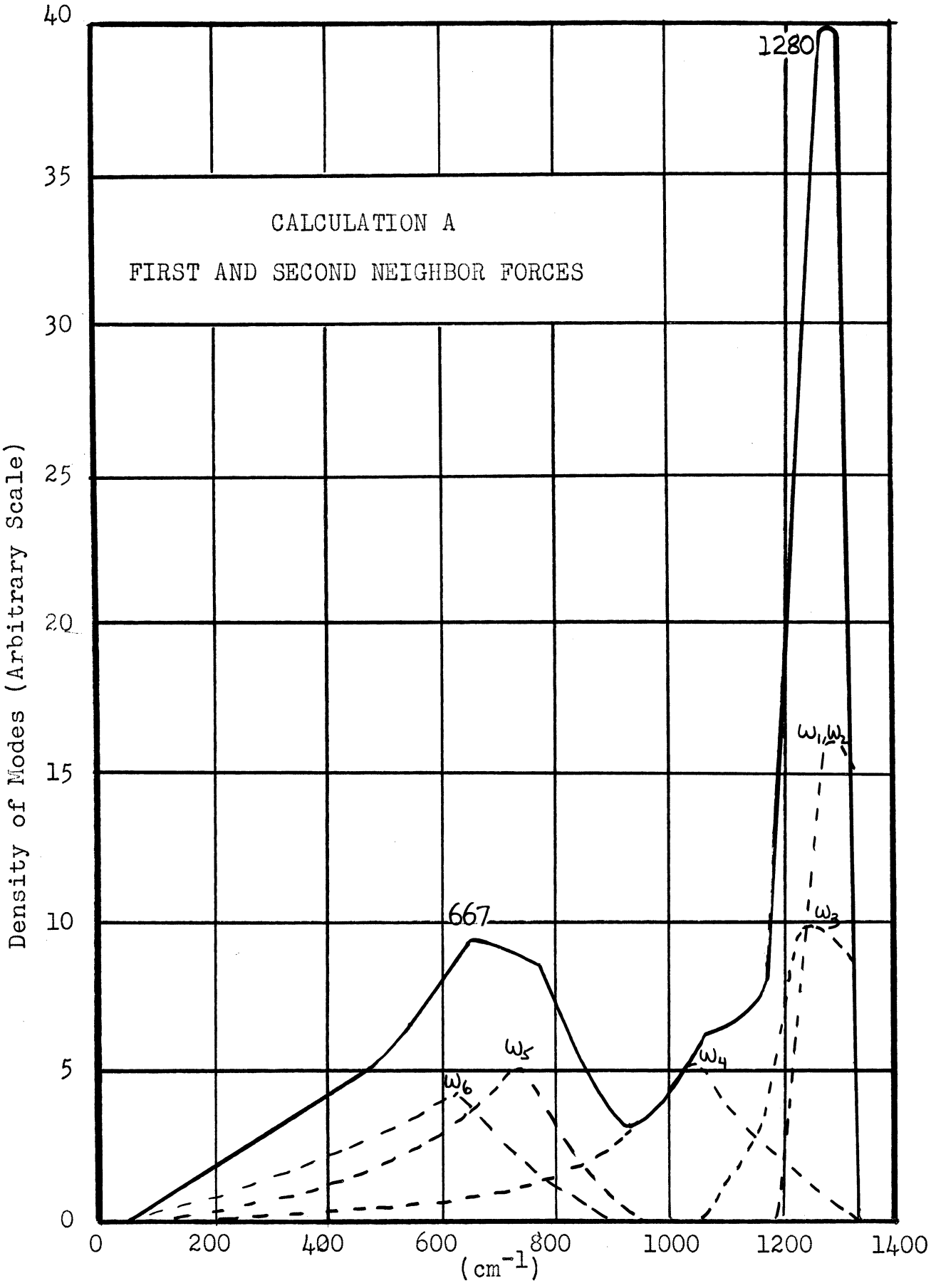

Fig. 25A

THE FREQUENCY DISTRIBUTION OF VIBRATIONAL MODES IN DIAMOND

(AFTER SMITH)

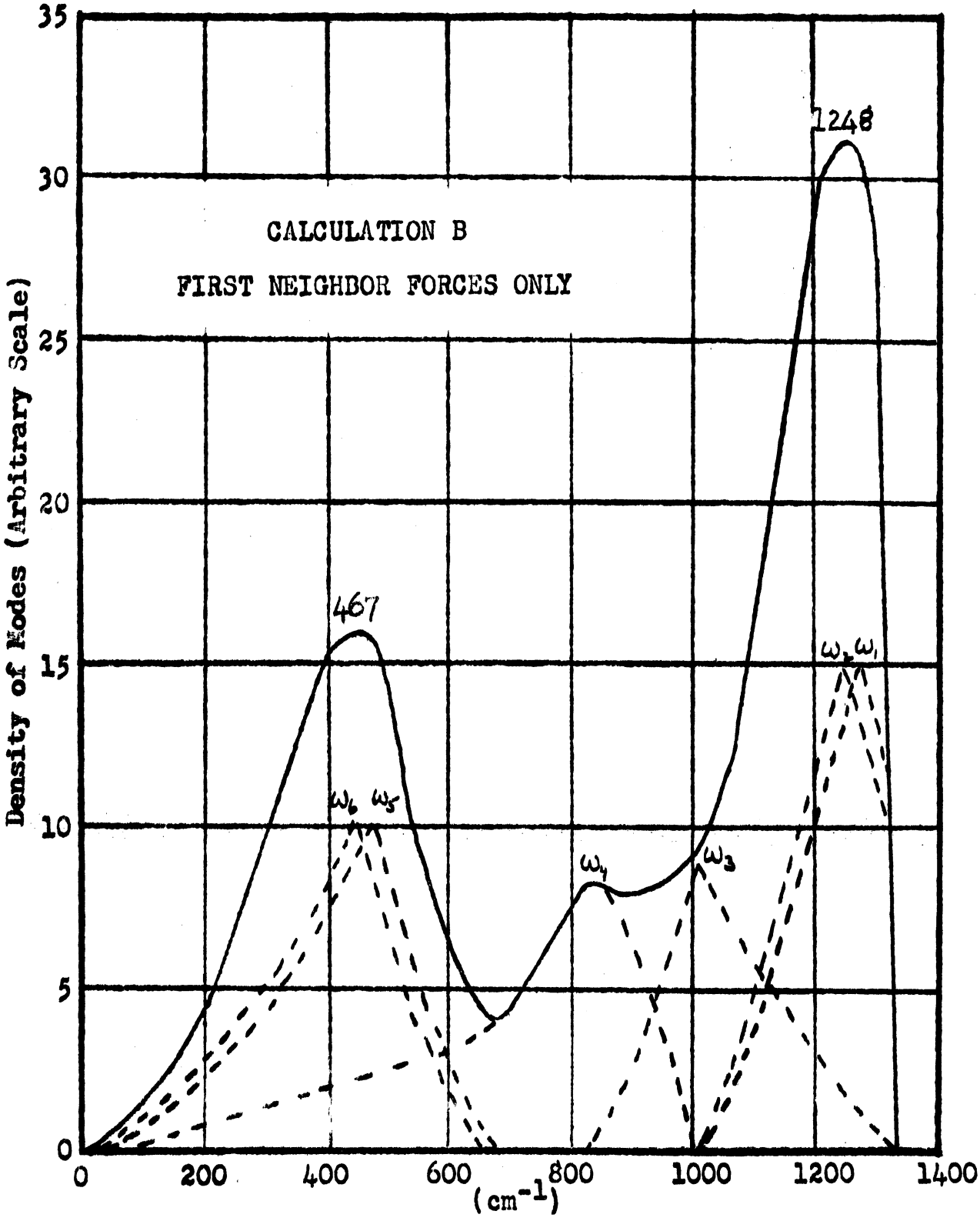

Fig. 25B

THE FREQUENCY DISTRIBUTION OF VIBRATIONAL MODES IN DIAMOND

(AFTER SMITH)

Table IIa

FREQUENCIES OF VIBRATION OF DIAMOND UNDER THE ACTION OF FIRST AND SECOND NEIGHBOR FORCES

Reciprocal Lattice Point			Branch Number					
P_x	P_y	P_z	ω_1	ω_2	ω_3	ω_4	ω_5	ω_6
8	4	0	2.51	2.51	2.12	2.12	1.48	1.48
8	2	2	2.48	2.48	2.27	2.12	1.53	1.30
8	2	0	2.51	2.51	2.17	2.17	1.44	1.44
8	0	0	2.48	2.48	2.23	2.23	1.40	1.40
7	3	1	2.50	2.50	2.24	2.07	1.55	1.33
7	1	1	2.48	2.48	2.30	2.06	1.43	1.35
6	6	0	2.48	2.48	2.27	2.12	1.53	1.30
6	4	2	2.51	2.51	2.28	2.07	1.35	1.16
6	4	0	2.51	2.51	2.34	2.01	1.47	1.25
6	2	2	2.49	2.49	2.33	1.96	1.37	1.21
6	2	0	2.51	2.51	2.40	1.90	1.34	1.23
6	0	0	2.49	2.49	2.43	1.97	1.28	1.28
5	5	1	2.49	2.49	2.27	2.00	1.46	1.15
5	3	3	2.49	2.49	2.32	2.06	1.13	1.06
5	3	1	2.51	2.51	2.35	1.88	1.30	1.05
5	1	1	2.50	2.50	2.42	1.68	1.17	1.14
4	4	4	2.50	2.50	2.34	2.11	0.99	0.99
4	4	2	2.50	2.50	2.38	1.96	1.14	0.99
4	4	0	2.50	2.50	2.44	1.78	1.38	0.99
4	2	2	2.50	2.50	2.49	1.71	0.98	0.98
4	2	0	2.51	2.51	2.49	1.54	1.09	0.88
4	0	0	2.51	2.51	2.51	1.35	0.97	0.97
3	3	3	2.50	2.50	2.45	1.84	0.91	0.91
3	3	1	2.50	2.50	2.43	1.55	1.01	0.80
3	1	1	2.51	2.51	2.51	1.21	0.77	0.74
2	2	2	2.51	2.51	2.51	1.34	0.69	0.69
2	2	0	2.51	2.51	2.51	1.07	0.73	0.54
2	0	0	2.51	2.51	2.51	0.71	0.52	0.52
1	1	1	2.51	2.51	2.51	0.71	0.37	0.37

H. M. J. Smith's Data

Units of ω are 10^{14} sec.$^{-1}$

Table 11B

FREQUENCIES OF VIBRATION OF DIAMOND UNDER THE ACTION OF FIRST NEIGHBOR FORCES ONLY

Reciprocal Lattice Point			Branch Number					
P_x	P_y	P_z	ω_1	ω_2	ω_3	ω_4	ω_5	ω_6
8	4	0	2.29	2.29	1.78	1.78	1.03	1.03
8	2	2	2.32	2.27	1.84	1.71	1.06	0.95
8	2	0	2.29	2.29	1.78	1.78	1.03	1.03
8	0	0	2.29	2.29	1.78	1.78	1.03	1.03
7	3	1	2.33	2.28	1.89	1.66	1.05	0.95
7	1	1	2.31	2.30	1.93	1.61	1.02	0.99
6	6	0	2.32	2.27	1.84	1.71	1.06	0.95
6	4	2	2.36	2.33	1.92	1.62	0.94	0.85
6	4	0	2.35	2.29	1.94	1.59	1.03	0.90
6	2	2	2.35	2.33	1.98	1.54	0.94	0.88
6	2	0	2.34	2.32	2.04	1.46	0.97	0.91
6	0	0	2.33	2.33	2.09	1.40	0.94	0.94
5	5	1	2.37	2.31	1.94	1.60	0.98	0.85
5	3	3	2.39	2.38	1.95	1.58	0.80	0.78
5	3	1	2.38	2.35	2.07	1.42	0.89	0.79
5	1	1	2.37	2.37	2.18	1.25	0.83	0.82
4	4	4	2.40	2.40	1.91	1.63	0.73	0.73
4	4	2	2.40	2.38	2.02	1.49	0.81	0.73
4	4	0	2.40	2.34	2.11	1.37	0.90	0.73
4	2	2	2.41	2.41	2.17	1.26	0.71	0.69
4	2	0	2.43	2.38	2.25	1.11	0.79	0.65
4	0	0	2.41	2.41	2.32	0.96	0.70	0.70
3	3	3	2.42	2.42	2.11	1.36	0.67	0.67
3	3	1	2.44	2.41	2.24	1.13	0.70	0.59
3	1	1	2.46	2.45	2.36	0.86	0.55	0.52
2	2	2	2.46	2.46	2.33	0.95	0.50	0.50
2	2	0	2.48	2.46	2.40	0.75	0.50	0.39
2	0	0	2.48	2.48	2.46	0.49	0.37	0.37
1	1	1	2.50	2.50	2.46	0.48	0.27	0.27

H. M. J. Smith's Data

Units of ω are 10^{14} sec.$^{-1}$

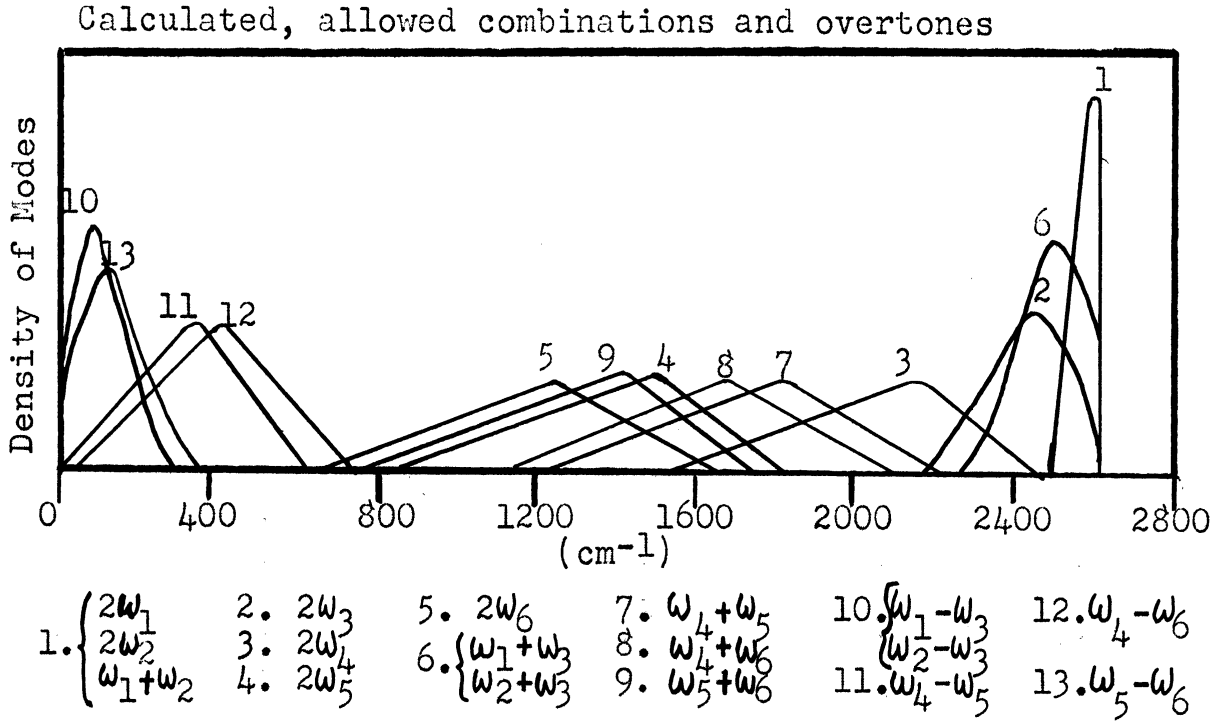

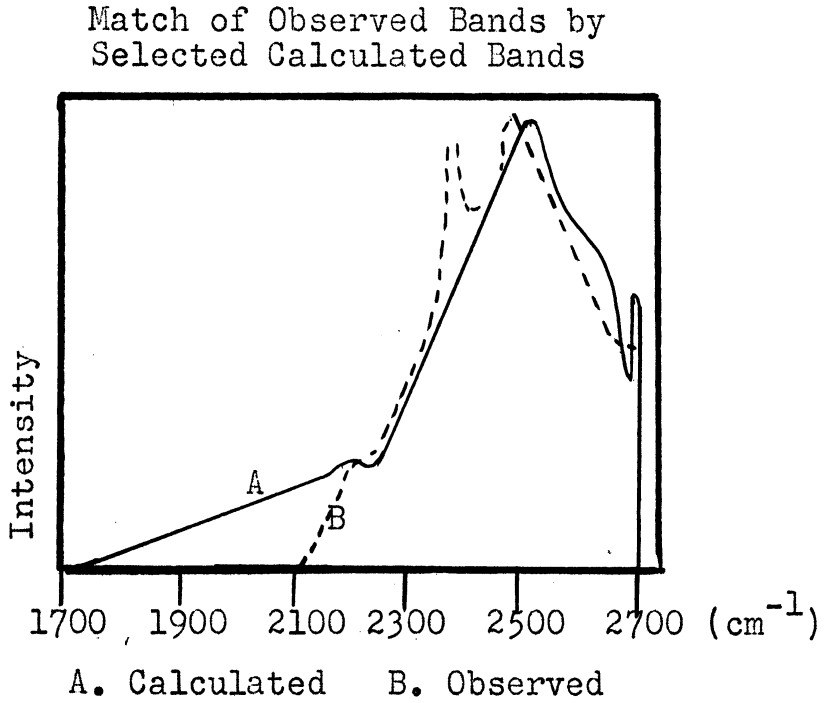

Fig. 26

THE SECOND ORDER RAMAN SCATTERING OF DIAMOND

(AFTER SMITH)

all other branches having zero intensity. Smith's calculated positions for the maxima of individual combinations and overtones are given below. Maxima in the observed Raman spectrum occur at 2460 cm^{-1} and 2176 cm^{-1}.

Table 12

CALCULATED MAXIMA ALLOWED IN RAMAN SCATTERING

Combination	Maximum	Combination	Maximum	Combination	Maximum
$2\omega_1$	2602	$\omega_1 + \omega_3$	2522	$\omega_1 - \omega_3$	106
$2\omega_2$		$\omega_2 + \omega_3$		$\omega_2 - \omega_3$	
$2\omega_3$	2469	$\omega_4 + \omega_5$	1805	$\omega_4 - \omega_5$	345
$2\omega_4$	2177	$\omega_4 + \omega_6$	1683	$\omega_4 - \omega_6$	409
$2\omega_5$	1487	$\omega_5 + \omega_6$	1434	$\omega_5 - \omega_6$	133
$2\omega_6$	1258				

The important question is whether or not Smith's calculation of the second order Raman effect is an adequate test of her calculated frequency distribution. Out of thirteen allowed bands only four are used to determine the contours of the observed bands. In addition, no allowance has been made for the effect of anharmonicity in the potential on the frequencies of combinations and overtones. Finally, there are several branches whose maxima fall in the region of the maximum of the second order Raman scattering. We conclude that while Smith's method of interpreting the observed spectrum is correct, in principal, it does not afford

a rigorous test of the precise positions of the individual frequencies.

4.1.2 Germanium

The methods already discussed also apply to the lattice of germanium since it has the same crystal structure as diamond. By the introduction of the measured elastic constants, the frequency distribution for germanium can be obtained. A calculation has been made by Hsieh[77] in which he considers only first neighbor interaction. His result for $N(\nu)$ is shown in Figure 27.

We will now examine the identities calculated by Smith to determine the validity of Hsieh's assumption that second neighbor interaction is negligible. The elastic constants used are those recently measured by W. L. Bond[103] and differ only slightly from Hsieh's values.

	Our Calculation	Hsieh's Calculation
C_{11}	1.298×10^{12} dynes/cm	1.29×10^{12} dynes/cm
C_{12}	0.488×10^{12}	0.48×10^{12}
C_{44}	0.673×10^{12}	0.67×10^{12}

$m = 72.6$ atomic units

$2a = 5.62 \times 10^{-8}$ cm

With these constants identity 1 gives 1.017 vs 1; identity 2 gives $\nu_R = 369$ cm^{-1}. Because ν_R is not known for germanium, the second identity gives a numberical value for ν_R which has no direct experimental check. If we include second neighbor interaction for germanium, identity 3 gives $\nu_R = 396$ cm^{-1}.

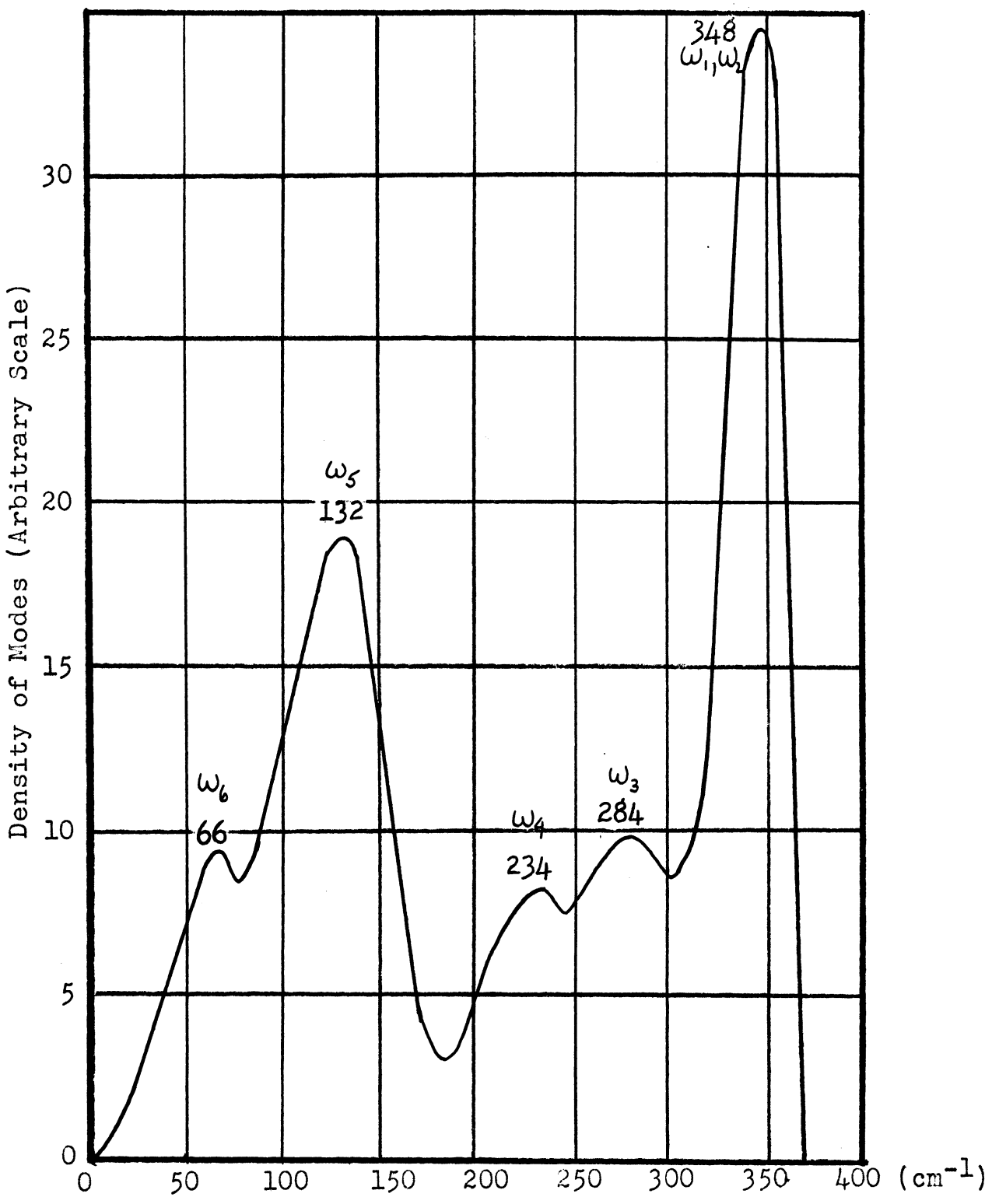

Fig. 27

THE FREQUENCY DISTRIBUTION OF VIBRATIONAL MODES IN GERMANIUM

(AFTER HSIEH)

We will now calculate the force constants which are determined by the measured elastic constants of germanium. We also make a similar calculation for diamond in which elastic constants (using Smith's altered C_{44}) are used. This calculation differs from Smith's calculation B in that the measured value of ν_R is not included as a parameter. In the following table those quantities with subscript "1" are calculated assuming first neighbor interaction alone and the listed values of the elastic constants are the only quantities used in determining the values. We shall call this "Calculation C". The quantities labelled with subscript "2" are calculated assuming both first and second neighbor interaction. For germanium the calculation depends only on the measured elastic constants, while for diamond, since we use the altered C_{44}, the calculation is equivalent to Smith's calculation A.

Table 13

ELASTIC AND FORCE CONSTANTS FOR DIAMOND AND GERMANIUM

	C_{11}	C_{12}	C_{44}	α_1	β_1
Germanium	1.298	0.488	0.673	.0725	.0497
Diamond	9.5	3.9	(5.0)	.338	.239
Ratio $\frac{\text{Diamond}}{\text{Germanium}}$	7.32	7.99	7.43	4.66	4.81
	α_2	β_2	μ_2	ν_{R_1}	ν_{R_2}
Germanium	.0839	.0582	-.0014	369	396
Diamond	.157	.104	+.0226	1951	1332
Ratio $\frac{\text{Diamond}}{\text{Germanium}}$	1.87	1.79	-16.14	5.30	3.36

The sign of "μ" for germanium differs from that of diamond. This indicates a repulsion between second neighbors. Since the value is small, it seems likely that second neighbor interaction in germanium is negligible. It will be noticed that the effect of the introduction of second neighbor interaction is to reduce ν_R in diamond and to raise ν_R in germanium.

Since our calculation C for germanium and Smith's calculation B for diamond are both on the assumption that second neighbor interaction is negligible we can compare the two calculations by comparing the force constants used:

	α	β
Our calculation C for germanium:	.0725	.0497
Smith's calculation B for diamond:	0.157	0.104
Ratio B/C:	2.165	2.092
Average:	2.129	
Deviation:	± 2%	

Whether the agreement of the ratios of the force constants is fortuitous or not, the fact that the two ratios are closely the same can be used to develop relations between the frequency distribution from Smith's calculation B and Hsieh's calculation for germanium which is equivalent to our calculation C. In order to find the desired relations, we must return to Smith's formulation of the dynamical matrix. It is found that each element of that matrix contains a factor α or β. Since the α's and β's for the calculations B and C are mutually proportional, the proportionality factor may be removed to the front of the matrix. In addition, a factor 1/m occurs in front of the matrix. $m_{ge}/m_c = 6.05$. Therefore, the eigenvalues of

the matrix, V^2, for calculation B will be 2.129 x 6.05 times the corresponding eigenvalues of calculation C. Finally, the frequency scales for calculation B will be $\sqrt{2.129 \times 6.05} = 3.58$ times the frequency scale for Calculation C.

In order to check the results of these calculations we compare results obtained by Hsieh for germanium (calculation C) and by Smith in her calculation B for diamond. (Figure 27 and Figure 25B). Using the positions indicated we obtain:

	Diamond	Germanium	Ratio
First Maximum	1248 cm^{-1}	348 cm^{-1}	3.59
Second Maximum	467	132	3.55
Minimum	695	179	3.88

The variation in the ratio indicates that Smith and Hsieh did not perform their calculations in precisely the same manner. If we use individual maxima in Hsieh's curve arising from branch maxima and compare with Smith's branch maxima we obtain:

Table 14

CORRESPONDING MAXIMA IN FIGURE 27 AND FIGURE 25B

Germanium Maxima (Calculation C)		Diamond Maxima (Calculation B)	Ratio
$\omega_1\omega_2$	348 cm^{-1}	1248 cm^{-1}	3.59
ω_3	284	1007	3.55
ω_4	234	830	3.55
$\omega_5\omega_6$	132	467	3.55

The agreement of these ratios with the predicted value of 3.58 is very satisfactory. We have ignored the low frequency maximum

at 66 cm^{-1} in Hsieh's calculation. Calculations in a later section show that it is not a principal maximum of a branch. It is clear that the lack of agreement in the first comparison is due to a difference in the position of the minimum. Evidently, Smith and Hsieh used slightly different methods of numerical integration.

From the results of the preceding section we are assured that a scale factor of approximately 3.58 relates the numerical values obtained for frequencies in Smith's Calculation B and the frequencies for germanium.

Hsieh showed that his frequency distribution gives correct results for the variation of the specific heat of germanium with temperature. This indicates that the Calculation C for germanium corresponds to the true distribution. However, for diamond it is not the Calculation B which fits observed specific heat data. Instead, it is calculation A. Consequently, we can predict that the true distribution for germanium, while it is simply related to Smith's Calculation B for diamond, is not simply related to the true distribution for diamond, i. e. Calculation A. This prediction follows from the fact that there is no simple relation between the Calculation A and B made by Smith. Physically, the difference between the true distributions for germanium and diamond lies in the second neighbor interaction which is important in diamond, but negligible in germanium. We shall return to this point when we attempt to correlate the infrared spectra of diamond and germanium.

4.1.3 Silicon

For silicon we proceed in the same manner as with germanium.

There is no calculation comparable to Hsieh's for germanium. However, if the silicon force constants are related to those of germanium by a constant factor, Smith's B calculation can be used for silicon.[104] For silicon the elastic constants and corresponding force constants are as follows:

Table 15

ELASTIC AND FORCE CONSTANTS IN SILICON AND GERMANIUM

	C_{11}	C_{12}	C_{44}	α_1	β_1
Si	1.6740	.6523	.7957	.0909	.0763
Ge	1.298	.488	.675	.0725	.0497
Si/Ge	1.290	1.337	1.182	1.254	1.354

	α_2	β_2	μ_2	ν_{R_1}	ν_{R_2}
Si	.1537	.1101	-.0078	663	862
Ge	.0839	.0582	-.0034	369	396
Si/Ge	1.832	1.892	5.57	1.80	2.177

The second neighbor force constant, μ, is negative for silicon as for germanium and also relatively small. The identities for silicon give: Identity 1: 1.087 vs 1; Identity 2: ν_{R_1} = 663 cm^{-1}; Identity 3: ν_{R_2} = 862 cm^{-1}. The results are very similar to those obtained for germanium. We therefore compare the force constants for the calculations where second neighbor interaction is neglected (Calculation C). These values are listed above under α_1 and β_1. The ratios are 1.254

for α and 1.354 for β. The average value is 1.304; deviation is 5%. To find the scale factor for $N(\nu)$ we have $m_{Ge}/m_{Si} = \frac{72.6}{28.06} = 2.58$; $\nu_{Si}/\nu_{Ge} = \sqrt{1.304 \times 2.58} = 1.83 \pm .04$. The relation between the frequencies for silicon and Smith's values in Calculation B is given by $\frac{3.58}{1.83} = 1.95$. Therefore, for silicon we can expect that the maxima of the distribution of normal modes will lie at frequencies 1.83 times higher than for germanium, and 1.95 times lower than for Smith's Calculation B.

One check of our calculation is offered by the specific heat data. Keesom and Pearlman[105] have shown that a scale factor of 1.8 will superimpose the variation of θ_D vs T (θ_D = Debye temperature) for silicon and germanium. Since the Debye temperature is directly proportional to the frequency, it is expected that the ratio of 1.83 should appear. We discuss this point in Appendix A.

4.1.4 Analysis of the Branches of the Frequency Distribution

In the preceding treatment we have shown that the calculations made by H. M. J. Smith can be used to determine the frequency distribution of the normal modes for diamond, silicon, and germanium. Before applying Smith's results to the infrared absorption spectra of these substances, we will examine the contours of the individual branches. This procedure is necessary because we are not employing an analytical method but are forced to use the method of numerical integration. Figure 28 shows the contour of branch 3 (ω_3) from Smith's Calculation A using three methods of numerical integration.

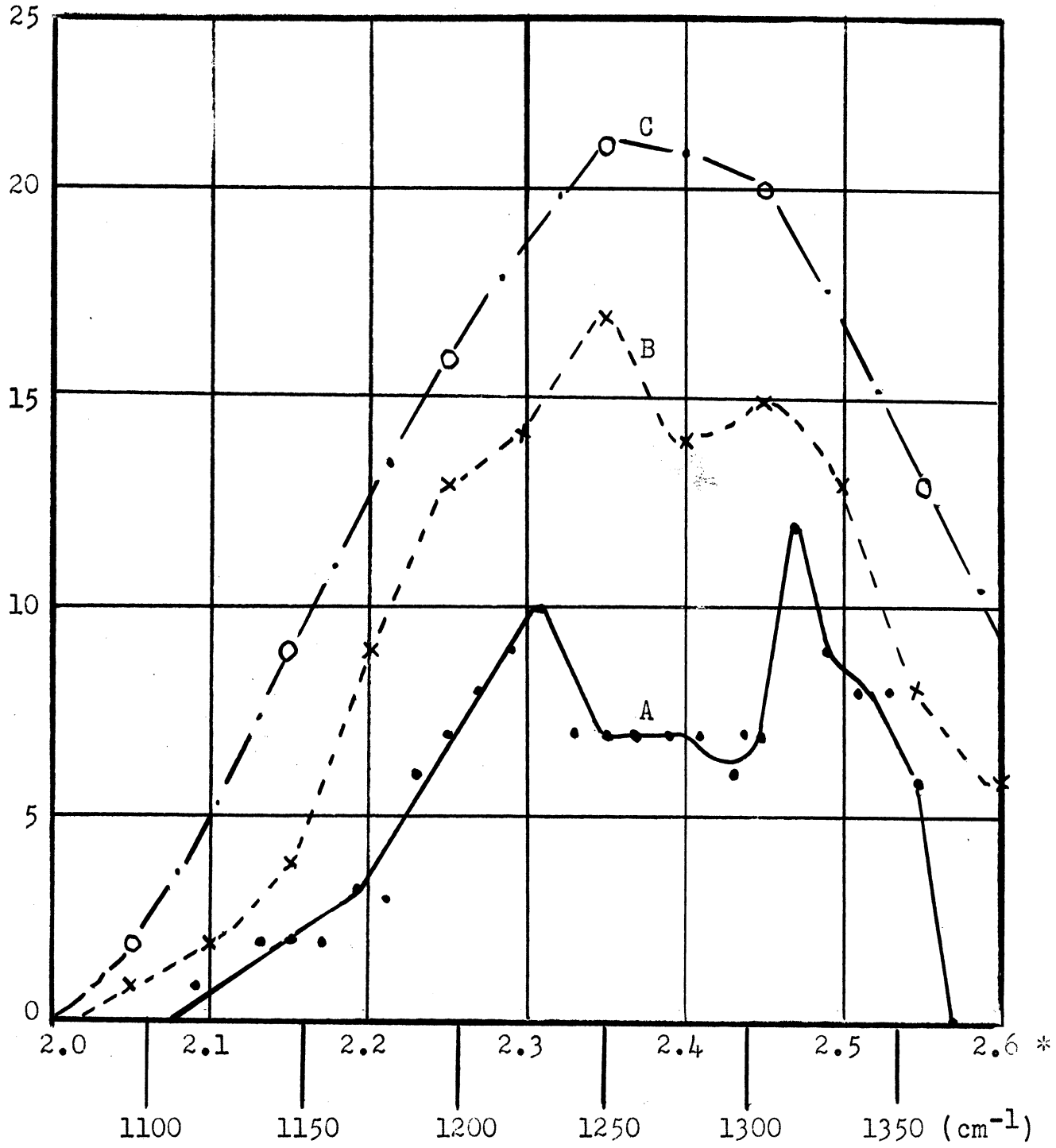

* Scale units are $2\pi\nu \cdot 10^{-14}$/sec.

	A	B	C	
$\Delta\nu$	19	38	57	(cm-1)
n	5	4	3	

Fig. 28

VARIATION IN BRANCH CONTOUR WITH NUMERICAL INTEGRATION PARAMETERS

The positions of the maxima as well as the upper and lower frequency limits are clearly functions of the parameter $\Delta\gamma$ introduced on page 101. In this example, we are already aware that the upper frequency limit of the branch is 1332 cm^{-1} (2.51 in Smith's units), because it is possible to solve for the roots at φ = (0,0,0), and general theory predicts that these roots will give the limiting frequencies of the branches. However, the lower limiting frequency of an optical branch and the upper limiting frequency of an acoustical branch is not given by the roots at φ = (0,0,0). Without introducing further theory, we would be compelled to leave these frequency limits as unknowns. This difficulty, in combination with the approximation inherent in numerical integration, gives poor prospects for establishing the contours of the individual branches. In addition, it tells us that we cannot accept Smith's contours of the branches without careful scrutiny. We will first examine Smith's calculation of branch contours and then try to refine the methods she used.

Examination of the branches Smith uses indicates that she has not been consistent in her representation of branch 4, Calculation A. Shown as a fundamental, this branch extends to an upper limit of 2.51 (in her units) = 1332 cm^{-1}. Shown as an overtone, it extends to approximately 4.7.

$$4.7/2 = 2.35 \neq 2.51$$

Since an overtone branch is the same as the corresponding fundamental except for a scale factor of 2, these results are inconsistent. On the general theory, it can be predicted that only 3 branches are "optical", i. e. extend to 1332 cm^{-1}. Therefore,

it is certain that an error was made in drawing ω_4. Since Smith did not calculate each fundamental branch separately, this error is explainable. However, since Smith did calculate each separate distribution for the overtone of each branch, the results for the overtones can be carried over directly to the fundamentals.

Branch	Smith's 1st Overtone Maximum	Fundamental Maximum
$\omega_1 = \omega_2$	2602 cm^{-1}	1301 cm^{-1}
ω_3	2469	1235
ω_4	2177	1089
ω_5	1487	744
ω_6	1258	629

In order to examine these results, we will go to a theory developed by van Hove.[106] He has shown that singularities will occur in $N_i(\nu)$, i. e. the distribution of modes in the ith branch, whenever the three derivaties $\partial\nu/\partial\varphi_1$, $\partial\nu/\partial\varphi_2$, $\partial\nu/\partial\varphi_3$ vanish simultaneously. It will be recalled that the solution of the determinental equation in the dynamical calculation gave ν as a function of the φ_i. Van Hove shows further that there are four types of singularities which can appear. Using his notation the singularities in $\nu = \nu\ (\varphi_i)$ are (1) Maxima, (2) Saddle points of type 1, (3) Saddle points of type 2, (4) Non-vanishing minima. The nature of these singularities in $N_i(\nu)$ is as follows: $g(\nu) = N(\nu)/N$, N_0 = volume of unit cell, a > 0, N = total number of unit cells.

(1) Maximum:

$$g(\nu) = g_0(\nu) + \begin{cases} \frac{2\pi\nu_0}{a^{3/2}}\sqrt{\nu_c - \nu} & \text{for } \nu < \nu_c \\ 0 & \text{for } \nu > \nu_c \end{cases}$$

(2) Saddle pt. of 1st type:

$$g(\nu) = g_0(\nu) - \begin{cases} 0 & \text{for } \nu < \nu_c \\ \frac{2\pi\nu_0}{a^{3/2}}\sqrt{\nu - \nu_c} & \text{for } \nu > \nu_c \end{cases}$$

(3) Saddle pt. of 2nd Type:

$$g(\nu) = g_0(\nu) - \begin{cases} \frac{2\pi\nu_0}{a^{3/2}}\sqrt{\nu_c - \nu} & \text{for } \nu < \nu_c \\ 0 & \text{for } \nu > \nu_c \end{cases}$$

(4) Non-vanishing minimum:

$$g(\nu) = g_0(\nu) + \begin{cases} 0 & \text{for } \nu < \nu_c \\ \frac{2\pi\nu_0}{a^{3/2}}\sqrt{\nu - \nu_c} & \text{for } \nu > \nu_c \end{cases}$$

In Figure 29 the behavior of the function $g(\nu)$ at each type of singularity is shown. The function $g_0(\nu)$ is analytic and hence smoothly continuous at the critical frequency. The contribution of $\sqrt{\nu - \nu_c}$ is discontinuous at ν_c. Hence, even though $g_0(\nu)$ is not known, it is necessary that the total function $g(\nu)$ follow the general patterns shown in the Figure. The following points are made by van Hove. (1) Singularities of two or more types can occur at the same ν_c. In this case,

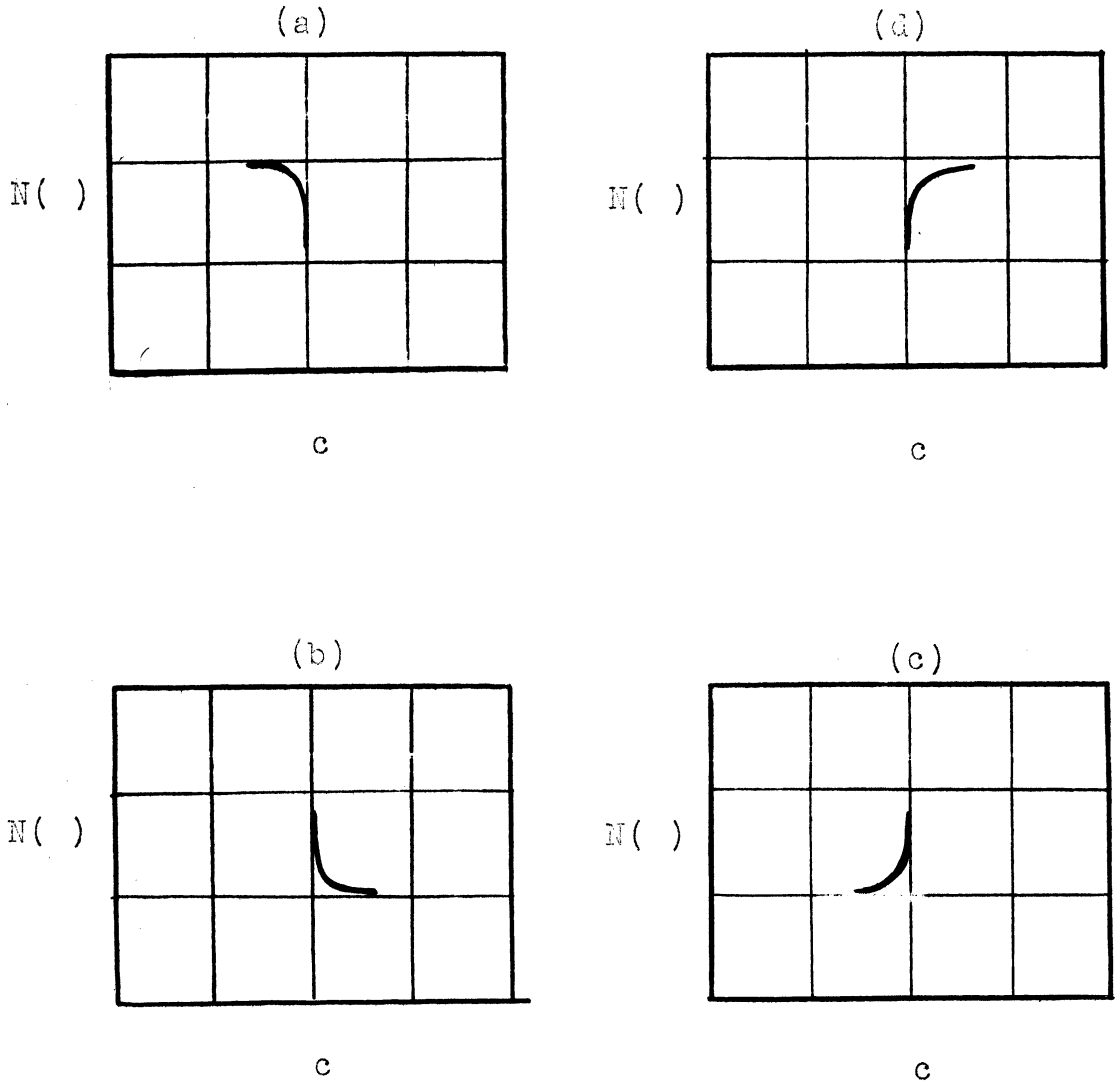

Fig. 29

THE CONTOUR OF THE FREQUENCY DISTRIBUTION NEAR SINGULAR POINTS

the resultant is the sum of the singularities. (2) At least one maximum, one saddle point of type 1, and one saddle point of type 2 must occur in every acoustical branch. (3) At least one non-vanishing minimum must occur in each optical branch. It should be noted that since the $g_o(\nu)$ are analytic functions, the singularity at ν_c is always in the slope, i. e.

$$\frac{\partial g(\nu)}{\partial \nu} \longrightarrow \pm \infty .$$

In order to apply this theory to a particular case, it is necessary to examine the analytic expressions for each branch: $\nu = \nu(\varphi)$ to determine points at which $\frac{\partial \nu}{\partial \varphi_1} = \frac{\partial \nu}{\partial \varphi_2} = \frac{\partial \nu}{\partial \varphi_3} = 0$.

Using the diamond lattice as our example, we first examine the shape of the reciprocal lattice. The first zone of a face centered lattice is described by Smith as an octahedron with its vertices cut off. Its analytic description is

$$q_x = \pm 1,\ q_y = \pm 1,\ q_z = \pm 1,\ q_x \pm q_y \pm q_z = \pm 3/2.$$

We have adopted Smith's notation where our φ_i = her q_i. The q_i are the variables of the reciprocal space and, as mentioned before, represent the phases of the triply periodic solutions to the dynamical problem. To simplify, Smith introduces variables $P_i = 8q_i$. The first zone boundary is now

$$P_x = \pm 8,\ P_y = \pm 8,\ P_z = \pm 8,\ P_x \pm P_y \pm P_z \pm 12.$$

Due to the symmetry of the reciprocal lattice, it is sufficient to consider that portion of the first zone bounded by

$$0 \leq P_x \leq P_y \leq P_z \leq 1;\ P_x + P_y + P_z \leq 12.$$

We know that $\partial\nu/\partial P_i$ will be zero at any zone boundary which is perpendicular to a reciprocal lattice axis. Therefore, the following point (P_x, P_y, P_z) will have $\frac{\partial \nu}{\partial P_x} = \frac{\partial \nu}{\partial P_y} = \frac{\partial \nu}{\partial P_z} = 0$:

(8,0,0). It can also be shown that the point (4,4,4) will satisfy the condition for the occurrence of a singularity. The procedure is to obtain the derivatives of the determinental equation with respect to q_x, q_y, q_z. All factors $\partial\nu/\partial q_i$ are set equal to zero. The coordinates of a given point (P_x, P_y, P_z) are substituted, and the result must vanish identically. In this procedure, we do not use numerical values for the force constants, but demand that the functions of q_x, q_y, q_z must cancel. In this way, we have shown that the points (8,0,0) and (4,4,4) identically satisfy the conditions for all branches. The method is rather laborious, and a return to symmetry considerations produces the result that the point (8,4,0) also satisfies conditions for the occurrence of singularities. This is shown as follows: The derivative of ν with respect to q_x is zero for any point (8,a,b) from general rules of zone theory; the derivative with respect to q_z is zero for any point (a,b,0) since the x,y plane is a plane of symmetry of the reciprocal lattice. It remains to show that $\partial\nu/\partial q_y$ is zero at (8,4,0). The direction parallel to the y axis through (8,4,0) passes through the following points: (8,0,0), (8,2,0) (8,4,0), (8,6,0), (8,8,0). Now the points (8,6,0) and (8,8,0) lie outside the first zone. However, it is found by transformation that they correspond to the points (8,2,0) and (8,8,0), respectively. That is, the function $\nu = \nu(q)$ must be symmetrical about (8,4,0) along the above line parallel to the y axis. Consequently, the contention that (8,4,0) represents a point at which singularities in the branches occur is proved.

The two points (6,6,0) and (8,2,2) can be shown to be equivalent by the allowed transformations of the reciprocal lattice. Due to their positions on the boundaries of the first zone, it was suspected that either maxima or minima in $\nu = \nu(q)$ would occur for every branch at these points. However, along the line (8,2,0), (8,2,2), (8,2,4), (8,2,6), it is found that the point (8,2,4) is equivalent to the point (0,4,6) and (8,2,6) is equivalent to (6,2,0). Therefore, one can only calculate the functions $\nu = \nu(q)$ along this line to see if a maximum or minimum occurs in a particular branch since the symmetry does not indicate that this will occur for all branches. Table 16 shows the values of ν. Since (8,2,2) is symmetrically placed with respect to the y and z axes, and since it lies on the boundary (8,a,b), the demonstration of a maximum or minimum in the Table is sufficient to guarantee the condition $\partial\nu/\partial q_x = \partial\nu/\partial q_y = \partial\nu/\partial q_z = 0$. Calculations for both the "1st Neighbor" (Calculation B) and "2nd Neighbor" (Calculation A) cases are shown. In each case, branches two and five demonstrate horizontal slopes. For branch two, ν reaches a minimum. For branch five, ν reaches a maximum. Consequently, we anticipate that the corresponding frequencies will denote singular points in $N_i(\nu)$ for these two branches.

The total result of the considerations of van Hove's theory is given in Table 17. It must be pointed out that there may be additional singular points.

The four types of singularities can be distinguished from one another by the examination of the $\partial\nu/\partial\varphi_i$ at each point. If all three $\partial\nu/\partial\varphi_i$ are maxima, the singular point

Table 16

SINGULAR POINTS IN BRANCHES ω_2 AND ω_5 AT POINT 8,2,2 = 0,6,6 IN THE RECIPROCAL LATTICE DIRECTION PARALLEL TO EITHER y OR z AXES

Point in Reciprocal Lattice	ω_1	ω_2	ω_3	ω_4	ω_5	ω_6
		First Neighbor Calculation (B)				
8,2,0 = 0,6,8	2.29	2.29	1.78	1.78	1.03	1.03
8,2,2 = 0,6,6	2.32	2.27	1.84	1.71	1.06	0.95
8,2,4 = 0,6,4	2.35	2.29	1.94	1.59	1.03	0.90
8,2,6 = 0,6,2	2.34	2.32	2.04	1.46	0.97	0.91
		Second Neighbor Calculation (A)				
8,2,0 = 0,6,8	2.51	2.51	2.17	2.17	1.44	1.44
8,2,2 = 0,6,6	2.48	2.48	2.27	2.12	1.53	1.30
8,2,4 = 0,6,4	2.51	2.51	2.34	2.01	1.47	1.25
8,2,6 = 0,6,2	2.51	2.51	2.40	1.90	1.34	1.23
		Units: 2.51 = 1332 cm^{-1}				

Table 17

LOCATIONS OF SINGULARITIES IN THE FREQUENCY DISTRIBUTIONS OF DIAMOND, SILICON, AND GERMANIUM

	ω_1	ω_2	ω_3	ω_4	ω_5	ω_6
			Diamond			
8,0,0	1316(d)	1316(d)	1185(b)	1185(a)	743(c)	743(c)
4,4,4	1326	1326	1240(d)	1120(a)	525(d)	525
8,4,0	1332	1332	1125(d)	1125(b)	786(a)	786(a)
8,2,2 = 6,6,0		1316(d)			812(a)	
			Silicon			
8,0,0	624(d)	624	485	485	281	281
4,4,4	654	654	520(d)	444(a)	198	198
8,4,0	624(d)	624	485	485	281	281
8,2,2 = 6,6,0		618(d)			284(a)	
			Germanium			
8,0,0	340(d)	340	264	264	153	153
4,4,4	356	356	283(d)	242(a)	108	108
8,4,0	340(d)	340	264	264	153	153
8,2,2 = 6,6,0		337(d)			155(a)	

is a "maximum" as described by equation (1) page 124. Similarly two maxima and one minimum give a saddle point of the first type; two minima and one maximum give a saddle point of the second type; and three minima give a non-vanishing minimum. Using these criteria we have labelled each singular point in Table 17 with letters (a) Maximum, (b) Saddle point of the First Type, (c) Saddle point of the Second Type, (d) Non-vanishing minimum. Many of the points are not labelled, particularly for the calculation in which no second neighbor interaction is considered. This arises from the fact that along at least one direction parallel to an axis through the point in question, the values of ν are constant. We are not aware of the significance of this point since we have not examined the situation analytically. However, there is probably some relation to the fact that in the simple cubic lattice Newell[107] finds that only when second neighbor interaction is introduced do the van Hove singularities appear. In the second neighbor calculations, only a few cases occur in which the singular points cannot be identified. For branches 1 and 2 the values of ν are very close together, so that the accuracy of the calculation is insufficient to define the singularities. The point (4,4,4) in branch 6 for the second neighbor calculation is the only point in the four remaining branches which cannot be identified. Since (4,4,4) is symmetrically located with respect to the three axes, this point must be either an (a) or (b) type singular point.

In order to utilize the singularities it is necessary to consider each branch in detail. Let us compare Smith's

maxima with singular points for diamond. (See Table 18).

Table 18

COMPARISON OF MAXIMA AND SINGULAR POINTS
IN DIAMOND'S DISTRIBUTION

Branch	Smith Maximum	Singular Points
1 = 2	1301	1316, 1326, 1332
3	1235	1240, 1185, 1125
4	1089	1120, 1125, 1185
5	744	743, 525, 786, 812
6	629	743, 525, 786

In the same way, Hsieh's results for germanium can be compared to the results above.

Table 19

COMPARISON OF MAXIMA AND SINGULAR POINTS
IN GERMANIUM'S DISTRIBUTION

	Hsieh Maximum	Singular Points
1	348	340, 356, 337
2		
3	284	283, 264
4	234	242, 264
5	132	108, 153, 155
6		

It is seen that some of the various singular points lie near the maxima obtained by Smith and Hsieh. Since the calculated singularities are associated with infinites in the slope, we do not expect to find distribution maxima at precisely the frequencies of the singularities. However, the nature of a particular singularity indicates the general behavior of $N(\nu)$ in the immediate vicinity of the singularity. Consequently, we can hope to define the interval of frequency in which maxima may occur.

To facilitate the use of the calculated singularities, we have calculated all of the fundamental branches using Smith's data and our own numerical integration.

For diamond, in branches 3,4,5,6, the singular points are identified except in the single case already mentioned. Consequently, we have altered the contour obtained by numerical integration to incorporate the effect of these singularities. This procedure is purely qualitative since we do not know the magnitude of the effect of the singularities.

For silicon and germanium, the number of singular points which are identified is not so great. Rather than assuming that these points will correspond to the similar points for diamond, we have used only those points which are identified.

In all three distributions, the most useful part of this work with singular points is the identification of the upper limiting frequencies of the acoustical branches and the lower limiting frequencies of the optical branches. This identification allows the numerical integration to be applied with more certainty since points falling beyond the limits are known to

be spurious and are neglected. The results for this procedure are shown in Figure 30 and Figure 31. Maxima are given in Table 20.

The principal differences between our results and those obtained by Smith lie in the location of the limiting frequencies, as already mentioned. The most significant case occurs for branches 1 and 2 whose maxima lie above the top of Figure 30. In these branches the lower limiting frequency occurs at 1316 cm^{-1}. Smith places the maximum of the branches at 1301 cm^{-1}. The error arises from Smith's numerical integration in which she uses $\Delta\nu = 160\ cm^{-1}$ while the spread of the branch is only 16 cm^{-1}. This is equivalent in spectroscopy to using a spectral

Table 20

THE CALCULATED MAXIMA OF THE BRANCHES OF THE FREQUENCY DISTRIBUTIONS OF DIAMOND, SILICON, AND GERMANIUM

Branch	Diamond	Silicon	Germanium
1	1326	654	356
2	1326	625	341
3	1285, 1180	520	284
4	1080, 930, 680, 370	444	241
5	736, 570, 330	281, 230, 122	153, 126, 67
6	700, 525	230, 122	126, 67

Note: Some of the secondary maxima listed for branches 4, 5, and 6 may be spurious due to the uncertainty in the numerical integration.

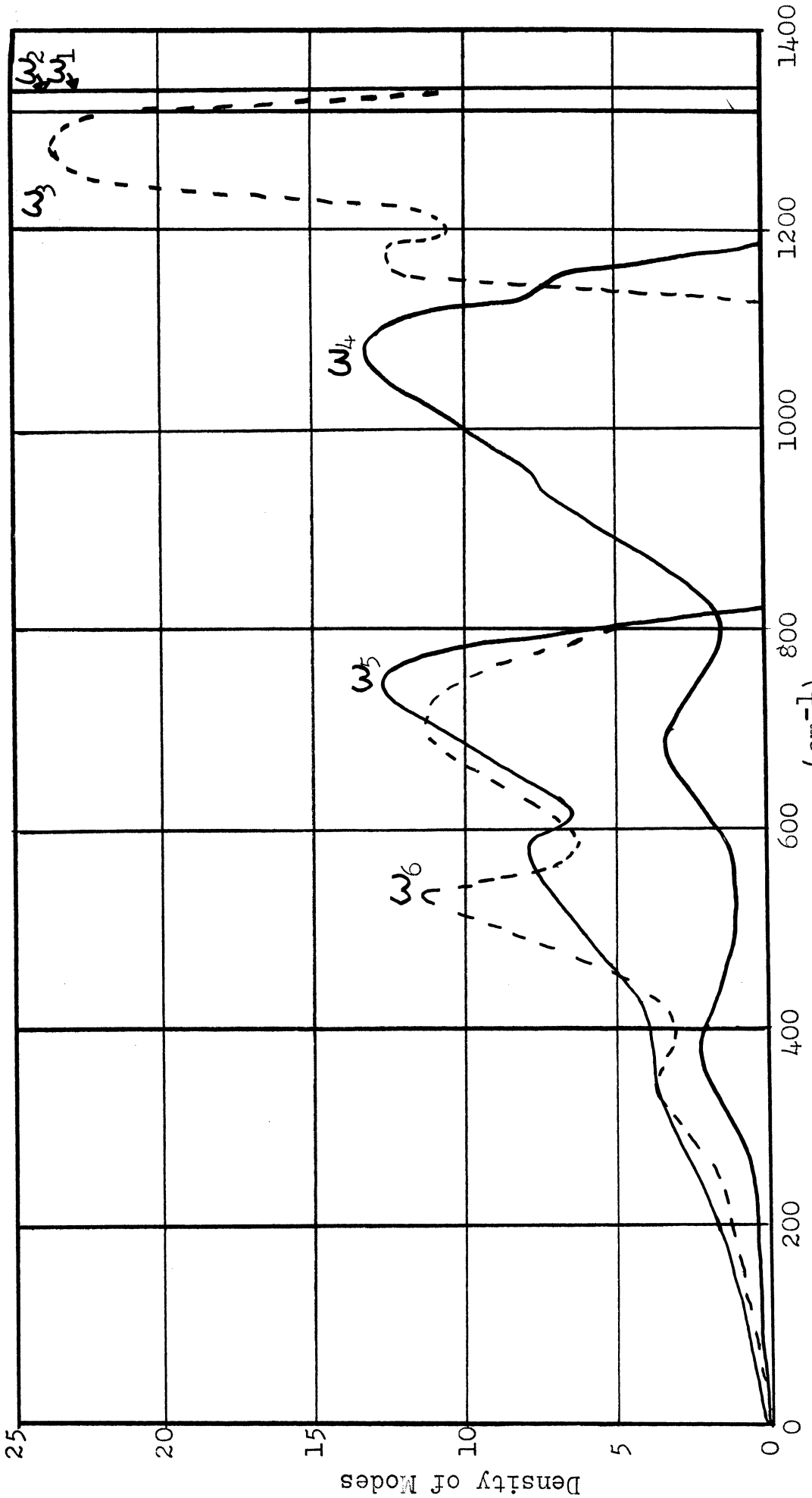

Fig. 30

THE BRANCHES OF THE DISTRIBUTION OF VIBRATIONAL MODES IN DIAMOND

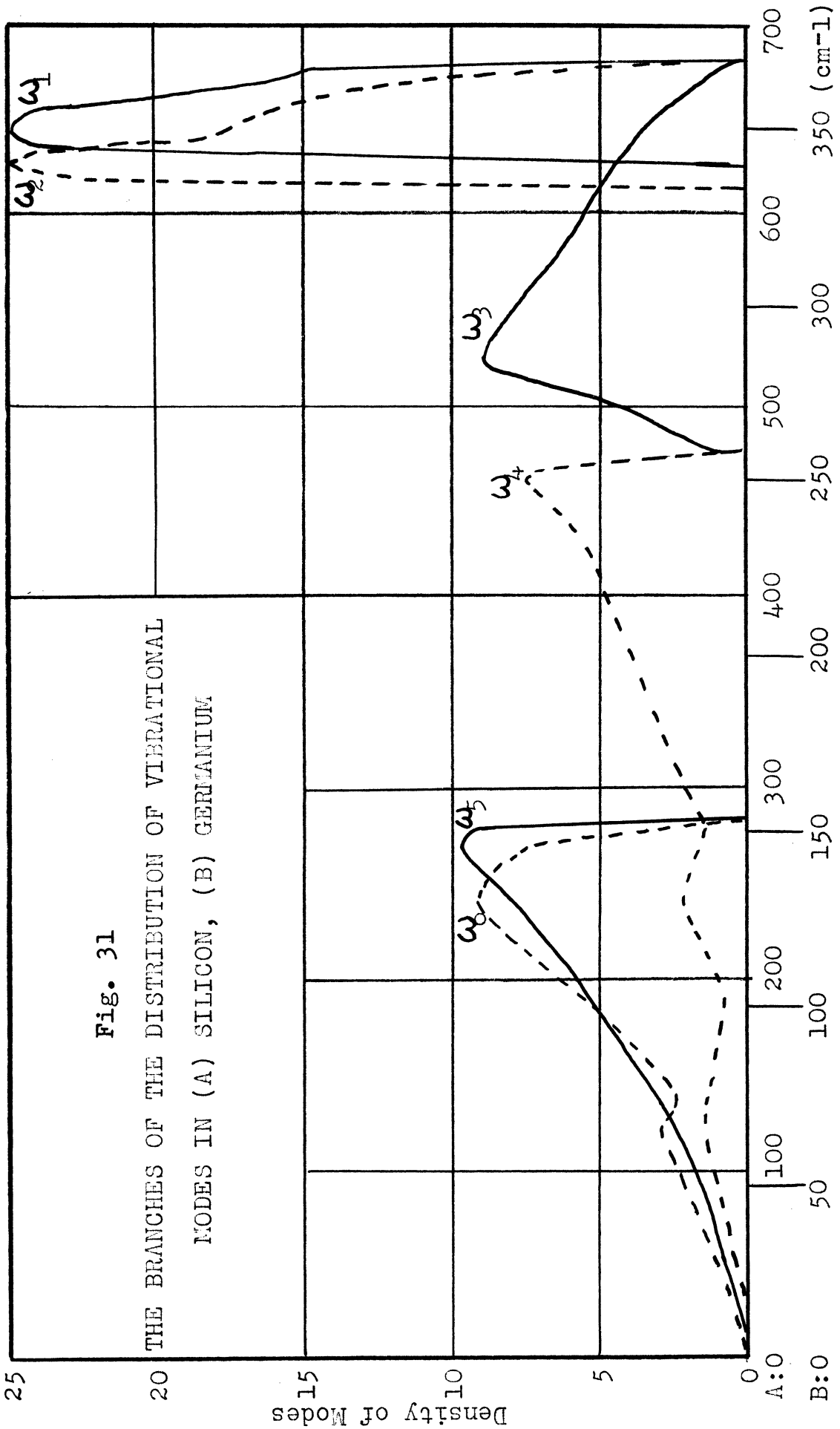

Fig. 31

THE BRANCHES OF THE DISTRIBUTION OF VIBRATIONAL MODES IN (A) SILICON, (B) GERMANIUM

slit width ten times the width of a line one is trying to resolve. This means that the principal maximum of the total distribution cannot lie at 1280 cm^{-1} as Smith calculates, but it must lie closer to 1332 cm^{-1}. The precise height of the maximum is difficult to determine because slight variations in the position of the lower limiting value of 1316 cm^{-1} will alter the height of the branches, since the area under the branches is fixed. Because of the high concentration of normal modes in such a narrow frequency interval, it is likely that the second neighbor calculation has its principal maximum at about 1320 cm^{-1}, i. e. the maximum will be determined by branches 1 and 2 with little contribution from branch 3.

4.2 Application of Lattice Dynamics to the Infrared Absorption Spectra of Diamond, Silicon, and Germanium

(4.2.1 Selection Rules)
(4.2.2 Analysis of the Observed Binary Combination Bands)
(4.2.3 Assignment of the Second Overtone Bands)
(4.2.4 Analysis of the Observed Fundamental Bands)

4.2.1 Selection Rules

The selection rules for the normal modes of a crystalline lattice are given by Teller,[81] Lifshitz,[16] and others.[90] The selection rules are as follows:

(1) Of all those frequencies occurring in the branches of the frequency distribution of a crystal, only those frequencies corresponding to $\varphi = (0,0,0)$ can be active in infrared absorption. The modes corresponding to these frequencies are elastic waves of infinite wavelength, i. e. the phase change is zero between similar atoms in different unit cells. This selection

rule follows from the fact that for all other modes, corresponding atoms in neighboring unit cells vibrate out of phase with one another, so that over a region comparable in size to the wavelength of the incident radiation a dipole moment change existing in one unit cell is cancelled by summing over many cells. For any mode at $\varphi = (0,0,0)$, the symmetry of the mode determines whether or not it is infrared active.

(2) Combinations and overtones of branches can be infrared active. In this case, it is possible to pick certain combinations for which the phase change between unit cells is zero. This is possible because for each frequency in one branch there is one corresponding frequency in every other branch for which the phase $\varphi_i = -\varphi_j$. That is, since the frequency is independent of the sign of φ, one adds the frequencies of each branch occurring at the same reciprocal lattice point. The distribution of the resultant combination frequencies can then be active in the infrared if the modes involved have the proper symmetry.

On the basis of these selection rules, we can state the following general rules which are independent of symmetry considerations: (1) The fundamental absorption spectrum of an ideal crystal is composed of narrow lines associated with limiting frequencies $\varphi = (0,0,0)$. (2) The overtone and combination absorption spectrum of an ideal crystal is composed of broad bands associated with the combinations of the branches which make up the distribution, $N(\nu)$. Whether or not any of the above lines and bands appear in absorption is governed by the symmetry of the modes involved. Symmetry selection rules can forbid

transitions allowed under (1) and (2) but cannot allow any transitions forbidden under (1) and (2).

Similar selection rules hold for the Raman effect with the same conclusions concerning the nature of the fundamental and overtone regions. The Raman effect of diamond corresponds to these rules. The single sharp line at 1332 cm^{-1} is the only feature of the fundamental region. The second order spectrum is composed of broad bands whose analysis by Smith has already been discussed.

Since the ideal diamond lattice has a center of symmetry at the center of each C-C bond, one may expect that the infrared and Raman spectra will be mutually exclusive.[102] There is only one limiting frequency, i. e. the three optical branches have a common root at $\varphi = 0,0,0$ and since this frequency is Raman active, no fundamental bands are expected to appear in infrared absorption. Further, Smith has calculated the selection rules for combinations and overtones in the Raman effect. If the rule of mutual exclusion holds, none of these combinations or overtones is allowed in the infrared. On this basis we would predict that the maximum number of allowed infrared combinations and overtones is (1) No first overtones, (2) $\omega_1 \pm \omega_4$, $\omega_1 \pm \omega_5$, $\omega_1 \pm \omega_6$, $\omega_3 \pm \omega_4$, $\omega_3 \pm \omega_5$, $\omega_3 \pm \omega_6$. Branches one and two are degenerate in Smith's calculation for diamond, so that all statements for ω_1 also hold for ω_2. The degeneracy is a consequence of the central force field which is assumed to exist between second neighbors. This force is not used in the calculation for silicon and germanium. Therefore, for silicon and germanium, these branches are not degenerate, and

separate combination maxima occur.

The above statements are based on the assumption that the diamond lattice is centrosymmetric. However, a real diamond having the ideal Bragg structure is not strictly centrosymmetric due to the presence of more than one isotope of carbon. Similarly, silicon and germanium, to which the selection rules apply, have more than one stable isotope. In Table 21, the stable isotopes of the three substances are listed together with their abundances.[67] In a later section we will discuss the effect of a random distribution of isotopes on the selection rule $\phi = (0,0,0)$ for fundamental modes. At this point, we shall assume that the selection rule requiring $\phi = (0,0,0)$ still holds. However, it is clear that at least some sites of each crystal will contain atoms of weight different from that of neighboring atoms. Consequently, the lattice is not strictly centrosymmetric. For diamond and silicon the abundances of the less predominant isotopes are relatively small. In germanium, however, there is a distribution over several isotopes having comparable abundances.

In diamond, silicon, and germanium, the masses of the various isotopes are not greatly different. The limiting mode involves the motion of one face centered lattice against the other. In such a mode, the amplitudes of two different isotopes will be only slightly different and the dipole moment change will be small. At least on this qualitative basis, no fundamental absorption is anticipated at the upper limiting frequency because of this isotope effect.

Similar reasoning leads us to the conclusion that the selec-

Table 21

THE STABLE ISOTOPES OF CARBON, SILICON, AND GERMANIUM

Substance	Isotope (Mass No.)	Abundance
Carbon	12	98.9%
	13	1.1
Silicon	28	92.3
	29	4.7
	30	3.0
Germanium	70	20.6
	72	27.4
	73	7.6
	74	36.8
	76	7.6

tion rules involving mutual exclusion can be expected to hold for the combination and overtone spectra. However, due to the presence of isotopes, particularly in the case of germanium the combinations allowed in the Raman effect may appear in absorption without violating symmetry selection rules. These combinations are $\omega_1 \pm \omega_2$, $\omega_1 \pm \omega_3$, $\omega_2 \pm \omega_3$, $\omega_4 \pm \omega_5$, $\omega_4 \pm \omega_6$, $\omega_5 \pm \omega_6$.

4.2.2 Analysis of the Observed Binary Combination Bands

In general, the maximum of a combination branch does not lie at the sum of the frequencies of the maxima of the two branches forming the combination. The variation of frequency with φ is different for each branch (see Tables 11A and B). In particular acoustic branches tend to low frequencies and optical branches tend to high frequencies as φ approaches zero. Consequently, when combination branches are formed by adding the frequencies for two branches at each point φ, the resulting variation of frequency with φ will be different, in general, from either of the contributing fundamental branches. Similarly, the distribution of combination frequencies, formed by numerical integration, will, in general, have its maximum at a frequency not equal to the sum of the frequencies of the maxima of the contributing fundamental branches. Teller[81] discusses this point. It is necessary to calculate the distribution for each allowed combination. We have done this using Smith's data and employing numerical integration. Singular points were utilized to identify the frequency limits of the combinations. Diamond combinations are obtained using Smith's

Calculation A. Silicon and germanium branches are obtained using Smith's Calculation B and then dividing the frequency scale by 1.95 and 3.58 respectively. The maxima of the combination branches are listed in Table 22. The calculated distributions are shown in Figure 32 and Figure 33. The anticipated shift of the combination maxima with respect to the individual fundamental maxima occurs (see Figures 30 and 31 and Table 20).

From our calculations we are certain that a frequency scale factor of approximately 1.83 connects the distributions of silicon and germanium. However, since second neighbor interaction is used for the diamond calculation, there is not a simple scale factor between the distributions of diamond and the other substances (see page 118). Consequently, while observed bands due to the same combinations in silicon and germanium should be recognizable from their positions and general similarity, the corresponding observed diamond bands can be identified only through the assignment of observed combinations in terms of calculated branches.

The observed infrared spectra of diamond, silicon,[52, 54] and germanium in the combination region are shown in Figure 34. The diamond frequency scale is 3.6 times the germanium scale and twice the silicon scale.

In Figure 35, the contours for the whole combination region are calculated on the assumption that every branch is equally intense. Comparing with Figure 34, it is clear that such an assumption does not correspond to the facts.

In Table 23, the observed maxima are listed together with the calculated maxima lying closest to them. This table

Table 22

THE MAXIMA OF CALCULATED COMBINATIONS ALLOWED IN INFRARED ABSORPTION

Combination*	Diamond	Silicon	Germanium
$\omega_1 + \omega_4$	2400 to 2450 cm^{-1}	1100 cm^{-1}	598 cm^{-1}
$\omega_2 + \omega_4$	2400 to 2450 cm^{-1}	1100	598
$\omega_3 + \omega_4$	2260	960	520
$\omega_1 + \omega_5$	2040	905	492
$\omega_2 + \omega_5$	2040	880	480
$\omega_3 + \omega_5$	1920	800	440
$\omega_1 + \omega_6$	1940	875	478
$\omega_2 + \omega_6$	1940	870	475
$\omega_3 + \omega_6$	1860	760	415
Total**	1900, 2350, 2450	790, 870 1090	430, 475, 600

* See Figure 34

** See Figure 35

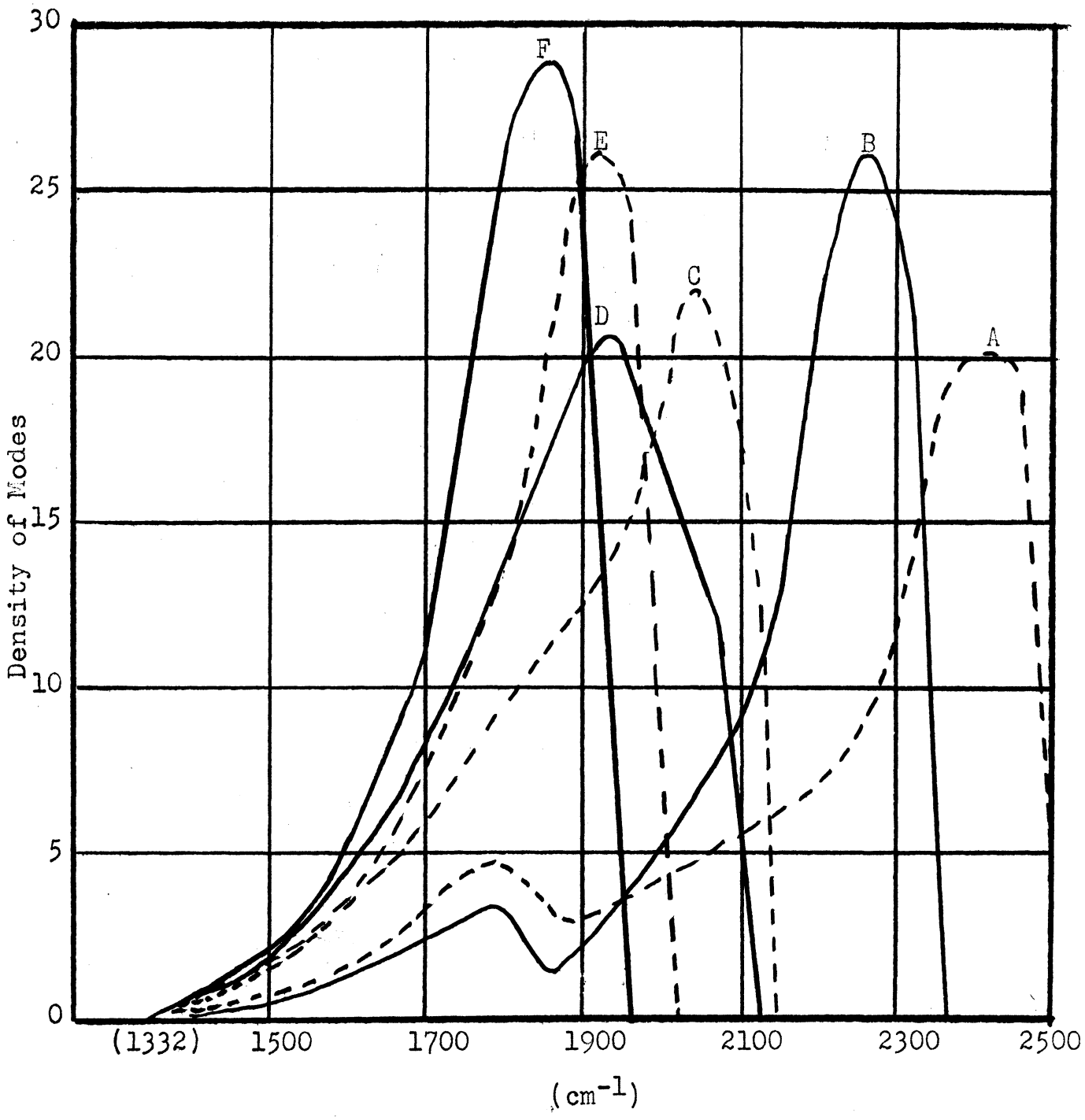

A: $\omega_1+\omega_4$; $\omega_2+\omega_4$. C: $\omega_1+\omega_5$; $\omega_2+\omega_5$ E: $\omega_3+\omega_5$

B: $\omega_3+\omega_4$ D: $\omega_1+\omega_6$; $\omega_2+\omega_6$ F: $\omega_3+\omega_6$

Fig. 32

CALCULATED COMBINATIONS ALLOWED IN INFRARED ABSORPTION IN DIAMOND

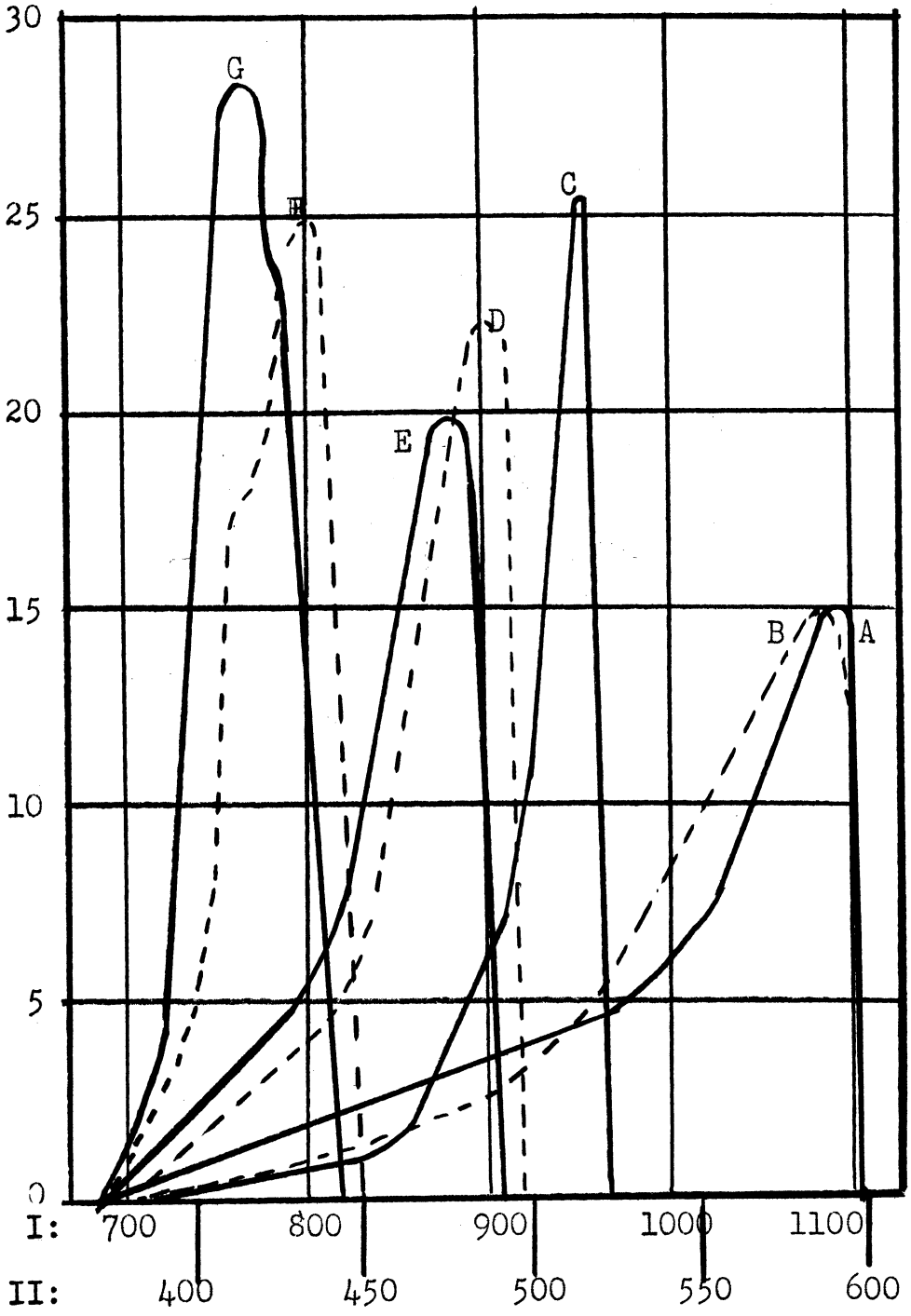

A: $w_1 - w_4$

B: $w_2 - w_4$

C: $w_3 - w_4$

D: $w_1 - w_5$

E: $w_2 - w_5$, $w_1 - w_6$, $w_2 - w_6$

F: $w_3 - w_5$

G: $w_3 - w_6$

Fig. 33

CALCULATED COMBINATIONS ALLOWED IN INFRARED ABSORPTION IN (I)SILICON, (II)GERMANIUM

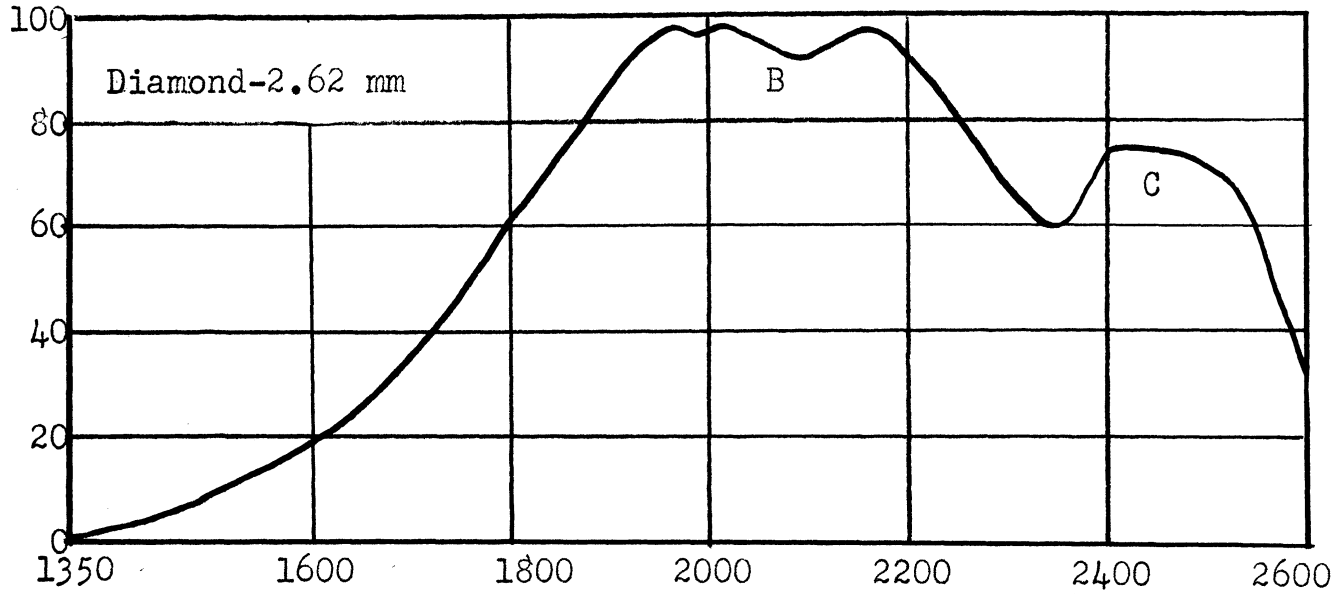
Diamond-2.62 mm
B
C
100
80
60
40
20
0
1350
1600
1800
2000
2200
2400
2600

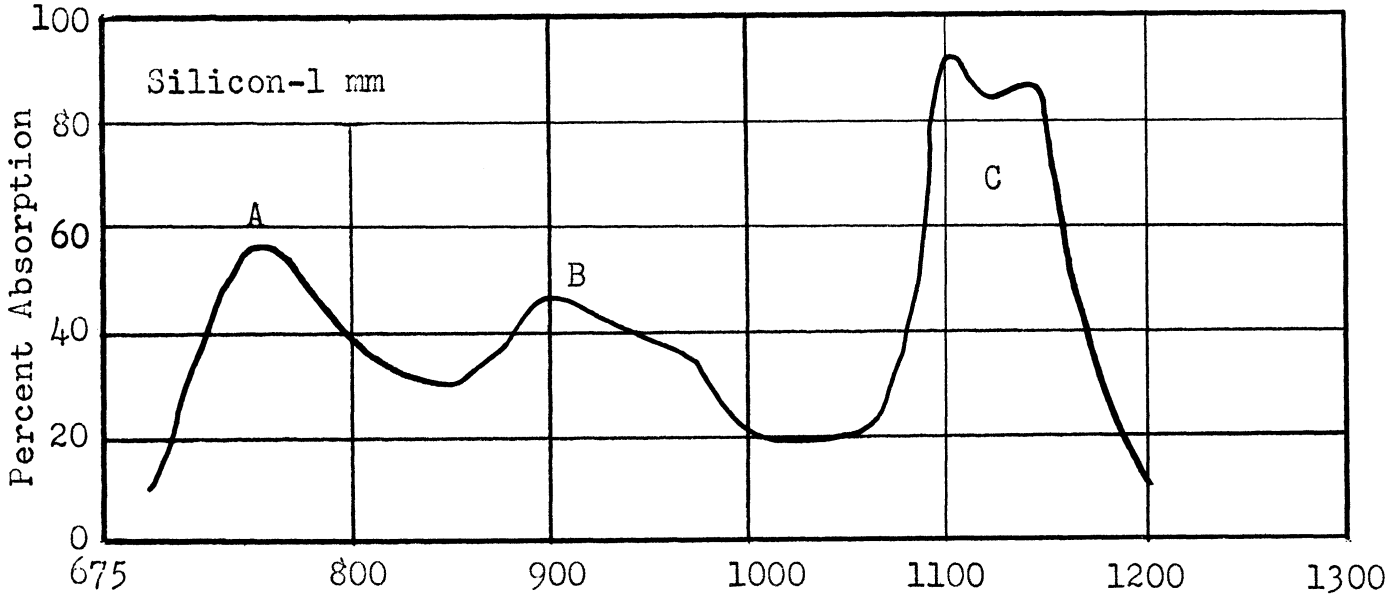
Silicon-1 mm
Percent Absorption
A
B
C
100
80
60
40
20
0
675
800
900
1000
1100
1200
1300

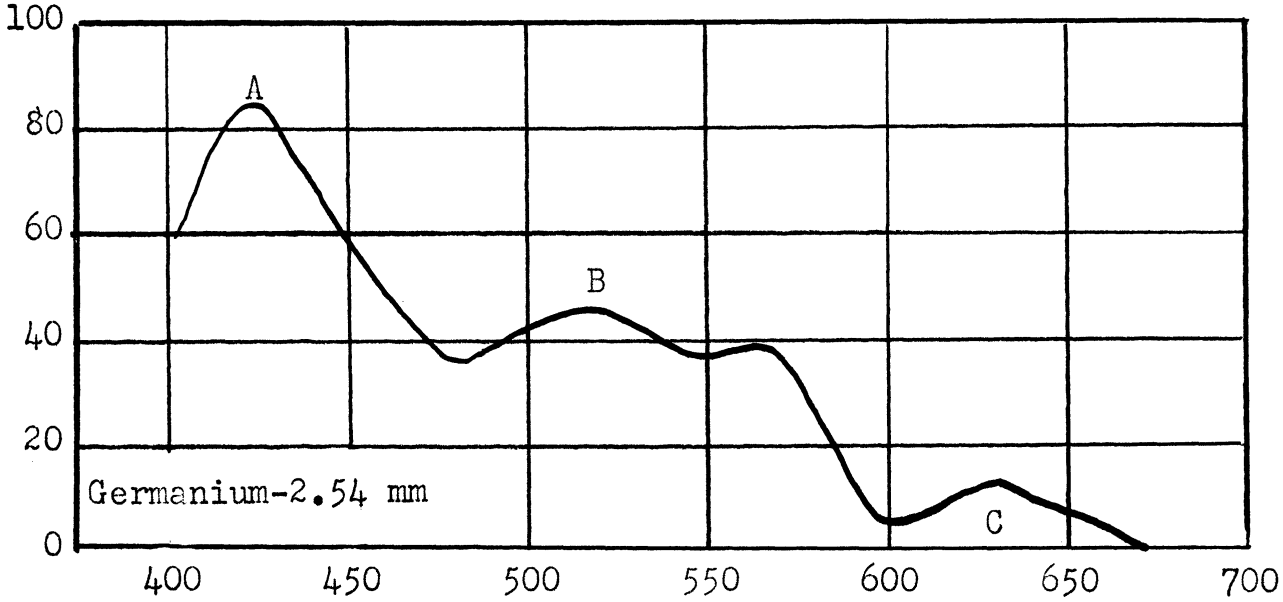
A
B
C
Germanium-2.54 mm
100
80
60
40
20
0
400
450
500
550
600
650
700

FIG. 34

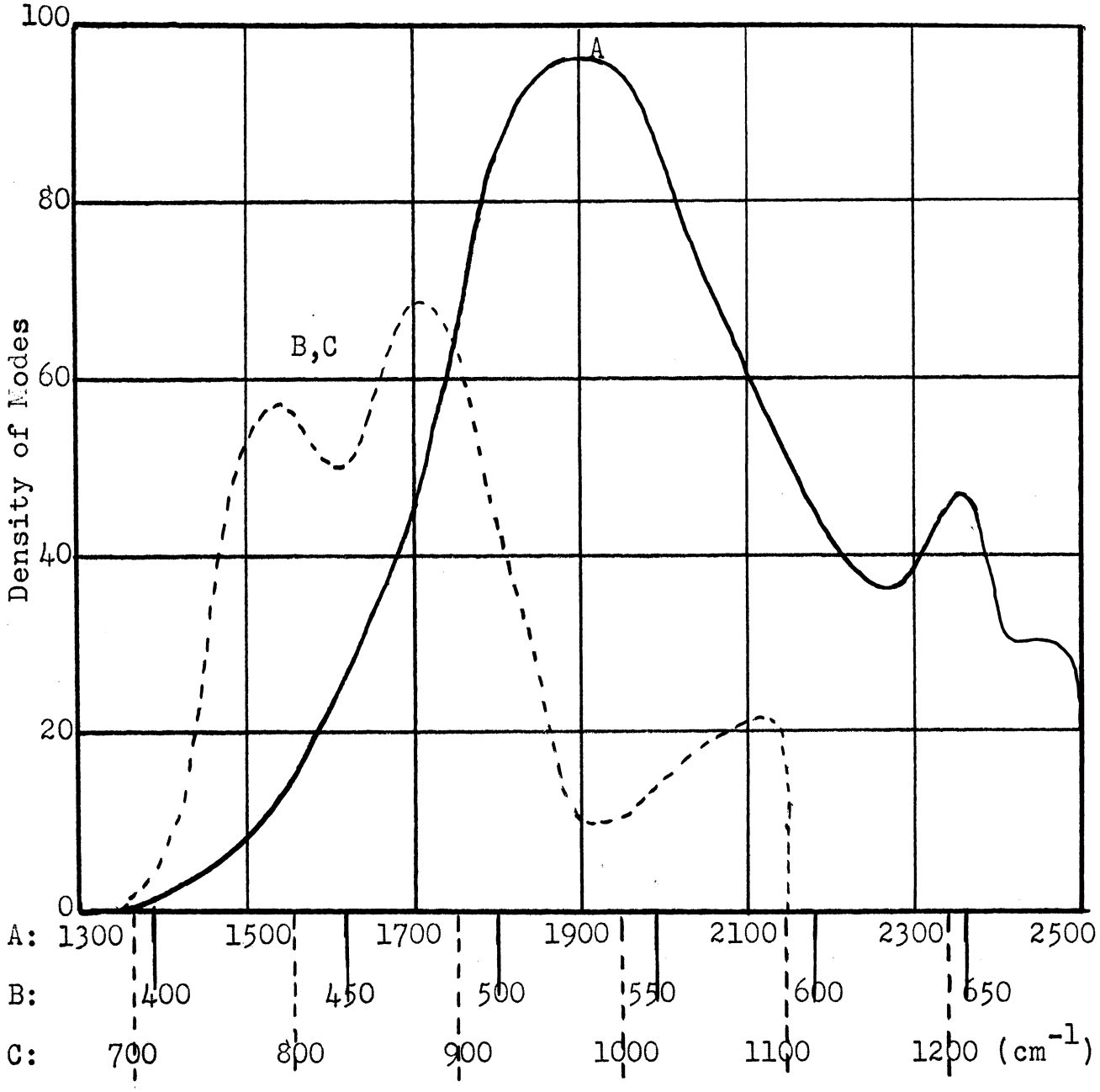

A: Diamond; B: Germanium; C: Silicon

Fig. 35

CALCULATED CONTOUR IF EACH ALLOWED

COMBINATION HAS THE SAME INTENSITY

Table 23

TENTATIVE ASSIGNMENT OF COMBINATION BANDS ON THE BASIS OF POSITIONS OF MAXIMA

Observed	Assignment	Calculated
	Diamond	
2400-2500	$\omega_1 + \omega_4$	2400-2450
	$\omega_2 + \omega_4$	
2165	$\omega_3 + \omega_4$	2260
1960-2020	$\omega_1 + \omega_5$	2040
	$\omega_2 + \omega_5$	
	$\omega_1 + \omega_6$	1940
	$\omega_2 + \omega_6$	
	Silicon	
1100-1150*	$\omega_1 + \omega_4$	1100
	$\omega_2 + \omega_4$	
900-960	$\omega_3 + \omega_4$	960
	$\omega_1 + \omega_5$	905
736	$\omega_3 + \omega_6$	760
	Germanium	
640	$\omega_1 + \omega_4$	598
	$\omega_2 + \omega_4$	
520-560	$\omega_3 + \omega_4$	520
	$\omega_1 + \omega_5$	492
420	$\omega_3 + \omega_5$	440
	$\omega_3 + \omega_6$	415

* See text

represents a tentative assignment on the basis of the positions of the maxima, but without consideration of the shapes of the bands. In Figures 36, 37 and 38 we have plotted the observed bands in terms of absorption coefficients. Also shown are calculated combinations whose component branches have been adjusted in relative intensity to produce the best fit with the observed bands. In the following paragraphs we discuss each case separately. In Table 24, the final assignments are listed together with the relative intensities of the individual bands. The individual combination maxima shift slightly when the various bands are superimposed. The maxima of the combined distribution are given in the table. All combinations not listed are assigned zero intensity.

DIAMOND: Several calculated maxima fall near the observed doublet at 2000 cm^{-1}. In our fit of the observed spectrum, we have included all of the calculated bands which fall close to 2000 cm^{-1}, i. e. those listed as tentative assignments. However, both $\omega_1 + \omega_6$ and $\omega_2 + \omega_6$ could be deleted without greatly altering the band shape, simply by increasing the intensities of $\omega_1 + \omega_5$ and $\omega_2 + \omega_5$. Since the observed maximum is a doublet, at least two combination bands must contribute to it. Our calculations are too approximate to justify showing fine structure in the calculated contour at 2000 cm^{-1}, although since several bands contribute to the calculated maximum, the observed doublet is essentially explained.

The second main maximum in the observed spectrum at 2165 cm^{-1} lies approximately 100 cm^{-1} below the closest maximum, $\omega_3 + \omega_4$, at 2260 cm^{-1}. However, the observed band shape is similar to

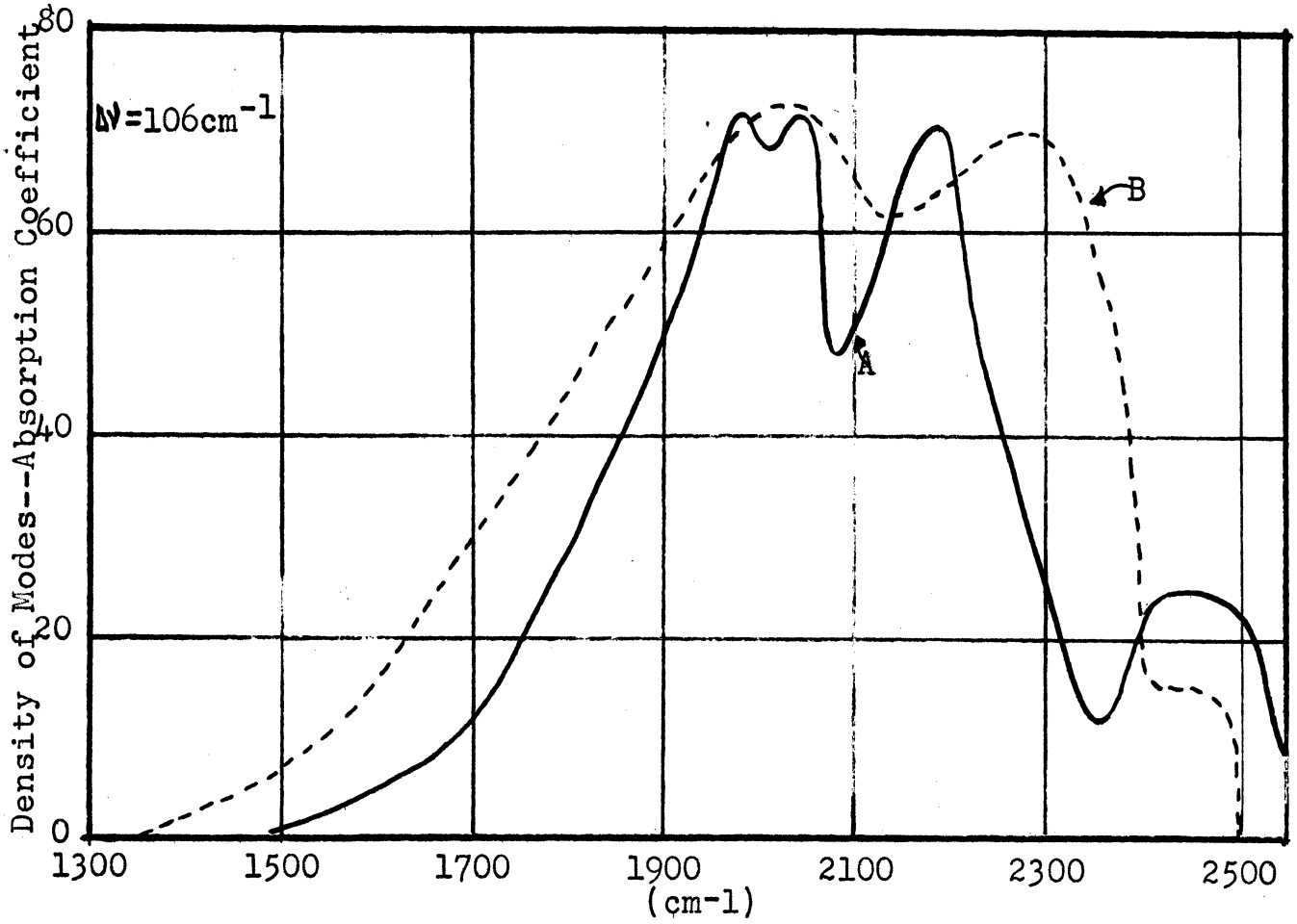

Branch : $w_1+w_4 : w_1+w_5 : w_1+w_6 : w_2+w_4 : w_2+w_5 : w_2+w_6 : w_3+w_4$

Intensity: ½ : 1 : 1 : ½ : 1 : 1 : 2

Fig. 36

CALCULATED (B) VS OBSERVED (A) COMBINATION BANDS IN DIAMOND

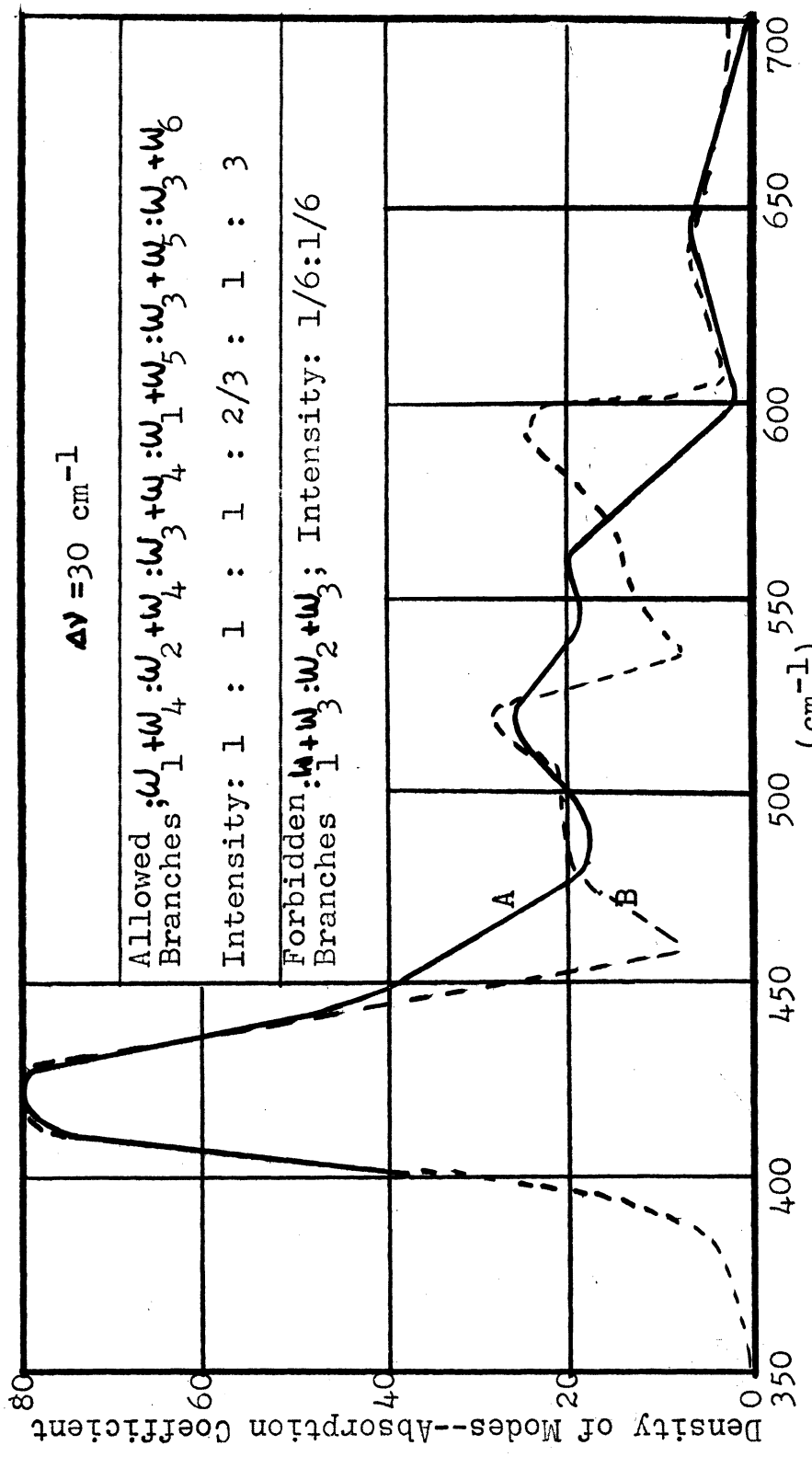

Fig. 37

CALCULATED (B) VS OBSERVED (A) COMBINATION BANDS IN GERMANIUM

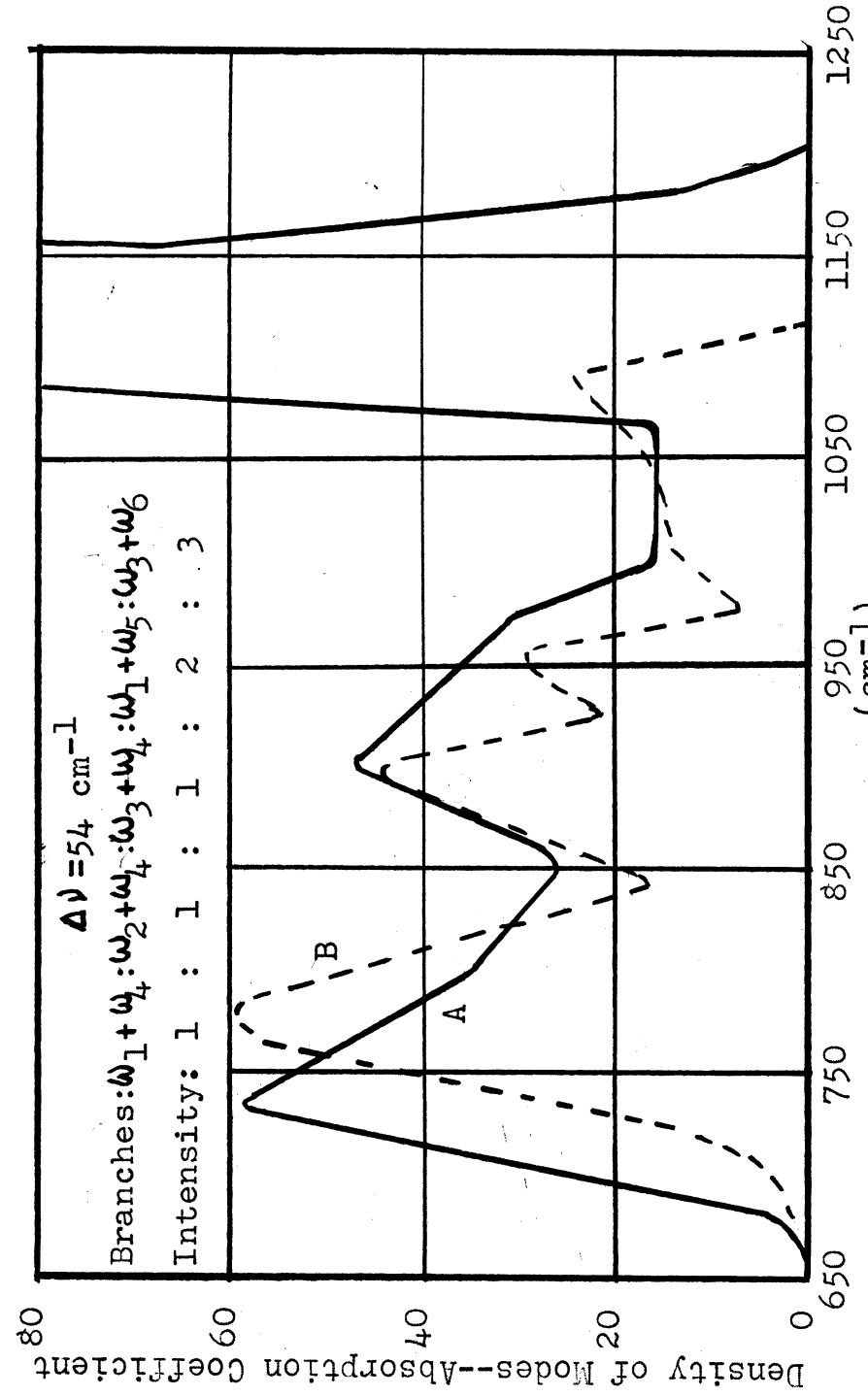

Fig. 38

CALCULATED (B) VS OBSERVED (A) COMBINATION BANDS IN SILICON

Table 24

FINAL ASSIGNMENT OF COMBINATION BANDS

Observed (cm^{-1})	Assignment	Intensity	Calculated* (cm^{-1})
	Diamond		
2400-2500	$\omega_1 + \omega_4$	1	2400-2450
	$\omega_2 + \omega_4$	1	
2165	$\omega_3 + \omega_4$	2	2270
1960-2020	$\omega_1 + \omega_5$	1	2000-2050
	$\omega_2 + \omega_5$	1	
	$\omega_1 + \omega_6$	1	
	$\omega_2 + \omega_6$	1	
	Silicon		
*1100-1150	$\omega_1 + \omega_4$	1	1100
	$\omega_2 + \omega_4$	1	
960	$\omega_3 + \omega_4$	1	950
900	$\omega_1 + \omega_5$	2	900
736	$\omega_3 + \omega_6$	3	770
	Germanium		
640	$\omega_1 + \omega_3$	1/6	640
	$\omega_2 + \omega_3$	1/6	
560	$\omega_1 + \omega_4$	1	590
	$\omega_2 + \omega_4$	1	
520	$\omega_3 + \omega_4$	1	520
	$\omega_1 + \omega_5$	2/3	
420	$\omega_3 + \omega_5$	1	420
	$\omega_3 + \omega_6$	3	

* See text

the calculated shape. The inaccuracy of the numerical integration ($\Delta\nu$ = 106 cm^{-1}) in addition to the effect of anharmonicity contribute to the discrepancy between observation and calculation.

The third observed maximum at 2480 cm^{-1} extends from 2400 to 2500 cm^{-1} and is well approximated by the calculated $\omega_1 + \omega_4$, $\omega_2 + \omega_4$. The fact that the calculated value of $\omega_3 + \omega_4$ lies at too high a frequency accounts for the overlapping of the calculated bands at 2325 cm^{-1}. The calculated intensity at 2450 cm^{-1} is below the observed intensity because it is found that further increase of the 2450 cm^{-1} band intensity moves the maximum at 2260 cm^{-1} to higher frequencies. Clearly, if $\omega_3 + \omega_4$ fell closer to the observed frequency, the difficulty with $\omega_1 + \omega_4$, $\omega_2 + \omega_4$ would not occur, and the observed spectrum could be more accurately reproduced.

GERMANIUM: In Table 23 it will be seen that there is a discrepancy between the observed maximum at 640 cm^{-1} and the calculated position of the assigned maximum at 598 cm^{-1} which is in the wrong direction to arise from anharmonicity. If, however, we consider the "forbidden" combinations, which we have stated may appear in germanium, it is found that the combinations $\omega_1 + \omega_3$ and $\omega_2 + \omega_3$ fall precisely at the location of the 640 cm^{-1} band, and have a similar contour (Table 24, Figure 37). Since absorption exists at 560 cm^{-1}, and since the $\omega_1 + \omega_4$, $\omega_2 + \omega_4$ maxima occur at 598 cm^{-1}, it is likely that they contribute to the absorption at 560 cm^{-1}. No other allowed or forbidden combination branch in the calculated set, has a non-zero density at 560 cm^{-1}. The only other possibility

is an overtone, which falls in the "forbidden" class. When overtones are considered it is found that 2 ω_3 falls at 568 cm^{-1}. However, its contour does not fit the observed band, especially the sharp drop at 600 cm^{-1}. Since the contour of $\omega_1 + \omega_4$, $\omega_2 + \omega_4$ is similar to the 560 cm^{-1}, although the maximum is displaced by 30 cm^{-1}, we assign the 560 cm^{-1} band to $\omega_1 + \omega_4$, $\omega_2 + \omega_4$. Although $\omega_1 + \omega_5$ does not have a corresponding maximum in the observed spectrum, its inclusion improves the agreement between the contours of the calculated and observed bands. The remaining observed bands are well explained by the calculated spectrum.

It should be noticed that the assigned bands in germanium differ from those for diamond. Aside from the inclusion of two weak "forbidden" bands germanium also has a strong $\omega_3 + \omega_6$ band and a somewhat weaker $\omega_3 + \omega_5$ band, neither of which occur in diamond. (Note: The Germanium contour can be reproduced in all important aspects by setting the intensity of $\omega_3 + \omega_5$ equal to zero and increasing the relative intensity of $\omega_3 + \omega_6$ from 3 to 4). Finally, neither $\omega_1 + \omega_6$ nor $\omega_2 + \omega_6$ occurs in germanium. As we have mentioned above, these last two bands are not vital to the explanation of the diamond spectrum and may not be present. The different intensities for various bands indicate that the anharmonic constants differ between germanium and diamond.

SILICON: We have made no observations of the silicon spectrum. Unfortunately, the published spectra do not overlap, i. e. Briggs[52] published the spectrum from 1 to 12μ and Lord[54] published the spectrum beyond 12μ. However, near 12μ there

are no data available. In addition, the absorption coefficient of the 1100 cm^{-1} band appears to be too strong to be comparable with the combination bands near it nor is it similar to any band in germanium or diamond. In the experimental section we have shown that in powder form silicon displays this band, and we have also shown (page 62) that SiO_2 has a similar strong band near 1100 cm^{-1}. For these reasons we consider that the band at 1100 cm^{-1} in silicon is due to SiO_2 impurities. Lord[53] holds this same opinion. The remainder of the spectrum can be explained in terms of the combinations listed in Figure 38. The inclusion of $\omega_1 + \omega_4$, $\omega_2 + \omega_4$ is arbitrary since we are excluding the 1100 cm^{-1} band from consideration. However, the level of general absorption between 1000 and 1050 cm^{-1} is consistent with the inclusion of these combinations. In addition, these two bands have appeared in our assignments for both germanium and diamond, and are included to show that their presence in silicon is not inconsistent with the experimental data.

Except for the assigned "forbidden" band in germanium, the assigned bands and their relative intensities are very similar for the two substances, espcially since $\omega_3 + \omega_5$ is not essential to the explanation of the germanium spectrum. This similarity points to the similarity of the force fields existing in these substances. Diamond clearly differs, as we have already anticipated in our original calculations.

4.2.3 Second Overtone Bands

We have not considered the two highest frequency maxima that occur in diamond (see Figure 6), silicon (see reference

52), and germanium (see Figure 19). These bands are weak and broad in all three substances and lie above the upper frequency limit for binary combinations and first overtones. We have not investigated the selection rules for higher order combinations and overtones, and will merely list second overtones falling close to the observed maxima.

Substance	Observed (cm^{-1})	Assignment	Calculated (cm^{-1})
Diamond	3125	$3\ \omega_4$	3240
	3570	$3\ \omega_3$	3755
Silicon	1300	$3\ \omega_4$	1332
	1470	$3\ \omega_3$	1560
Germanium	750	$3\ \omega_4$	722
	845	$3\ \omega_3$	852

Considering the possible effects due to anharmonicity as well as the accuracy of our calculations, the agreement can be considered satisfactory. We shall find that ω_3 and ω_4 occur in the fundamental spectra. In a centrosymmetric system, one expects that the second overtone of an active fundamental will be allowed.[102]

4.2.3 Analysis of the Observed Fundamental Absorption Bands

It has been stated in section 4.2.1 that the general selection rules for ideal crystals forbid infrared absorption due to all fundamental modes except those corresponding to limiting frequencies of branches. In the diamond type structure there is only one limiting frequency. It is triply degenerate. This frequency is forbidden in absorption by symmetry selection rules.

However, the absorption spectra of many diamond crystals and of all those silicon and germanium crystals which have been studied show broad absorption bands in the wavelength region where fundamental vibrations may be expected to occur. These broad bands cannot be explained as combination or difference bands. It will be shown that many of the observed maxima do correspond to the calculated maxima of the frequency distribution.

Broad bands are also observed in the fundamental absorption spectrum of NaCl.[120] Born and Blackman[121, 122] have shown that anharmonic terms in the potential can cause normally forbidden fundamentals to appear. According to this theory the appearance of forbidden transitions depends on the fact that the upper limiting frequency in NaCl is allowed in absorption,[90] even in the harmonic approximation. The upper limiting frequency is forbidden in diamond, silicon, and germanium. Consequently, the Born, Blackman theory does not apply.

It is necessary to explain, therefore, how the selection rules for fundamentals can be broken. For the explanation we shall consider the work by I, M. Lifshitz[16] concerning the effect of imperfections on crystal selection rules. Since Lifshitz's work is a mathematical treatment with very little interpretation, it is useful to discuss a model of an imperfect crystal on general terms to provide some connection between physical phenomena and the mathematical results. Accordingly, we will present a few general considerations based on qualitative reasoning.

If the periodicity of an ideal lattice is interrupted by the presence of randomly distributed imperfections which are separated by an average distance which is short compared to the wavelength of the incident radiation, then for at least some modes, for which the dipole moment change averages to zero in the ideal case, the averaging will now take place over a shorter distance (fewer number of unit cells), and a net dipole moment change may result. It appears that a net dipole moment change will occur only for those modes whose wavelengths are comparable to or longer than the average spacing of the imperfections. For modes of much shorter wavelength, the averaging over unit cells will produce a net dipole moment change of zero, just as in the ideal lattice.

The number and frequency distribution of the modes which will become active in an imperfect crystal will be determined by (1) the average separation of the imperfections (2) the distribution of vibrational frequencies with respect to the wavelengths of the corresponding modes, (3) the dipole moment change in a single unit cell associated with each particular mode.

The normal modes of a crystalline lattice are uniformly distributed in phase space. If we measure phase (the phase of an elastic wave equals the reciprocal of the wavelength times the unit cell dimension) in terms of the radial distance, φ_r, of a point in phase space from the origin, then the number of modes between φ_r and $\varphi_r + d\varphi_r$ is $4\pi\rho\varphi_r^2 d\varphi_r$ where ρ is the number of modes per unit volume of phase space. Since ρ is constant the number of modes increases as φ_r^2. This means that there are many more modes of short wavelength than of long

wavelength. In turn, we infer that imperfections must be spaced, relatively close together if many frequencies are to be active in absorption. Since optical branches tend to high frequencies near $\varphi = (0,0,0)$, and acoustical branches tend to low frequencies near $\varphi = (0,0,0)^{90}$, (see Table 11), imperfections will cause selection rules to break down for the higher frequencies of optical branches and the lower frequencies of acoustical branches.

In the preceding qualitative discussion it has been assumed that the normal modes can be represented as plane waves even in the imperfect crystal. In addition, no consideration has been given to the effect of imperfections on the normal frequencies and their distribution. To test the validity of our qualitative deductions we will now consider the work by Lifshitz.[16]

Lifshitz has written a series of three articles on the general subject "Optical Behavior of Non-Ideal Crystal Lattices in the Infrared." He shows that, in general, without reference to the nature of imperfections, the presence of imperfections in crystals can be expected to cause normally inactive frequencies to be allowed in absorption. In contrast to the qualitative results given above, Lifshitz finds that not just some of the modes but all of the modes are allowed in absorption in imperfect crystals. According to Lifshitz, this occurs because the normal modes are no longer plane waves. Returning to our qualitative model, if one says that the frequencies are primarily determined by the nature of the interaction forces, while the phase relationships between unit cells (which depend on the wave forms of the normal modes) are determined by the long range order of the crystal, then it is possible to understand how the frequency

distribution of the normal modes can remain essentially unchanged even though the selection rules are broken for all of the modes. Nevertheless, the extent to which the dipole moment change is preserved over several unit cells may vary between different modes.

Lifshitz has considered two special cases for which he can obtain a solution: (1) arbitrary concentration of small distortions, randomly distributed, (2) small concentration of centers with an arbitrary distortion. Case (1) corresponds to the effect due to the presence of more than one stable isotope. Case (2) corresponds to the effect due to the presence of impurity atoms or vacant sites.

Case (1): The isotope effect varies according to the frequency under consideration. We shall consider two ranges of frequency: (a) Frequencies comparable in magnitude to the upper limiting frequency. In diamond, silicon, and germanium the upper limiting frequency is normally inactive. For a case in which only two isotopes occur, Lifshitz finds that there will be weak, uniform absorption with the absorption coefficient proportional to $C(1-C)(\mu/m^*)^2$ where $\mu = m^{II} - m^{I}$, m^i = mass of i^{th} isotope, $m^* = m^{II}C + m^{I}(1-C)$, C = concentration of one isotope, 1-C = concentration of other isotope. "Uniform absorption" for all frequencies implies absorption bands which follow the contours of the branches of the frequency distribution. (b) Frequencies very small with respect to the upper limiting frequency. In this case, the absorption decreases with increasing frequency as the fifth power of the frequency. Since this range starts from $\nu = 0$, the modes involved will be primarily sonic

and very long infrared waves. Presumably, the strong decrease in absorption with frequency will render this effect unobservable in the infrared region.

(2) The impurity effect depends on the nature of the impurity. In order to simplify the problem Lifshitz treated the problem in which the impurity atom differs from the atoms of the parent crystal in mass, but does not alter the force field. The case is highly idealized, and probably only applies to ionic mixed crystals. However, the results are instructive. For example, when the mass of the impurity atom approaches the mass of the atoms of the parent crystal, Lifshitz obtains results which agree with the results obtained for the isotope effect, i. e. his treatment is consistent. For masses much greater or much less than the atoms of the parent crystal, absorption for high frequencies is uniform as in the isotope effect, but it depends only on the concentration of the impurity atoms and is independent of their mass. Also, the impurity atoms may cause new frequencies to appear which may lie either within or outside the frequency intervals of the ideal crystal branches. These new frequencies will, in general, form a set of continous bands whose positions and intensities depend on the impurity concentration.

We shall now consider how Lifshitz's results can be applied to explain the absorption in the fundamental region by diamond, silicon, and germanium in terms of the presence of imperfections in the lattice. The appearance of bands characteristic of the ideal lattice can be due either to an isotope effect or to the presence of impurity atoms, or perhaps to other imperfections

which have not been investigated specifically. If frequencies not characteristic of the lattice appear in absorption, these may be attributed to the effect of impurity atoms.

Before we consider the observed spectra we will make some estimates of the average distance between isotopes of the same mass. For diamond, C_{13} is present as 1.1% of the atoms while C_{12} makes up the remaining 98.9%. Therefore, 1 atom in 90 is C_{13}. Since each unit cell contains two atoms, 90 atoms fill 45 unit cells. If the isotopes are uniformly distributed (an approximation to the mean spacing of a random distribution), then the distance between unit cells containing C_{13} atoms is $3\sqrt{45} = 3.8$ unit cell sides. That is, approximately 4 unit cells separate C_{13} atoms, on the average. Such a separation is small enough to affect even the shortest mode, which has a wavelength comparable to one unit cell side. In silicon and germanium the various isotopes are present to an even greater extent. (See Table 21). We conclude that the imperfections introduced by isotopes are close enough together to break down selection rules for all elastic waves. The question now becomes one of the magnitude of the absorption coefficient. Since the mechanism of absorption in valency crystals is not clear, (see, for example, Matossi[108]), we will attempt no quantitative estimate of the absorption coefficient. One can calculate the factors which depend on the mass and concentration of the isotopes. In Table 25 we have calculated the quantity

$$K' = \sum_i \frac{(m^* - m_i)^2}{m^{*2}} \frac{C_i}{(1-C_i)}$$

where m^* is the atomic weight of the substance when the isotopes are present in their normal proportions, m_i is the mass of the

i^{th} isotope, and C_i is the concentration of the i^{th} isotope. This expression for K' is the extension of Lifshitz's expression for two isotopes (page 162) to the case of more than two isotopes.

Table 25

RELATIVE ABSORPTION COEFFICIENTS K'

Substance	Mass No.	C_i	m*	K'.10^5
Diamond	12	.989	12.01	7.7
	13	.011		
Silicon	28	.923	28.06	25.6
	29	.047		
	30	.030		
Germanium	70	.206	72.6	71.5
	72	.274		
	73	.076		
	74	.368		
	76	.076		

The absorption coefficient is proportional to K'. However, we have no good estimate of the relative effects of the remaining terms in the total expression for the absorption coefficient. These terms depend on the charge distribution and the force field. Under these conditions, we cannot compare the observed absorption coefficients with calculated expressions. Table 25 does show that the contribution of the terms depending on isotope concentration and mass becomes progressively greater as we go from diamond to silicon and germanium.

At the strongest absorption band in the fundamental spectra the observed absorption coefficients are

$$K_{Dia} : K_{Si} : K_{Ge} = (0\text{-}20) : 5.5 : 13.5$$

These observed coefficients also increase from diamond through germanium, if we use the IR II diamonds (K = 0) for the comparison. The fact that diamond sometimes exhibits no fundamental absorption indicates that either the isotope C_{13} is absent from IR II diamonds, or the isotope effect in diamond is not sufficient by itself to bring about observable absorption. In order to test this point, measurements of the C_{12}/C_{13} ratio in diamonds of varying IR properties were planned. Unfortunately, while tentative arrangements were made with the University of Chicago to do this work, no measurements have been made. However, results on other material containing carbon as well as some diamonds,[109] which were not classified as to Type, indicate that the maximum variation in the ratio C_{12}/C_{13} in naturally occurring substances is of the order of 5% of the ratio. The corresponding variation in the total number of C_{13} atoms, i. e. from 1 part in 90 to about 1.05 parts in 90, is insignificant from the standpoint of infrared absorption. Also, since isotope concentration can have at most very minor effects on the electronic properties whose variations are correlated with the variation in infrared absorption, it follows that the isotope effect by itself, is not responsible for infrared absorption. However, in silicon and germanium, the observed infrared absorption coefficients in pure samples do not vary from sample to sample. It seems reasonable to conclude that the absorption in silicon and germanium may be due to the isotope effect. If this is true, one must explain the fact that diamond evidently has no observable isotope effect. Such an explanation can be obtained only by a consideration of

the contribution to the absorption coefficient by the factors depending on charge distribution and the force field. We do know that the force field in diamond is different from that in silicon and germanium (see section 4.1). Consequently, there is no reason to expect that the neglected factors will be the same order of magnitude for all three substances.

We will now consider the observed spectra, shown in Figure 39. The frequency scales have been adjusted to the calculated factor of 1.95 (Dia/Si) and 3.58 (Dia/Ge). The principal maxima of all three substances fall in the same general region. The narrow diamond band at 1372 cm^{-1} has no counterpart in the silicon spectrum. The shoulders in the germanium spectrum at 360 and 375 cm^{-1} are similar to the 1372 cm^{-1} band. We will consider this point later.

In Table 26 are shown the calculated maxima which fall closest to the observed maxima. In Figures 40 and 41 the contours of the observed spectra are compared with the calculated branches which most nearly fit the observed bands. Intensity factors used for this comparison are shown in Table 26. We will now consider the fit between observation and calculation. Since the results for germanium and silicon are less complex than those for diamond, we will consider them first.

GERMANIUM: The contour of the observed spectrum is well matched in the high frequency portion by ω_1, ω_2, and ω_3. The maximum at 200 cm^{-1} is not so well explained by ω_4. The true shape of ω_4 may be somewhat different from our calculated result, and our observed spectrum in this region is not of high accuracy. In any event, the calculated bands appear to follow the contour

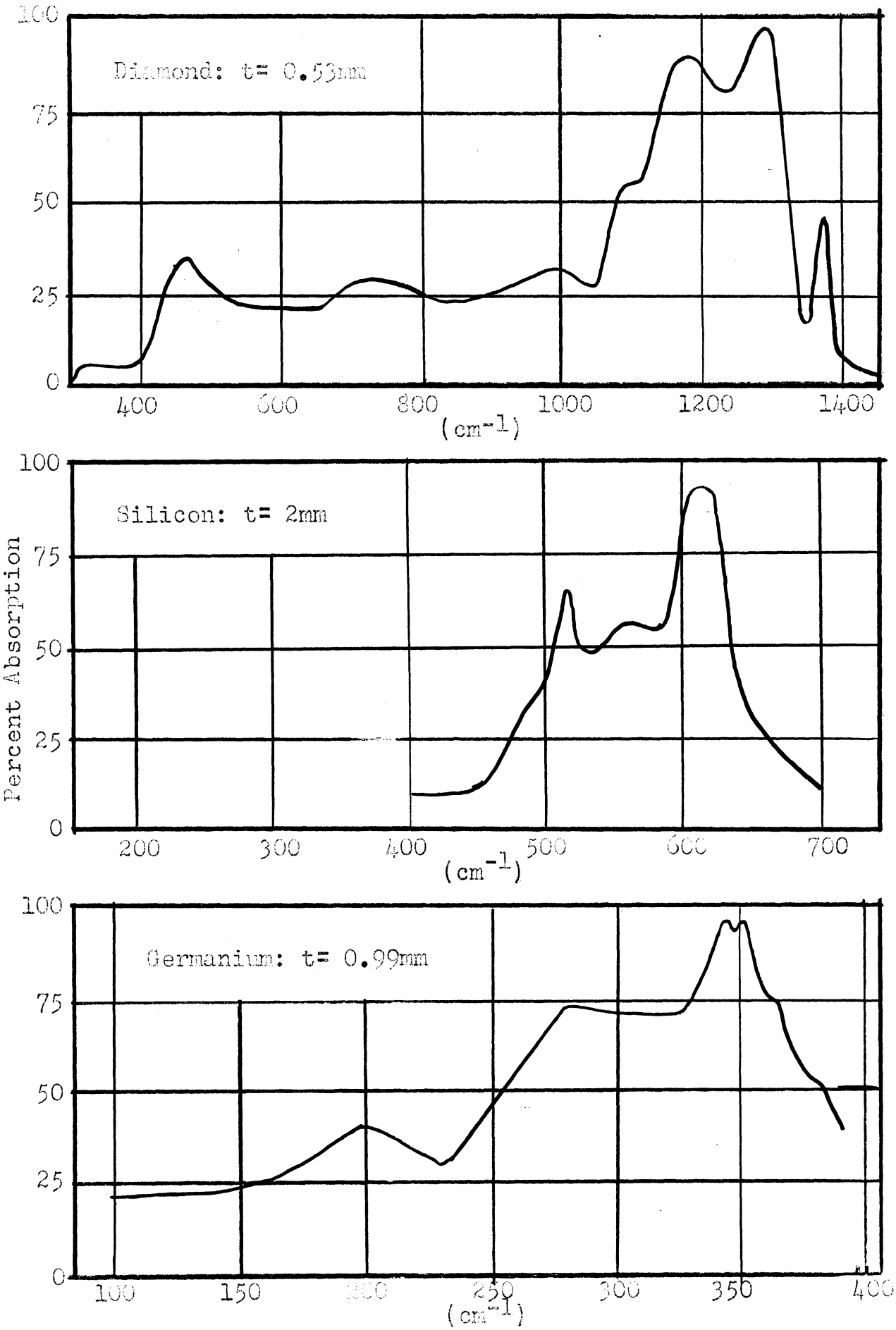

Fig. 39

OBSERVED FUNDAMENTAL ABSORPTION

Table 26

OBSERVED VS CALCULATED MAXIMA IN THE FUNDAMENTAL ABSORPTION SPECTRA OF DIAMOND, SILICON AND GERMANIUM

Substance	Observed (cm^{-1})	Calculated (cm^{-1})	Branch	Intensity
Diamond				
A:	1280	1285	ω_3	3
	1203	1180	ω_3	3
	1088	1080	ω_4	1
	480	(680)	ω_4	1
		(370)		
B:	1400	None		
	1372	None		
	1332	1326	ω_1, ω_2	0.1, 0.1
	1170	None		
	1004	None		
	770	736	ω_5	1
	368	330	ω_5	1
Silicon	610	654, 625	ω_1, ω_2	1, 1
	520	520	ω_3	2
Germanium	345	356, 341	ω_1, ω_2	1, 1
	275	284	ω_3	2
	200	241	ω_4	1.3

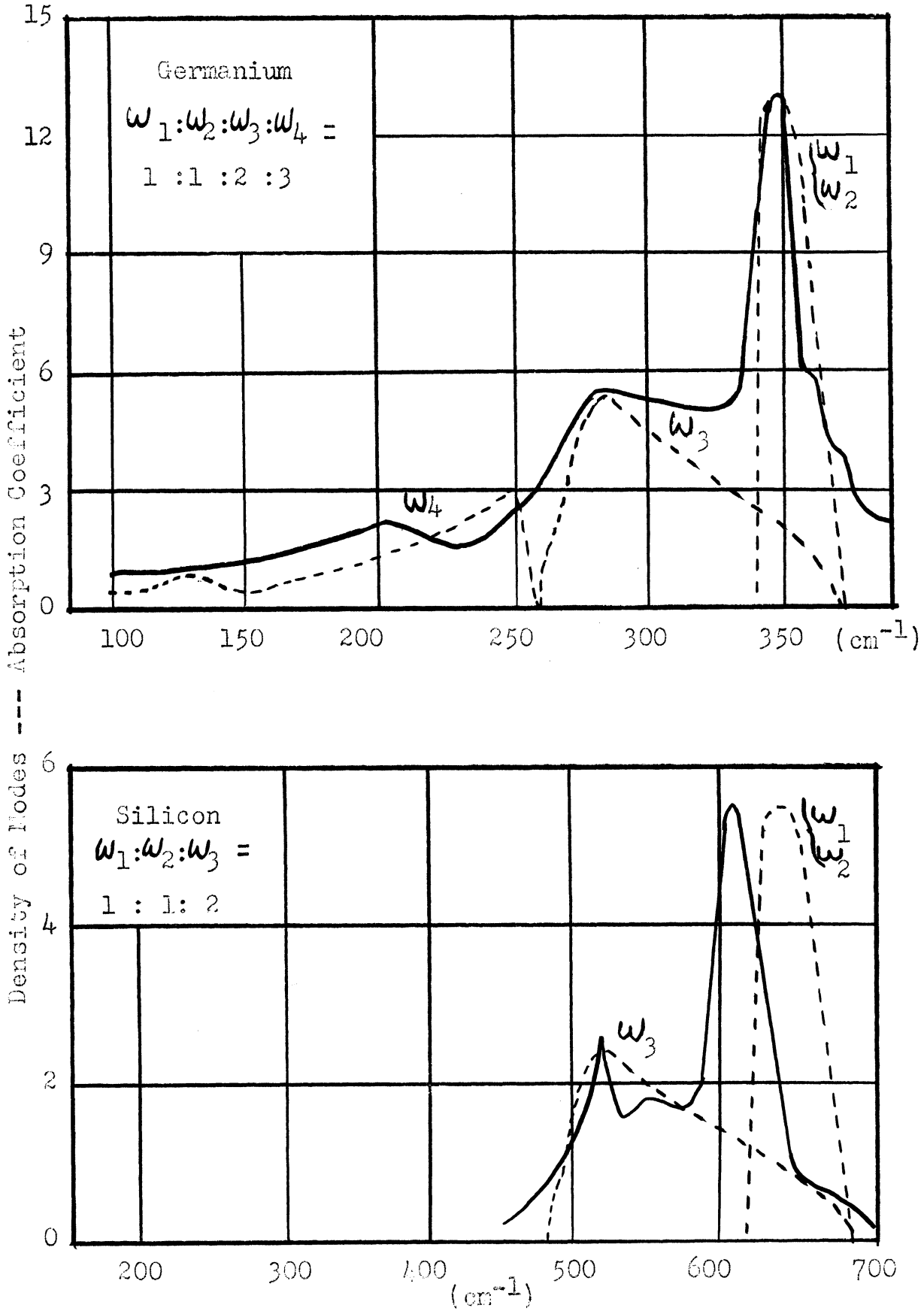

Fig. 40

CALCULATED VS OBSERVED FUNDAMENTAL BANDS

IN SILICON AND GERMANIUM

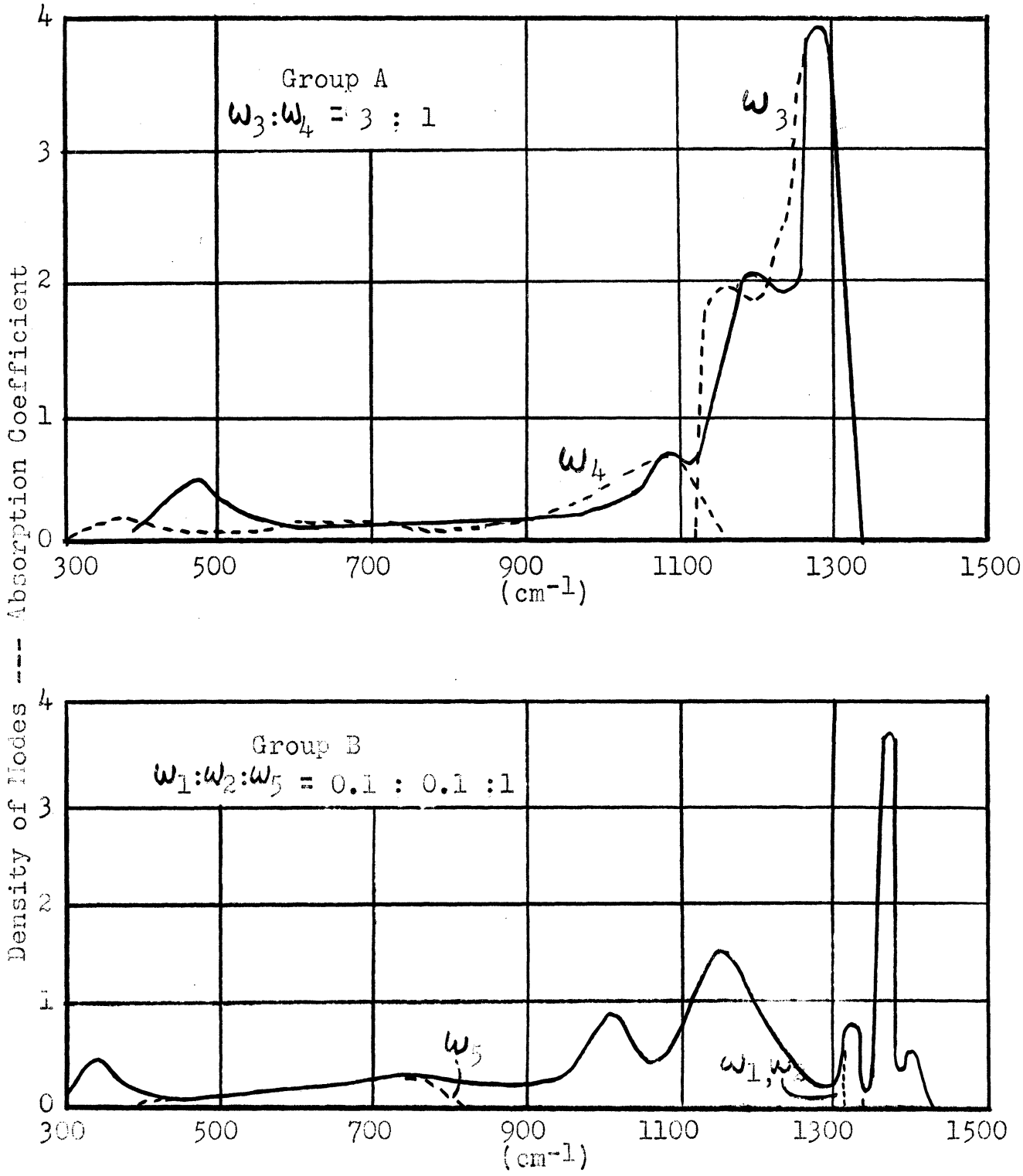

Fig. 41

CALCULATED VS OBSERVED FUNDAMENTAL BANDS IN DIAMOND

of the observed bands if the relative intensities of the branches are $\omega_1 : \omega_2 : \omega_3 : \omega_4 = 1:1:2:1:3$. The shoulder at 360 cm^{-1} falls within the calculated interval of fundamental frequencies and could be due to a shoulder on ω_1 or ω_2. The shoulder at 375 cm^{-1} falls just at the upper frequency limit of the calculated interval. However, we have no exact data on the position of this upper frequency limit, and it is possible that the 375 cm^{-1} absorption is also a shoulder on ω_1 or ω_2 rather than a non-lattice band.

SILICON: The calculated position of ω_1, ω_2 falls at a higher frequency than the observed maximum at 610 cm^{-1}. This indicates that our calculations for silicon are less accurate than those for germanium. The difference between the observed and calculated maxima is 640-610 = 30 cm^{-1}, or about 5% of the observed frequency. The original calculation (section 4.1.3) showed a deviation of 5% in the ratios of the force constants. Therefore, the observed error of 5% is compatible with the accuracy of the calculation. The calculated ω_3 matches the observed spectrum near 520 cm^{-1}, although the detail of the spectrum is somewhat more complex than that of our calculated branch. If the observed peak is as sharp as it appears to be from Lord's data, then singularities may be responsible. The calculation (section 4.1.4) of the fundamental branches using no second neighbor interaction (B) gave an unidentified singular point near 520 cm^{-1} (see Table 17). If we assume that the nature of the singularities in our Calculation B is the same as in the alternative calculation which does include second neighbor forces (A), then the peak observed at 520 cm^{-1} can be explained in terms of a singular

point of type (b) at the lower frequency edge of the branch (see Table 17 and Figure 28). The relative intensities $\omega_1 : \omega_2 : \omega_3 = 1:1:2$ are the same as those used to match the germanium spectrum.

DIAMOND: In diamond, the situation is complicated by the fact that the observed absorption coefficients are not constant. In addition, the relative intensities of the bands vary. We have constructed separate approximate contours for Group A and Group B type bands where the relative magnitudes of the absorption coefficients have been obtained from Blackwell's correlation charts, and, in the case of the long wavelength bands, from our experimental results.

Group A: The observed bands at 1280, 1203, and 1088 cm^{-1} are reasonably well explained by the calculated contours of ω_3 and ω_4 with a relative intensity of 3:1. The band at 21μ (480 cm^{-1}) is not well explained. Because the methods of calculation are quite inaccurate away from the principal maxima of the branches, it is quite possible that the 480 cm^{-1} band is due to a secondary maximum on ω_4. In Figure 40 we show two weak maxima on ω_4, both of which may be spurious; however, their presence in the calculated contour indicates the manner in which a secondary maximum can occur in the region where the calculations are inaccurate. The interpretation of the band at 480 cm^{-1} is more fully discussed below.

It will be noted that ω_1 and ω_2 are not used to account for Group A absorption, although those branches are responsible for the strongest absorption in silicon and germanium. Analogy with silicon and germanium would have led to the assignment of the 1280 cm^{-1} band to ω_1, ω_2 and 1203 cm^{-1} to ω_3. However, we

have shown (section 4.1.4) that the calculated position of the maxima of ω_1 and ω_2 lies near 1326 cm^{-1}. In addition, the calculated primary maximum of ω_3 lies at too high a frequency to be responsible for the 1203 cm^{-1} band. However, it is possible that the force field used for diamond is in error, especially since one elastic constant was altered to fit relations arising from the nature of the assumed force field (section 4.1.1). The principal argument in favor of retaining the present calculation is that no change can be made in the predicted values of ω_1, ω_2, and ω_3 without a corresponding change in ω_4, ω_5, ω_6. The maxima of ω_5 and ω_6 determine the position of the secondary maximum of the total frequency distribution. It is shown in Appendix A that the specific heat results at low temperatures are sufficiently sensitive to establish the position of the secondary maximum close to the position obtained with the present force field. Another argument in favor of our representation of ω_1 and ω_2 is that the calculated maxima of combinations involving ω_1 and ω_2 give good agreement with the observed combination bands.

Group B: In this group there are at least two bands (1372, 1400 cm^{-1}) which lie beyond the upper limit of the frequency distribution of diamond. It will be recalled that the Raman line at 1332 cm^{-1} fixes this limit. The weak band at 1540 cm^{-1} which has not been correlated to either Group A or B probably belongs to Group B because of its position with respect to the upper frequency limit. The remaining bands in Group B fall within the frequency distribution of the ideal diamond. Of these bands, the maxima at 1332 and 770 cm^{-1} correspond to

the calculated ω_1, ω_2, and ω_5. The absorption band at 1332 cm^{-1} is wider than the Raman line at the same frequency. For this reason we assign it to the ω_1, ω_2 bands rather than to the single upper frequency. The bands at 1170 and 1004 cm^{-1} fall in the vicinity of strong Group A absorption and near the dense portions of ω_3 and ω_4. However, their maxima do not correspond to calculated maxima, and they can be regarded as new frequencies caused by a perturbation of the diamond lattice. The 328 cm^{-1} band (like the 480 cm^{-1} band) falls in the region where our calculations are too inaccurate to make an assignment.

We will add a note on the long wavelength bands. If difference bands are considered, it is found that the maximum of $\omega_3 - \omega_5$ falls at the position of the 480 cm^{-1} band. However, that this assignment is unlikely is proved by the fact that the corresponding summation band does not occur in absorption (section 4.2.2). In addition, the absorption coefficient at 480 cm^{-1} is variable and appears to be associated with the Group A bands. The only other maximum calculated to be near 480 cm^{-1} is the maximum at 525 cm^{-1} in ω_6. The reason that this band has not been used in assignment, is that ω_6 has another calculated maximum near 740 cm^{-1}. However, the absorption observed near 770 cm^{-1} belongs to Group B while that at 480 cm^{-1} belongs to Group A, so that they can have their origins in the same branch only if the branch is not uniformly excited. While the assignment of the other branches has been made on the assumption that they are uniformly excited, it is not unlikely that the low frequencies of acoustical branches may be non-uniformly excited (see page 161). However, if this were

true, it would be difficult to assign bands, simply because the observed maxima might fall anywhere within the interval of frequencies of the branch under consideration. For this reason, we shall not speculate further on this point.

We see from the above discussion, that the absorption bands in the fundamental frequency range of diamond follow the general behavior predicted by Lifshitz. That is, frequencies which can be associated with the ideal frequency distribution appear in absorption with variable intensity, and, in addition, certain diamonds show additional absorption which cannot be associated with the ideal frequency distribution. It should be emphasized that the non-ideal bands always appear in the same positions although their intensities vary. This indicates that if the bands are due to impurities, the impurities do not correspond to Lifshitz's idealized case (2), page 163, in which the impurity atom does not alter the force field, for in that case the positions of non-ideal frequencies vary with concentration. One might infer that the primary effect of the imperfections responsible for Group B absorption is through a change in the force field.

4.3 Summary

We have calculated the branches of the frequency distributions for diamond, silicon, and germanium, using certain of H. M. J. Smith's numerical results on diamond. For silicon and germanium we have assumed that there is a constant proportion between the force constants of silicon and germanium and

the constants used in one of Smith's calculations (B) in connection with diamond. The validity of this assumption has been discussed and the proportionality factors evaluated.

The observed combination spectra of diamond, silicon, and germanium have been explained in terms of allowed combinations, with the exception of one weak band in germanium which has been shown to agree with a combination band which could become active through an isotope effect.

The observed fundamental spectra of silicon and germanium and Group A of diamond can be accounted for in terms of calculated branches of the frequency distributions of these substances. The diamond Group B absorption has two weak maxima lying near calculated branch maxima, but it is chiefly composed of bands which cannot be associated with calculated maxima for the ideal lattice. These results, coupled with the fact that the absorption coefficients for bands in pure silicon and germanium are constant while those in diamond vary, are consistent with the conclusion that the isotope effect is responsible for absorption in pure silicon and germanium, but that impurities account for absorption in diamond.

We conclude that (1) The infrared absorption spectra of diamond, silicon and germanium can be accounted for in terms of the Born theory of lattice dynamics. (2) Analysis of the infrared absorption spectrum of diamond in terms of the Born theory shows that the experimental facts which led Blackwell and Sutherland to propose the impurity theory are, in fact, consistent with such a theory.

Appendix A

THE VARIATION OF SPECIFIC HEAT WITH TEMPERATURE

In section 3.1, the effective Debye temperature has been defined as θ in $C_v = D(\theta/T)$ where $D(\theta/T)$ is the Debye expression for specific heat as a function of temperature. The variation of specific heat with temperature can be expressed as θ vs T where deviation from constant θ denotes deviation from an ideal Debye solid. In Figures 42 and 43, θ vs T is plotted for diamond [110], boron carbide [111], silicon carbide [111], silicon [112], germanium [113, 117], and grey tin [113]. Where necessary specific heat data in the literature have been reduced to θ data. All of the substances except boron carbide have the diamond type crystal structure [114]. Boron carbide has a complex structure not comparable to that of diamond [115]. It is included because it is normally considered to be a "valency" crystal like diamond and it has properties such as melting point and hardness which are intermediate between silicon carbide and diamond.

All of the substances display a minimum in θ vs T. This minimum is a consequence of the secondary maximum of the frequency distribution of vibrational modes. Nakamura [118] has shown that for $T \ll \theta$, $4(T/\theta) \approx \nu/\nu_L$ where ν_L = the upper limiting frequency of the distribution and ν denotes the frequency region making the dominant contribution to the specific heat at temperature T. In Table 27, the frequency, ν, evaluated from Nakamura's approximation, corresponding to the

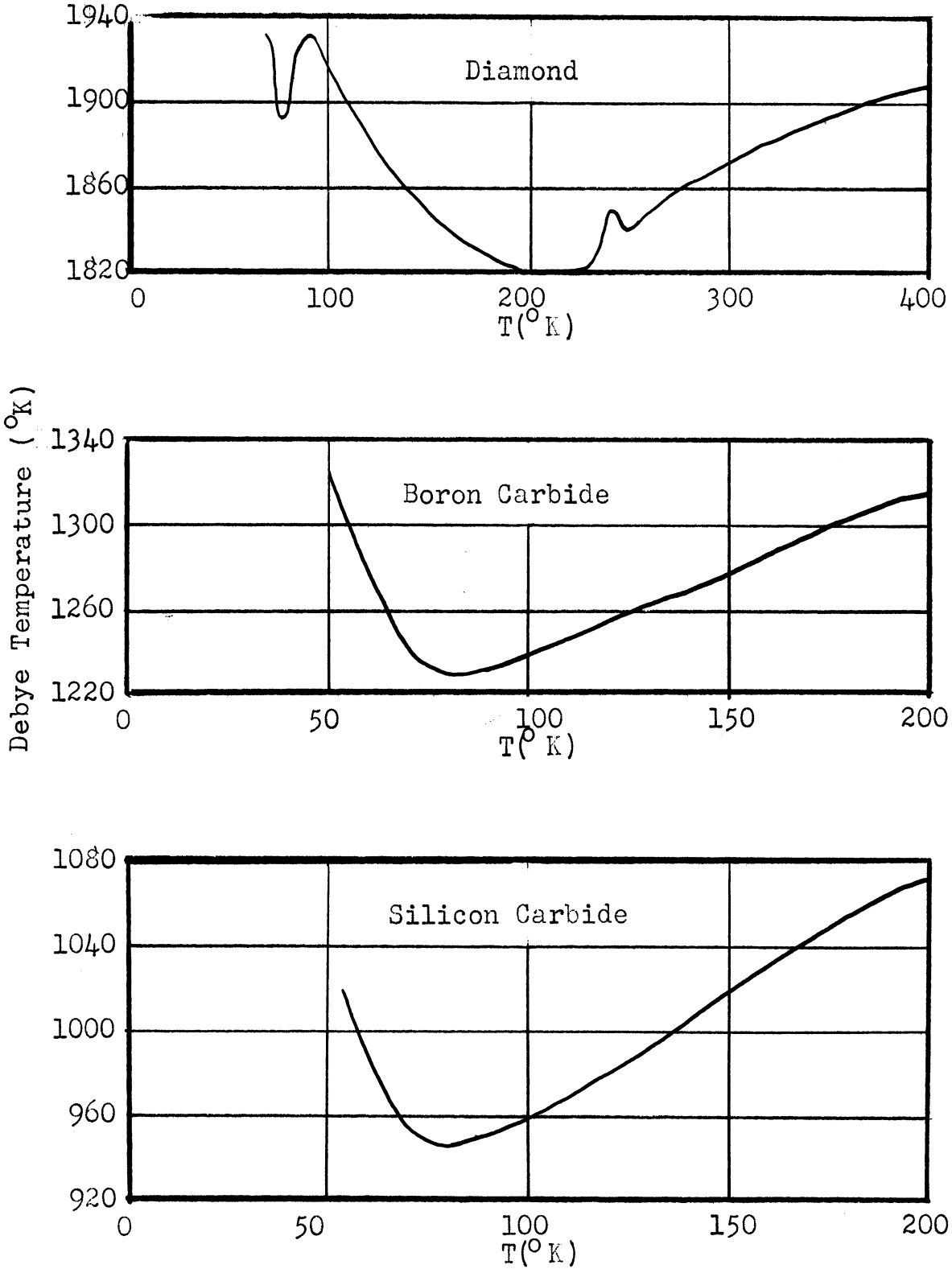

Fig. 42

VARIATION OF DEBYE TEMPERATURE: DIAMOND, B_4C, SIC

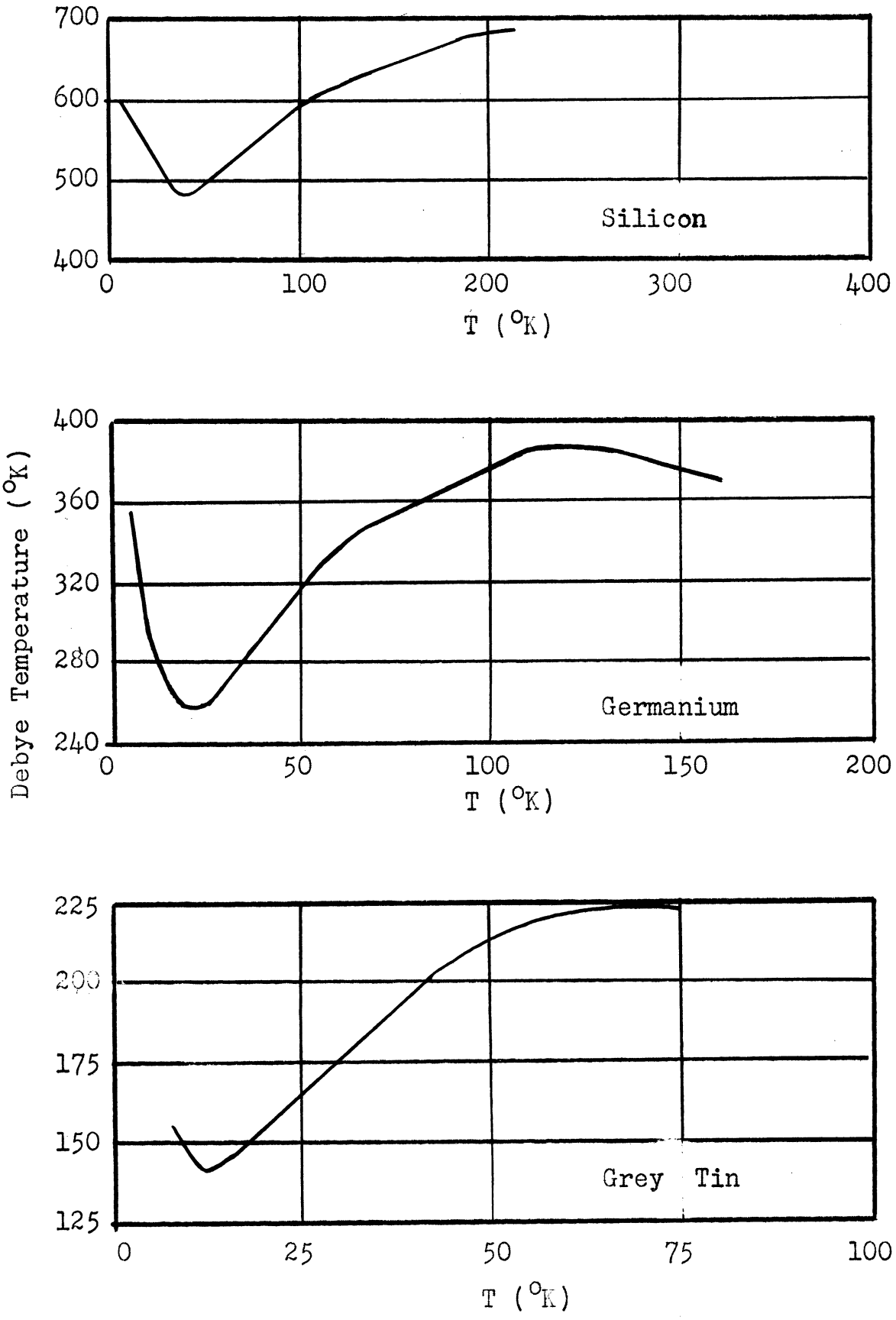

Fig. 43

VARIATION OF DEBYE TEMPERATURE: SI, GE, GREY SN

minimum in θ vs T is given for each of the six substances. For diamond, silicon, and germanium, our calculated values for the frequency of the secondary maximum are also listed.

Table 27

FREQUENCY OF THE SECONDARY MAXIMUM OF N(ν)

Substance	Position of Minimum in $\frac{\theta}{\theta}$ vs T T	ν_L	Secondary Maximum by Nakamura Equation	Secondary Maximum from Calculated Distribution
Diamond	1820°K	220°K	1332 cm^{-1}	648 cm^{-1}	680 cm^{-1}
Boron Carbide	1230	84	---	---	---
Silicon Carbide	946	80	---	---	---
Silicon	460	40	665	231	238
Germanium	256	22	372	128	132
Grey Tin	142	11	---	---	---

The agreement in the last two columns is very good. It explains the success by Smith and by Hsieh in calculating specific heat from their distributions for diamond and germanium, i. e. the secondary maxima fell at the correct position to account for the observed minimum in θ vs T. On the other hand, it is also clear that the specific heat is sensitive only to the low frequency portion of the distribution (see Katz [119]).

It is important to note that the frequencies listed in Table 27 depend on the use of "Second Neighbor" calculations for diamond (Calculation A) and "First Neighbor" calculations

for silicon, and germanium (Calculation B). Calculation B for diamond places the secondary maximum at 470 cm^{-1} which is considerably removed from the 645 cm^{-1} predicted from specific heat data. This is evidence that the 480 cm^{-1} band observed in absorption is not due to absorption at the secondary maximum. It is also evidence favoring the "second neighbor" calculation for diamond.

In Figure 44 are plotted curves for θ/θ_m vs T/θ_m for the six substances. θ_m is the average high temperature value of θ . The curves for silicon and germanium superimpose over the range of temperatures considered. The scale factor between corresponding θ's and T's is 1.8. In section 4.1, we stated that this result follows from our result that the frequency scales of the distributions for silicon and germanium are related by a factor of 1.83. From the definition of $\theta = \frac{h\nu_{max}}{k}$ and the Nakamura approximation one sees that this statement is valid.

The remaining curves in Figure 44 show two trends. There is a displacement to lower values of both θ/θ_m and T/θ_m as we go from diamond to grey tim. The minima of all the diamond like substances fall on a smooth curve while the boron carbide minimum is displaced from that curve. One sees that some of the properties of the substances such as melting point and hardness can be correlated with the variation in these curves i. e. diamond at one extreme and grey tin at the other. The deviation of boron carbide is to be expected since its crystal symmetry differs from the other substances. The fact that the

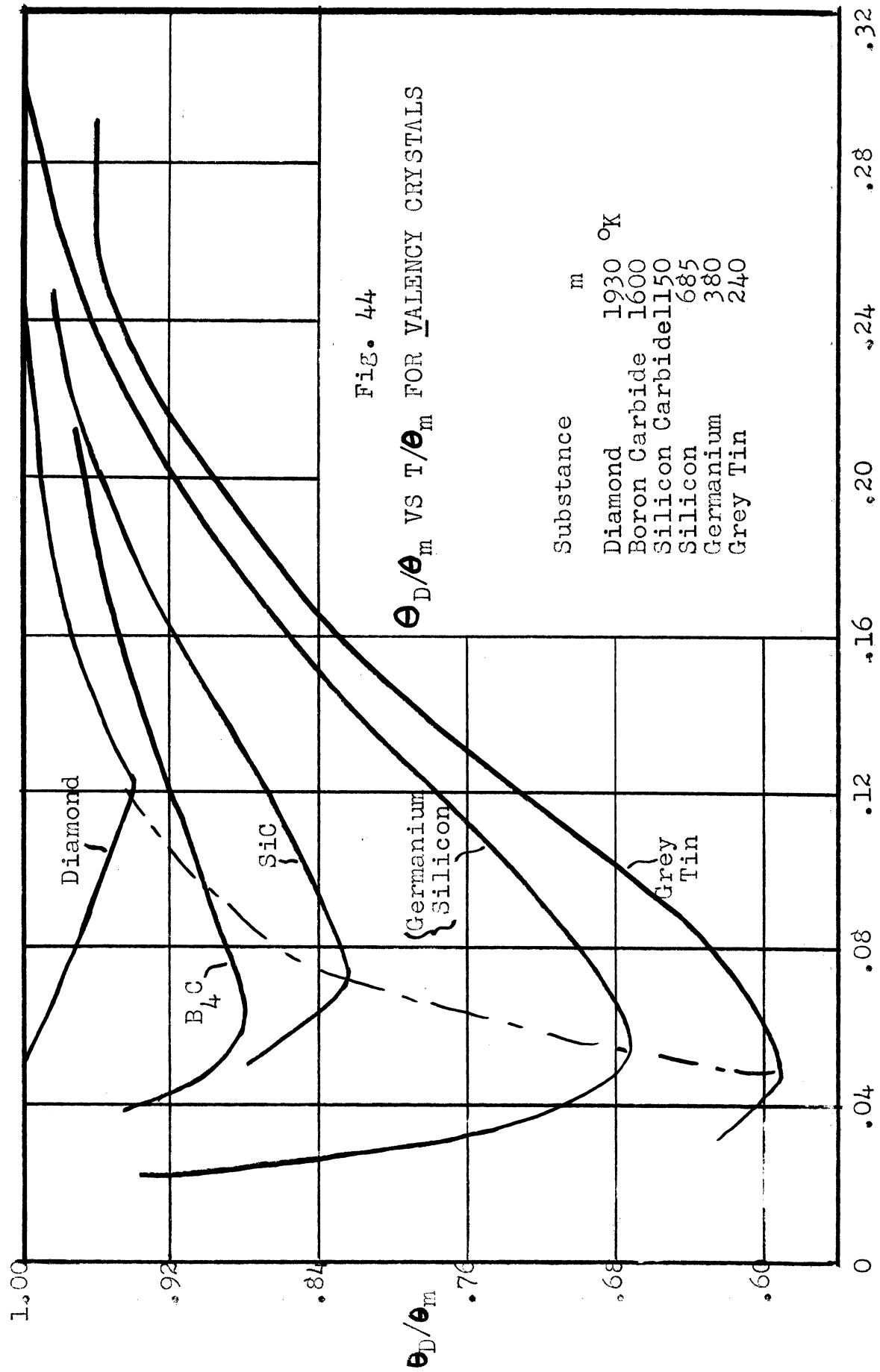
Fig. 44
Θ_D/Θ_m VS T/Θ_m FOR VALENCY CRYSTALS
Substance m °K
Diamond 1930
Boron Carbide 1600
Silicon Carbide 1150
Silicon 685
Germanium 380
Grey Tin 240
Diamond
SiC
B_4C
Germanium
Silicon
Grey Tin
Θ_D/Θ_m
T/Θ_m
1.00
.92
.84
.76
.68
.60
0
.04
.08
.12
.16
.20
.24
.28
.32

curves for all the diamond-like substances do not superimpose indicates a difference in the forces between atoms in these crystals, i. e. their frequency distributions are not related by simple frequency scale factors.

Appendix B

LIST OF DIAMONDS USED IN EXPERIMENTAL WORK

Diamond	IR
K 1	II
2	WI
3	SI
4	SI
5	SI
6	WI
7	WI
M 4	WI *
S 1	SI
2	SI
3	SI
T 15	WI
22	II
37	II *
38	WI
B 2	SI
BP 2	II *
3	II
CR 1	SI
F 1	SI *
2	SI
3	SI
G 1	MI
2	SI
3	SI

DIAMOND	IR
GM 12	MI
38	MI
39	SI
40	SI
41	SI
74	II
75	WI
GR 1	MI
2	SI
3	SI
I 7	MI
13	WI
20	WI
25	II
30	II
SLF1 27	SI *
SLO 9	SI
15	SI
15P	SI
25	SI
25P	SI
42	SI
44P1	SI
44P2	SI *
SYR 1	SI
8	SI *
8P	SI *
9	SI

Note: All diamonds listed were examined for uniformity of transmission at 2537 A. U.

* Stones tested in the vacuum ultraviolet.

Code: K - Kaplan; M - Parkinson; S - Slawson; T - Triefus;

All others - Diamond Trading Company.

BIBLIOGRAPHY

1. Robertson, R., Fox, J. J., and Martin, A. E., Phil. Trans. Roy. Soc. 232, 463 (1934).
2. Raman, C. V. and Nilakantan, P., Proc. Ind. Acad. Sci. 11, 379 (1940).
3. Lonsdale, K., Phil. Trans. Roy. Soc. A240, 219 (1947); Proc. Roy. Soc. A179, 315 (1942).
4. Ramanathan, K. G., Proc. Ind. Acad. Sci. 24, 137 (1946).
5. Sutherland, G. B. B. M. and Willis, H. A., Trans. Faraday Soc. 41, 289 (1945).
6. Raman, C. V. and Coworkers, Proc. Ind. Acad. Sci. 19, 189-342 (1944).
7. Raman, C. V., Proc. Ind. Acad. Sci. 18, 237 (1943); A34, 141 (1951).
8. Raman, C. V., Proc. Ind. Acad. Sci. 19, 189, 199 (1944).
9. Born, M., Proc. Phys. Soc. 54, 362 (1942).
10. Blackwell, D. E., Thesis, Cambridge (1949).
11. Blackwell, D. E. and Sutherland, G. B. B. M., J. Chim. Phys. 46, 9 (1949).
12. Grenville-Wells, H. J., Thesis, London (1951).
13. Herman, F., Phys. Rev. 88, 1210 (1952).
14. Smith, H. M. J., Phil. Trans. Roy. Soc. A241, 105 (1948).
15. Born, M., Dynamik der Kristallgitter, Teubner, Leipzig (1915).
16. Lifshitz, I. M., J. of Phys. (USSR) 7, 215, 249 (1943); 8, 89 (1944).
17. Bragg, W. H. and Bragg, W. L., Proc. Roy. Soc. A89, 277 (1913).
18. Straumanis, M. E. and Aka, E. Z., J. Am. Chem. Soc. 73, 5643 (1951).
19. Ehrenberg, W., Ewald, P. P., and Mark, H., Zeits. F. Krist. 66, 547 (1928).
20. Faxen, H., Z. Phys. 17, 266 (1923).
21. Waller, I., Z. Phys. 17, 398 (1923).
22. Lonsdale, K., Proc. Phys. Soc. 54, 314 (1942).
23. Lonsdale, K., Rep. Prog. Phys. 9, 256 (1942).
24. Hoerni, J. and Wooster, W. A., Experientia 8, 297 (1952).
25. Brill, R., Acta, Cryst. 3, 333 (1950).
26. Grenville-Wells, H. J., Proc. Phys. Soc. 65, 313 (1952).
27. James, R. W., The Optical Principles of the Diffraction of X-rays, Bell, London (1948).
28. Heidenreich, A. D., Phy. Rev. 77, 271 (1950).
29. Moffett and Coulson, Phil. Mag. 40, 1 (1949).
30. Born, M., Rep. Prog. Phys. 9, 294 (1942).

31. Danielson, G. C. and Willardson, R. K., J. Opt. Soc. Am. 42, 42 (1952).
32. Mani, A., Proc. Ind. Acad. Sci. 19, 231 (1944).
33. Bhagavantam, S., Ind. J. of Phys. 5, 35, 169, 573 (1930).
34. Krishnan, R. S., Proc. Ind. Acad. Sci. 24, 45 (1946).
35. Krishnan, R. S., Proc. Ind. Acad. Sci. 24, 25 (1946).
36. Tu, Y., Phys. Rev. 40, 662 (1932).
37. Bearden, J. A., Phys. Rev. 54, 698 (1938).
38. Raman, C. V. and Jayaraman, A., Proc. Ind. Acad. Sci. A32, 65 (1950).
39. Ramanchandran, G.N., Proc. Ind. Acad. Sci. 24, 65 (1946).
40. Chesley, F. G., Amer. Min. 27, 20 (1942).
41. White, J. U. and Liston, M. D., J. Opt. Soc. Am. 40, 36, 93 (1950).
42. White, J. U., J. Opt. Soc. Am. 37, 713 (1947).
43. Williams, V. Z., Symposium on Molecular Structure, Ohio State University (1952).
44. Walsh, A., Nature 167, 810 (1952).
45. Wood, D. L., Rev. Sci. Inst. 21, 764 (1950).
46. Schwartzschild, K., Abh. Ges. der Wiss. zu Gottingen neue Folge 4 Mathematische-Physikalische Klasse II, (1905-6).
47. Burch, C. R., Proc. Phys. Soc. 59, 41 (1947).
48. Wood, D. L., Thesis, Ohio State University (1950).
49. Randall, H. M., Rev. Mod. Phys. 10, 72 (1938).
50. Harrison, G. R., Lord, R. C., and Loofbourow, J. R., Practical Spectroscopy, Prentice-Hall, New York (1948).
51. Platt, J. R., Private Communication.
52. Briggs, H. B., Phys. Rev. 77, 727 (1950).
53. Lord, R. C., Private Communication
54. Lord, R. C., Phys. Rev. 85, 140 (1952).
55. Briggs, H. B., J. Opt. Soc. Am. 42, 686 (1952).
56. Conwell, E. M., Proc. I. R. E. 40, 1327 (1952).
57. Shockley, W., Proc. I. R. E. 40, 1289 (1952).
58. Collins, R. J. and Fan, H. Y., Bull. Am. Phys. Soc. 27, 2, 32 (1953).
59. Collins, R. J. and Fan, H. Y., Bull. Am. Phys. Soc. 28, 2, I10 (1952).
60. Platt, J. R., J. Am. Chem. Soc. 69, 3055 (1947).
61. Potts, W. J., J. Chem. Phys. 20, 809 (1952).
62. Crookes, W., Nature 72, 593 (1905).
63. Cork, J. M., Phys. Rev. 62, 80 (1942).
64. Blackwell, D. E., Private Communication.
65. Grenville-Wells, H. J., Atomic Scientists' News 1, 86 (1952).
66. Grenville-Wells, H. J., Min. Mag. 29, 803 (1952).
67. Cork, J. M., Nuclear Physics, Nostrand Co., New York (1950).
68. Einstein, A., Ann. Physik 22, 180, 800 (1906); 34, 170 (1911).
69. Nernst, W. and Lindemann, F. A., S. B. preuss. Akad. Wiss. 22, 494 (1911).
70. Debye, P. Ann. Physik 39, 789 (1912).
71. Born, M. and von Karman, Th. Physik. Z. 13, 297 (1912); 14, 15 (1913).
72. Kelsom and Clark, Physica 2, 698 (1935).
73. Blackman, M., Z. Physik 86, 421 (1933); Proc. Roy. Soc. 148 384 (1935); 159, 416 (1937); Proc. Cambridge Phil. Soc. 33, 94 (1937).

74. Fine, P. C., Phy. Rev. 56, 355 (1939).
75. Leighton, R. B., Rev. Mod. Phys. 20, 165 (1948).
76. Kellerman, E. W. Phil Trans. A238, 513 (1940).
77. Hsieh, Y., Bull. Amer. Phys. Soc. 26, 6, 34 (1951).
78. Krishnamurti, B., Proc. Ind. Acad. Sci. A34, 121 (1951).
79. Blackman, M., Proc. Phy. Soc. 54, 377 (1942).
80. MacDonald, D. K. C., Prog. in Metal Phys. 3, 42 (1952).
81. Teller, E., Euckenwolf, Hand. und Jahrbuch der Chemisch. Physik 9, II.
82. Raman, C. V., Proc. Ind. Acad. Sci A34, 61 (1951).
83. Krishnan, R. S. and Ramanathan, K. G., Nature 157, 45 (1946).
84. Sutherland, G. B. B. M., Nature, 157, 45, 582 (1946).
85. Kimball, G. E., J. Chem. Phys. 3, 560 (1935).
86. Pauling, L. J., Am. Chem. Soc. 53, 1367 (1931).
87. Slater, J. C., Phys. Rev. 37, 481 (1931).
88. Hall, G. G., Phil. Mag. 43, 338 (1952).
89. Shockley, W., "Electrons and Holes in Semiconductors," Van Nostrand, New York, 1950.
90. Seitz, F., Modern Theory of Solids, McGraw-Hill, New York, 1940.
91. Bishui, B. M., Ind. J. Phys. 24, 441 (1950).
92. Ahearn, A. J., Phys. Rev. 84, 798 (1951).
93. Champion, F. C. and Stratton, K., Proc. Phys. Soc. B65, 473 (1952).
94. Hofstadter, R., Phys. Rev. 73, 631 (1948).
95. Klemens, P. G., Phys. Rev. 86, 1055 (1952).
96. Klemens, P. G., Proc. Roy. Soc. A208, 107 (1951).
97. Born, M. and Begbie, G. H., Proc. Roy. Soc. A188, 179 (1946).
98. Bhagavantam, S. and Bhimasenachar, J., Nature 154, 546 (1944).
99. Born, M., Nature, 157, 582 (1946).
100. Adams, L. H., J. Wash. Acad. Sci., 11, 45 (1921).
101. Williamson, E. D., J. Franklin Inst. 193, 491 (1922).
102. Herzberg, G., Molecular Structure and Molecular Spectra II, Nostrand, New York, 1945.
103. Bond, W. L., Phys. Rev. 78, 176 (1950).
104. McSkimm, H. J., Phys. Rev. 83, 1080 (1951).
105. Pearlman, N. and Keesom, P. H., Bull. Amer. Phys. Soc. 26, 6, 34 (1951).
106. van Hove, L., Phys. Rev. 89, 1189 (1953).
107. Newell, G. F., Bull. Am. Phys. Soc. 28, 2, 29 (1953).
108. Matossi, F., Symposium on Molecular Structure, Ohio State University, 1952.
109. Craig, H. B., Applied Spectroscopy Conference, Pittsburgh (1952).
110. Nernst, W., Ann. Phys. 36, 395 (1926); Pitzer, J. Chem. Phys. 6, 68 (1938).
111. Kelley, K. K., J. Am. Chem. Soc. 63, 1137 (1941).
112. Pearlman, N. and Keesom, P. H., Phys. Rev. 88, 398 (1952).
113. Hill, R. W., and Parkinson, D. H., Phil. Mag. 43, 309 (1952).
114. Wyckoff, R. W. G., Crystal Structure, Interscience, New York (1951).
115. Clark and Howard, J. Am. Chem. Soc. 65, 2115 (1943).
116. Cristescu, S. and Simon, F., Z. Physik. Chem. 25B, 273 (1934).

117. Estermann, I. and Weertman, J. R., J. Chem. Phys. 20, 972 (1952).
118. Nakamura, T., Prog. of Theor. Phys. 5, 213 (1950).
119. Katz, E., J. Chem. Phys. 19, 488 (1951).
120. Barnes, R. B., Brattain, R. R., and Seitz, F., Phys. Rev. 48, 582 (1935).
121. Born, M. and Blackman, M., Z. Physik 82, 551 (1933); Blackman, M., Z. Physik, 86, 421 (1933).